

1. Report No. FHWA/TX-95-1342-1	2. Government Accession No.	3. Recipient's Catalog No.	
4. Title and Subtitle A CASE STUDY OF OVERLAY PERFORMANCE OF CONTINUOUSLY REINFORCED CONCRETE PAVEMENT (CRCP) LOCATED ON IH-35, BOWIE COUNTY, TEXAS		5. Report Date February 1994	
7. Author(s) B. F. McCullough, T. Dossey, J. Weissmann, Yoon-Ho Cho		6. Performing Organization Code	
9. Performing Organization Name and Address Center for Transportation Research The University of Texas at Austin 3208 Red River, Suite 200 Austin, Texas 78705-2650		8. Performing Organization Report No. Research Report 1342-1	
12. Sponsoring Agency Name and Address Texas Department of Transportation Research and Technology Transfer Office P. O. Box 5051 Austin, Texas 78763-5051		10. Work Unit No. (TRAIS)	
15. Supplementary Notes Study conducted in cooperation with the U.S. Department of Transportation, Federal Highway Administration Research study title: "Updating and Maintaining the Rigid Pavement Condition Survey Data Base"		11. Contract or Grant No. Research Study 0-1342	
16. Abstract <p>This report documents a case study of an overlaid PCC pavement on IH-30, Bowie County, Texas. The 16-km (10-mile) project, constructed in April 1972, was first rehabilitated with an ACP overlay in May of 1986. Condition surveys of this project have been taken continuously at varying intervals, from the point of construction to the present. In June 1993, the project was again scheduled to be rotomilled and overlaid with 5 cm (2 inches) of ACP overlay. This rehabilitation effort created a unique opportunity for studying overlay performance. Condition survey, deflection, and profile data were all collected on the project before rotomilling (on the old overlay), after overlay (on the exposed PCC), and after the new overlay had been placed. Three analyses were performed: First, the failure history of the pavement was evaluated; second, a spectral analysis of the pavement profile was performed to determine the roughness reduction benefit of the overlay; and, finally, back-calculations of the concrete, subbase, and subgrade moduli were obtained to determine the development of fatigue in the pavement and the extent to which it was mitigated by the ACP overlay.</p> <p>Taken together, this study shows that, while a thin overlay restores ride quality, reduces the rate of failure development, and minimizes dynamic loading, the overlay does little to reinforce or reverse the development of fatigue in the underlying layers.</p>		13. Type of Report and Period Covered Interim	
17. Key Words CRCP, ACP overlays, pavement rehabilitation, roughness evaluations, back-calculation procedures, pavement structure behavior, pavement structure performance		18. Distribution Statement No restrictions. This document is available to the public through the National Technical Information Service, Springfield, Virginia 22161.	
19. Security Classif. (of this report) Unclassified	20. Security Classif. (of this page) Unclassified	21. No. of Pages 93	22. Price

**A CASE STUDY OF OVERLAY PERFORMANCE OF CONTINUOUSLY
REINFORCED CONCRETE PAVEMENT (CRCP) LOCATED
ON IH-30, BOWIE COUNTY, TEXAS**

by

B. Frank McCullough
Terry Dossey
José Weissmann
Yoon-Ho Cho

Research Report 1342-1

Research Project 0-1342

Updating and Maintaining the Rigid Pavement Condition Survey Data Base

conducted for the

Texas Department of Transportation

in cooperation with the

**U.S. Department of Transportation
Federal Highway Administration**

by the

**CENTER FOR TRANSPORTATION RESEARCH
Bureau of Engineering Research
THE UNIVERSITY OF TEXAS AT AUSTIN**

February 1994

IMPLEMENTATION STATEMENT

As a result of this study, the Texas Department of Transportation (TxDOT) should specifically consider the following for implementation in pavement planning and design:

1. When a pavement has developed roughness as a result of swelling clay or differential soil movement, the effect of the increased dynamic impact loading can be minimized by the use of a thin overlay, i.e., 5 cm (2 inches) or less, to reduce the dynamic impact loading caused by the roughness. These overlays should be scheduled as soon as major roughness develops (indicated by the “bouncing” of trucks on the section) or when a rapid increase in the failure rate is noted.
2. The designer should recognize that, although a thin overlay decreases the rate of failure (by eliminating the increased stresses from the dynamic impact loadings), the pavement will continue to experience fatigue consumption at the original rate intended during the design process. Thus, any major rehabilitation or overlay scheduled for the future should not be postponed.
3. Because the rigid pavement data base can be valuable in design and research studies, it should be maintained and referred to as needed.

Prepared in cooperation with the Texas Department of Transportation and the U.S. Department of Transportation, Federal Highway Administration.

DISCLAIMERS

The contents of this report reflect the views of the authors, who are responsible for the facts and the accuracy of the data presented herein. The contents do not necessarily reflect the official views or policies of the Federal Highway Administration or the Texas Department of Transportation. This report does not constitute a standard, specification, or regulation.

NOT INTENDED FOR CONSTRUCTION,
BIDDING, OR PERMIT PURPOSES

B. F. McCullough, P.E. (Texas No. 19914)
Research Supervisor

TABLE OF CONTENTS

IMPLEMENTATION STATEMENT.....	iii
SUMMARY	vii
CHAPTER 1. INTRODUCTION	1
1.1 DESCRIPTION OF THE SPECIAL CASE STUDY SECTION	1
1.2 OBJECTIVES	1
1.3 METHODOLOGY AND SCOPE.....	1
1.4 HISTORICAL DATA	2
CHAPTER 2. OVERLAY EFFECT ON VISUAL CONDITION.....	3
2.1 INTRODUCTION.....	3
2.2 DATA COLLECTION.....	3
2.3 DATA ANALYSIS.....	3
2.4 DISCUSSION	8
CHAPTER 3. ROUGHNESS EVALUATION	9
3.1 INTRODUCTION.....	9
3.2 DATA ANALYSIS METHODOLOGY.....	9
3.3 RESULTS.....	12
3.4 DISCUSSION OF RESULTS	14
3.5 CONCLUSIONS AND RECOMMENDATIONS.....	15
CHAPTER 4. DEFLECTION ANALYSIS	17
4.1 DATA MEASUREMENTS	17
4.2 DELINEATION OF HOMOGENEOUS SECTIONS.....	19
4.3 LOAD TRANSFER	23
4.3.1 FWD Measurements.....	23
4.3.2 Load Transfer at Transverse Cracks in the Composite Pavement.....	24
4.3.3 Load Transfer Results.....	25
4.4. EVALUATION OF OVERLAYS.....	29
4.4.1 Comparison of Old and New ACP Overlays.....	29
4.4.2 Overlay Structural Contribution.....	31
4.4.3 Summary.....	32
4.5 BACK-CALCULATION PROCEDURES	32
4.5.1 Back-Calculation Programs.....	32
4.5.2 Results of Deflection Analysis	33

CHAPTER 5. DISCUSSION OF RESULTS.....	35
5.1 PAVEMENT STRUCTURE BEHAVIOR.....	35
5.1.1 Deflection Behavior.....	35
5.1.2 Material Properties.....	37
5.2 PAVEMENT STRUCTURE PERFORMANCE.....	40
5.2.1 CRCP-5 Predicted Performance.....	41
5.2.2 AASHTO Performance.....	43
5.3 PLANNING AND DESIGN IMPLICATIONS.....	44
 CHAPTER 6. CONCLUSIONS AND RECOMMENDATIONS	47
6.1 CONCLUSIONS.....	47
6.2 RECOMMENDATIONS.....	48
 REFERENCES	49
 APPENDIX A. SAS SPECTRAL ANALYSIS PROGRAM	51
APPENDIX B. DEFLECTION PLOTS ALONG MILEPOST	55
APPENDIX C. COMPARISON OF DEFLECTION.....	69
APPENDIX D. ANALYSIS OF BACK-CALCULATION PROCEDURES.....	77

SUMMARY

This report documents a case study of an overlaid PCC pavement on IH-30, Bowie County, Texas. The 16-km (10-mile) project, constructed in April 1972, was first rehabilitated with an ACP overlay in May of 1986. Condition surveys of this project have been taken continuously at varying intervals, from the point of construction to the present. In June 1993, the project was again scheduled to be rotomilled and overlaid with 5 cm (2 inches) of ACP overlay. This rehabilitation effort created a unique opportunity for studying overlay performance.

Condition survey, deflection, and profile data were all collected on the project before rotomilling (on the old overlay), after overlay (on the exposed PCC), and after the new overlay had been placed. Three analyses were performed: First, the failure history of the pavement was evaluated; second, a spectral analysis of the pavement profile was performed to determine the roughness reduction benefit of the overlay; and, finally, back-calculations of the concrete, subbase, and subgrade moduli were obtained to determine the development of fatigue in the pavement and the extent to which it was mitigated by the ACP overlay.

Taken together, this study shows that, while a thin overlay restores ride quality, reduces the rate of failure development, and minimizes dynamic loading, the overlay does little to reinforce or reverse the development of fatigue in the underlying layers.

CHAPTER 1. INTRODUCTION

This report presents a case study of overlay performance. Although the primary objective of Project 1342 is to maintain and update the Center for Transportation Research's Rigid Pavement Database, a secondary objective is to perform special case studies from time to time as requested by the Texas Department of Transportation (TxDOT). This special study, devised in cooperation with the Pavement Section of the Design Division, took advantage of a unique opportunity to study overlay effectiveness.

1.1 DESCRIPTION OF THE SPECIAL STUDY SECTION

The study section consisted of an 20.32-cm (8-inch) continuously reinforced concrete pavement (CRCP) located on IH-30 in Bowie County, District 19, with the segment running from Milepost 188 to Milepost 198. In the Center for Transportation Research (CTR) Rigid Pavement Database, it is identified as CFTR 19019, and in TxDOT control-section-job format it is 610-5-9. This 16-km (10-mile) pavement section was constructed in April 1972 using siliceous river gravel (SRG), coarse aggregate, and a cement-treated subbase. The subgrade consists of a swelling clay soil; the average yearly rainfall in the area is moderate, roughly 73.66 cm/yr (29 in/yr).

The project was first rehabilitated with an ACP overlay in May of 1986. The original ACP overlay was constructed to reduce the long wavelength roughness in the CRCP surface caused by swelling clay movement. The roughness resulted in significant dynamic impact loadings of heavy trucks moving at high speeds, which in turn increased the rate of punchouts and failures. Thus, with a smoother pavement, the stresses in the PCC layer were reduced back to conventional dynamic loadings as expected in design. Average daily traffic (ADT) at the time was approximately 13,600 vehicles, with an estimated 3.5 percent annual growth rate.

Because of the deteriorated state of the ACP, this project was rotomilled in June 1993 to remove the existing overlay. A new 5.08-cm (2-inch) ACP overlay was then placed onto the underlying PCC structure. Given that the rotomill grinds up and removes all of the old asphalt overlay (and some of the PCC beneath), we saw a unique opportunity to examine the CRC pavement condition before milling, after milling, and after the new overlay was in place.

1.2 OBJECTIVES

The objective of this study is to use the TxDOT Rigid Pavement Data Base developed as a part of Project 1342 and prior projects to evaluate the performance of the pavement and the rehabilitation strategies over the history of the facility (approximately 20 years).

1.3 METHODOLOGY AND SCOPE

Since the objective of the study is to determine overlay effect on pavement performance, three measures of pavement performance were selected. First, a condition survey would be performed, wherein raters would visually inspect the pavement section for such defects as punchouts, patches, and cracking. Next, the surface profile would be taken to determine

roughness. Finally, a series of Falling Weight Deflectometer drops would be performed to collect deflection basins that could be used to estimate subgrade support, load transfer, and, in general, the structural integrity of the pavement. The conclusions and recommendations are presented in Chapter 5.

All measurements were taken at three points: (1) on the old overlay surface, before milling, (2) directly on the underlying PCC surface, after milling, and (3) on the new overlay surface after placement. In this way, determinations could be made as to the effectiveness of the first ACP overlay in protecting the original PCC pavement. In addition, the amount of distress present in the PCC layer could be determined — including whether such distresses had reflected up through the ACP overlay. First, the distress-vs.-age curve experienced by the PCC pavement prior to overlay was determined. Extrapolating this curve seven years (as if the PCC had not been overlaid) and then comparing the predicted distress with the measured distress of the overlaid PCC gives the protection provided by the overlay. These results are discussed in Chapter 2. A detailed evaluation of the roughness measurements is included in Chapter 3, where a detailed spectral analysis of the profilometer data is documented. Chapter 4 documents the analysis of the Falling Weight Deflectometer (FWD) measurements and compares the different sets of readings obtained at the site at different stages of the pavement rehabilitation. Chapter 5 combines and integrates the results from the previous three chapters into pertinent observations for planning, design, and construction.

1.4 HISTORICAL DATA

We used the CTR Rigid Pavement Database (Ref 1) to determine the distress history of the PCC prior to overlay. This database is a comprehensive statewide collection of pavement performance data pertaining to selected PCC pavements collected since 1974. Visual condition surveys were performed on the study section in 1974, 1978, 1980, 1982, 1984, and 1987, giving a good historical distress curve with points at ages 2, 6, 8, 10, 12, and 15 years. Although a crack spacing survey was performed in 1987, no cracks were recorded, as the section had recently been overlaid in the spring 1986. A diagnostic survey (deflection testing) was performed in 1988, also after the first overlay. Curves were fit through these distress-vs.-age points to extrapolate how the distress would have developed had the section not been overlaid. This analysis is presented in Chapter 2.

CHAPTER 2. OVERLAY EFFECT ON VISUAL CONDITION

2.1 INTRODUCTION

The objective of the analysis documented in this chapter is to examine overlay effectiveness on slowing distress propagation in the underlying CRC pavements. This chapter will focus on visual condition, including punchouts, ACP patches, and PCC patches. Taken together, these three distresses may be used to define the present condition or failure — and hence the overall deterioration — of a given pavement, as expressed in failures per mile.

The 16-km (10-mile) special study section was scheduled to be overlaid in June 1993. The existing AC overlay was to be milled off before placing the new overlay. The original plan was to collect visual condition data at three points: (1) before the old overlay was removed, (2) after milling, from the exposed underlying PCC surface, and (3) after the new overlay had been placed.

This study presented a unique opportunity to test the effect of overlays on distress propagation on the underlying rigid pavement. Specifically, data from these three visual evaluations could be combined with the section's historical condition data that have been stored in the CTR database since the section's construction in March 1972.

2.2 DATA COLLECTION

Data collection teams accompanied the contractor's construction crew during implementation of the project. Distress data were collected on the AC overlay before it was removed, and on the CRCP after the AC overlay had been removed. This information provided a basis for evaluating the development of after-overlay distresses in CRCP. The information collected was used to test the theory that CRC pavement deteriorates at a slower rate after an ACP overlay is placed.

Figure 2.1 shows the availability of distress data for the 16-km (10-mile) section, both in terms of historical data from the CTR database and in what could be collected during the milling and paving operation. The original CRC pavement was first overlaid in April 1986, when it was 14 years old.

2.3 DATA ANALYSIS

The first data analysis task undertaken was to check whether the overlay reduced the rate at which distresses occur in the CRCP. In order to maintain consistency between the historical data taken over the years and the field data collected during this study, the number of failures was used as the distress indicator. Failures are defined as the sum of total numbers of AC and PCC patches and severe punchouts (parts of the pavement completely delineated by cracks). We emphasize that the term *failures* used in this report refers to the condition at a specific location on the pavement, and not to the functional condition of a section of road. Previous studies have

used these data to establish a functional rating. Figure 2.2 shows the development of failures with age for the 16-km (10-mile) section.

Year	Distress Type					
	Spalling	Pumping	Punchout	Patches	Cracking	Failures
1993**	Diagonal lines	Diagonal lines	Dark grey	Dark grey	Dark grey	Diagonal lines
1993*	Diagonal lines	Diagonal lines	Dark grey	Dark grey	Diagonal lines	Dark grey
1984	Dark grey	Dark grey	Dark grey	Dark grey	Diagonal lines	Diagonal lines
1982	Dark grey	Dark grey	Dark grey	Dark grey	Diagonal lines	Diagonal lines
1980	Dark grey	Dark grey	Dark grey	Dark grey	Diagonal lines	Diagonal lines
1978	Dark grey	Dark grey	Dark grey	Dark grey	Dark grey	Diagonal lines
1974	Dark grey	Dark grey	Dark grey	Dark grey	Diagonal lines	Diagonal lines

** After Milling
 * Before Milling
 Pavement overlaid April 1986



 Data available
 Data not available

Figure 2.1. Data availability by year

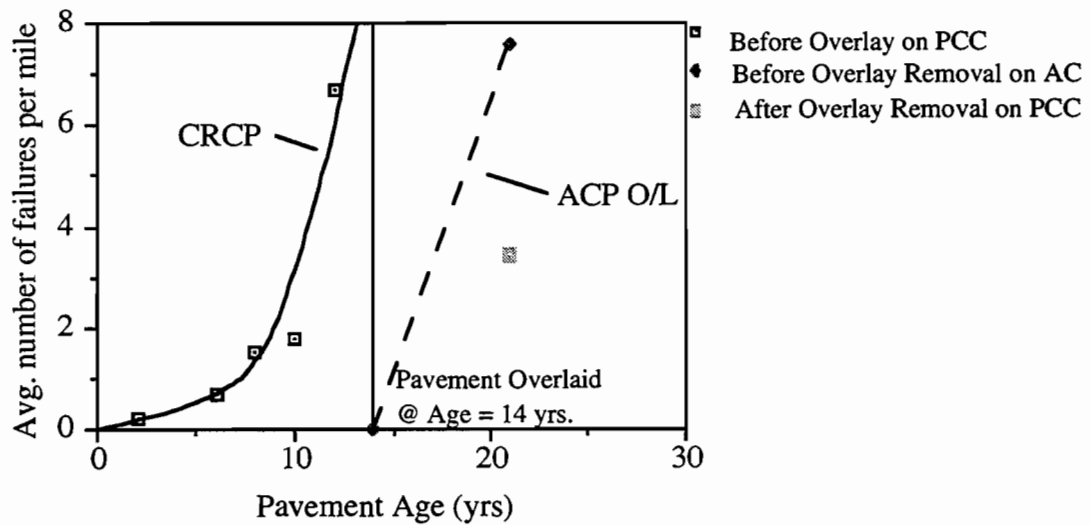


Figure 2.2. Average number of failures per mile vs. pavement age (1 mile=1.61 km)

In Figure 2.2, the solid curve shows the relationship between the average number of failures per mile for the entire project versus the age of the pavement before overlay. It is

assumed that when the CRC pavement was built, it showed zero failures. The original pavement was overlaid when it was 14 years old. The before-overlay curve for the CRCP section was extrapolated to determine how the CRC pavement would have behaved with no overlay.

The dashed line shows the propagation of failures after overlay on the AC overlay surface. The only condition survey on the AC overlay was made in June 1993, and it is assumed that the AC overlay exhibited zero failures when it was laid. Because there are only two data points to work with, a straight line is shown.

There is only one point available in the plot that shows the failures on the original PCC pavement when the AC overlay was removed. This point seems to be an anomaly, since it appears to show that the PCC pavement after the overlay removal has less distress than when the overlay was placed. This low failure count can be explained by a combination of two factors. First, it is common practice to repair all punchouts prior to overlay, as it was the case with this section, based on reports from the field; this resulted in larger patches covering more distress. Since the size of the patches was not taken into consideration, this could reduce the reported number of failures. Second, the milling process produced much debris, making it difficult to count failures and obtain reliable information. Crack spacing could not be measured at all.

Despite these difficulties, the extrapolated curve for failures on CRC pavement before overlay and failures on CRC pavement after the AC overlay was removed clearly indicates that the overlay did in fact reduce the rate at which distress developed in the underlying CRC pavement. Even if the survey team had undercounted the failures by a highly unlikely factor of 3, this would still be true. Currently, no data on the AC overlay thickness or the soil support could be obtained, so correlation of AC overlay effectiveness with AC overlay thickness or soil support could not be performed.

We next analyzed the distress for specific sections of the project. The sectioning of the project was based on the deflection analysis that will be discussed in Chapter 4. The results of the FWD analysis divided (in terms of the milepoints) the project into the sections shown in Table 1.1.

Table 1.1. Delineation of homogeneous sections using FWD data

Beginning Milepoint	Ending Milepoint
Start	192.1
192.1	192.8
192.8	194.7
194.7	End

Because condition survey data were collected for .32-km (0.2-mile) sections, the above sections were modified for this analysis, resulting in the analysis sections shown in Table 1.2.

Table 1.2. Modified delineation of homogeneous sections using FWD data

	Beginning Milepoint	Ending Milepoint
Section I	Start	192.2
Section II	192.2	193
Section III	193	194.6
Section IV	194.6	End

Figure 2.3 shows the propagation of failures with age for the 6.76-km (4.2-mile) section (Section I, Start – 192.2).

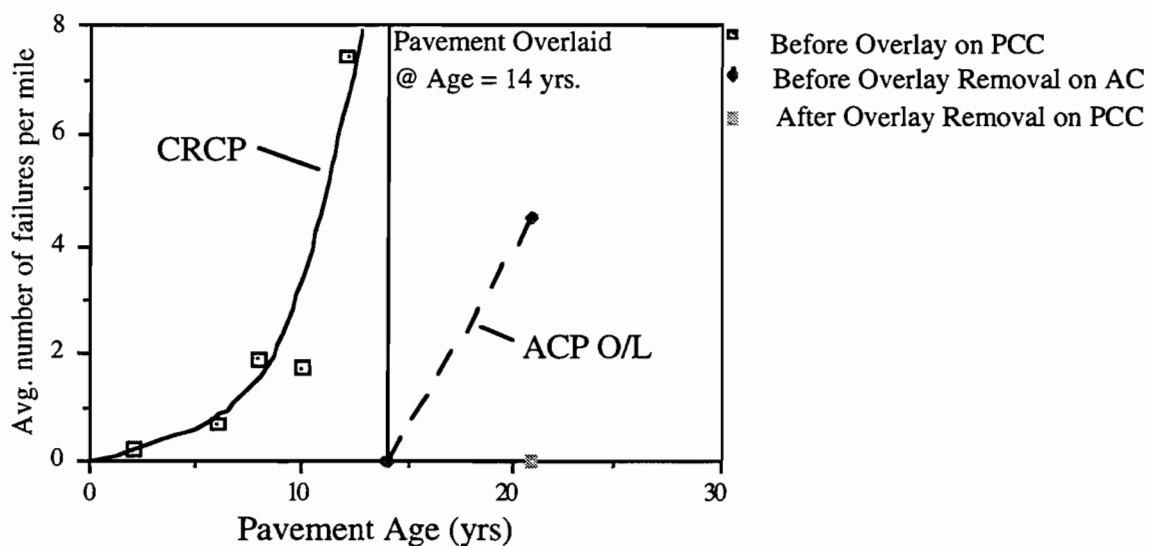


Figure 2.3. Average number of failures per mile vs. pavement age (Section I) (1 mile=1.61 km)

Figure 2.4 shows the propagation of failures with age for the 1.29-km (0.8-mile) section (Section II, 192.2 – 193.0).

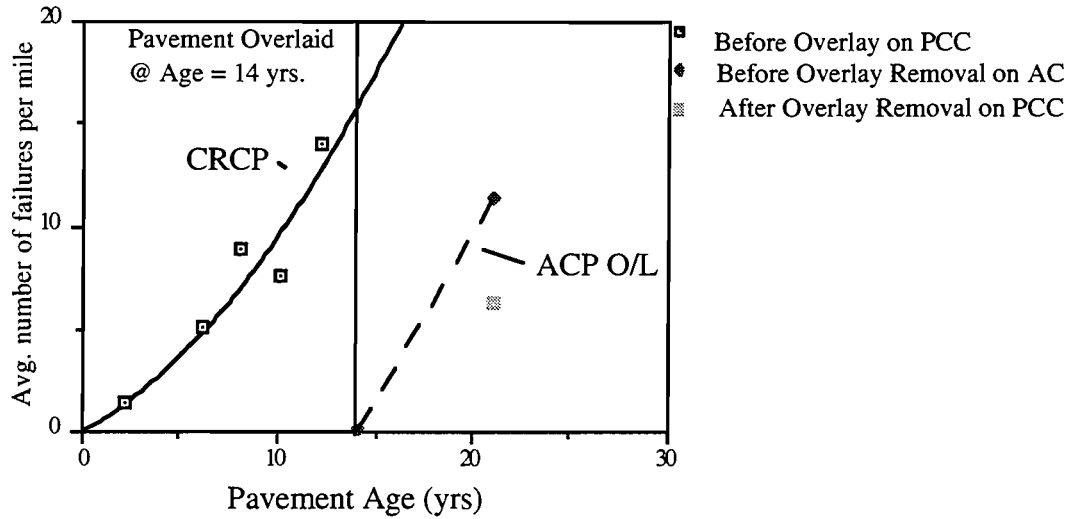


Figure 2.4. Average number of failures per mile vs. pavement age (Section II) (1 mile=1.61 km)

Figure 2.5 shows the propagation of failures with age for the 2.57-km (1.6-mile) section (Section III, 193.0 – 194.6).

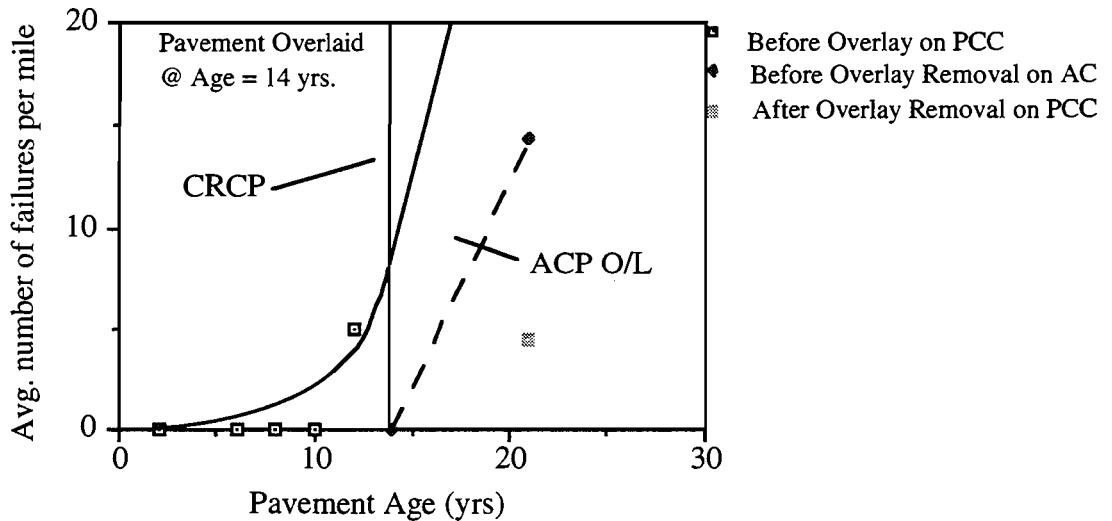


Figure 2.5. Average failures per mile vs. pavement age (Section III) (1 mile=1.61 km)

Figure 2.6 shows the propagation of failures with age for the 5.47-km (3.4-mile) section (Section IV, 194.6 – End).

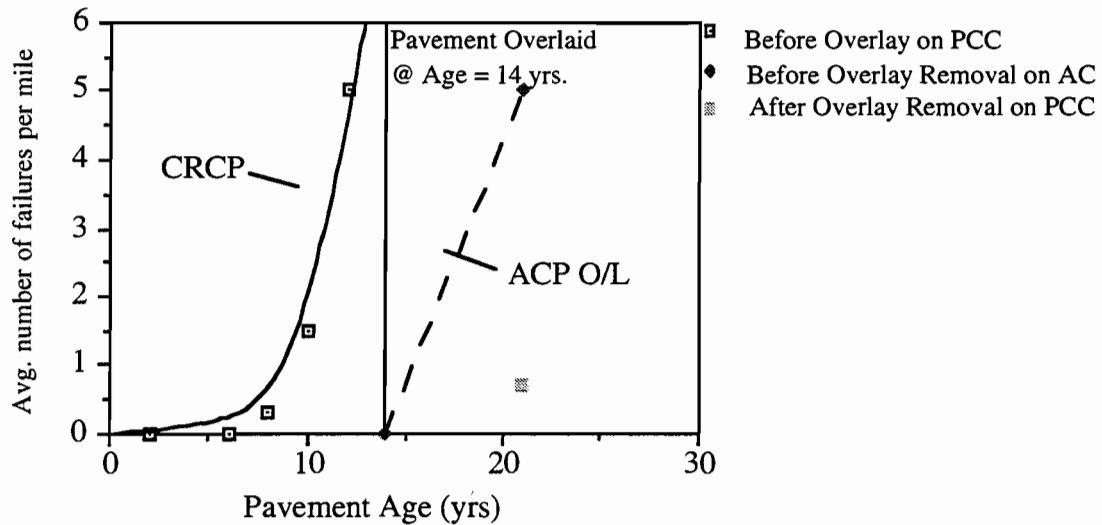


Figure 2.6. Average failures per mile vs. pavement age (Section IV) (1 mile=1.61 km)

2.4 DISCUSSION

Of the four detailed section analyses presented above, only one section — Section II, shown in Figure 2.4 — had already reached a failure criteria of 10 failures/1.61 km (1 mile) at the time of the original overlay. However, the other three sections, by extrapolation of the failure curve, could have reached the failure criteria within two years (Section I and Section III). Section IV had a much lower failure rate and could not be extrapolated safely.

What the data do show conclusively is that the rate of failure development in the PCC slab was greatly reduced by the application of the overlay. Three (and possibly all) of the pavement sections analyzed would have failed within two years or less if the overlay had not been applied. The pavement, when overlaid, provided six years of additional satisfactory performance.

CHAPTER 3. ROUGHNESS EVALUATION

3.1 INTRODUCTION

This chapter documents the roughness evaluation performed on the special study pavement section. The objective of the analysis documented in this chapter is to determine the amount of decrease in roughness supplied by the new overlay, both in terms of overall ride quality and in terms of reduction of vertical acceleration owing to changes in profile elevation at specific wavelengths along the roadway.

All of the analysis performed in this chapter is based on data collected by profilometer. Several runs were made in each direction on the pavement before removing the old overlay and after placement of the new overlay. We originally planned to take profile measurements on the old PCC surface after the old overlay had been milled off, but time constraints and limited equipment availability made this impossible: The original PCC surface was exposed only for a very short time, as the paving machine followed the milling machine closely.

Three methods of measuring roughness were used in the analysis. The first two were calculated directly by the profilometer software and express overall roughness in terms of two standard units — Serviceability Index (SI) and International Roughness Index (IRI). Both indices are intended to give a measure of the amount of roughness that would be perceived by a passenger in a car traveling over the roadway, and thus are expressed as a single number that represents a weighted average of amplitudes across specific wavelengths found in the vertical profile of the pavement.

The third method presented here is more general, and simply presents the amplitude of the peaks and dips at each component wavelength comprising the complex waveform that represents the road surface. Any complex periodic waveform can be shown to be formed by a sum of simple sine and cosine waves. Figure 3.1 illustrates this concept. Three sine waves (A, B, and C) with different amplitudes and wavelengths are added together algebraically to create the complex waveform labeled “Composite” in the figure. Thus, the apparently complex road profile can also be characterized as a sum of sines and cosines.

Algorithms have been developed to move in the other direction, that is, to decompose complex waveforms into their sine and cosine constituents, yielding the relative amplitude at each wavelength. Applying this to pavements, the relative smoothing effectiveness of an overlay can be determined at long wavelengths (hills, slopes, “built in roughness”), intermediate wavelengths (most likely to affect car and driver), and short wavelengths (microtexture).

The decomposition procedure used in this analysis was the Fast Fourier Transform (FFT). The SPECTRA procedure of the Statistical Analysis System (SAS) was the specific software package employed, as illustrated in Appendix A.

3.2 DATA ANALYSIS METHODOLOGY

Profile data were collected on the section before milling and after the new overlay had been placed, though not on the exposed CRCP surface prior to overlay as discussed previously. (Again,

we were unable to collect the bare CRCP data because of the short time span between milling and paving operations.) Profile data were furnished by TxDOT to CTR in the form of seven IBM PC diskettes. Most of the diskettes contained data from other CTR test sections in District 19, not from the milled section. The CFTR number for this special study section is 19019.

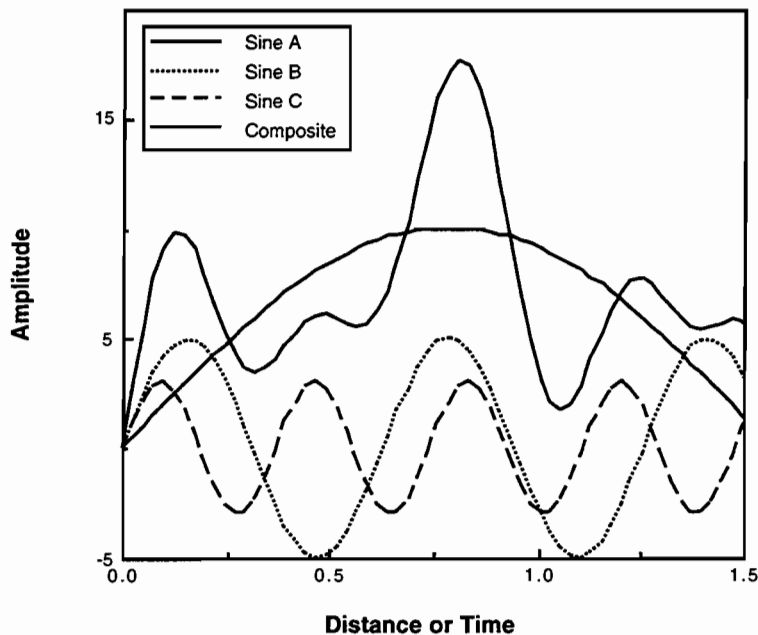


Figure 3.1. A complex waveform created from simple sine waves

The analysis was performed on a 4.67-km (2.9-mile) subsection of the outside westbound lane, using the right wheel path data (assumed to be the worst case in terms of roughness). Because of discrepancies in matching the files from the various profiling runs, only 4.67 km (2.9 miles) of the entire 8.05-km (5-mile) section could be analyzed. However, a comparison of the measured roughness with the printouts furnished by TxDOT indicate that the 4.67-km (2.9-mile) analysis section is fairly representative of the entire 16-km (10-mile) project, and more than adequate for determining the benefit of the overlay.



Figure 3.2. Position of old and new overlay profile data

Figure 3.2 shows the alignment of the profile data from the before and after overlay files. Because the old overlay data begin at milepost 198.0 and the new data begin at milepost 197.7, it was necessary to include a 0.48 km (0.3 mile) (3168 sample) offset in the analysis program. Since these beginning and ending mileposts were furnished by the operators and assumed to be approximate, precise alignment was visually checked by plotting the before-and-after profile together and noting the positions of large elevation changes in the road surface that would not have been affected by the overlay (Figure 3.3). By this criteria, alignment was judged to be adequate for performing the analysis.

TxDOT also provided a hard copy analysis of roughness on the test section before and after overlay, in terms of Serviceability Index (SI) and International Roughness Index (IRI). These indicators were calculated from the road profile every 0.16 km (0.1 miles), or 1056 sample points. By contrast, spectral analysis provides a power distribution for every 256 points or 39.01 m (128 feet). In order to facilitate comparison between the TxDOT roughness analysis and the spectral analysis, a data framing methodology was employed, as shown in Figure 3.4.

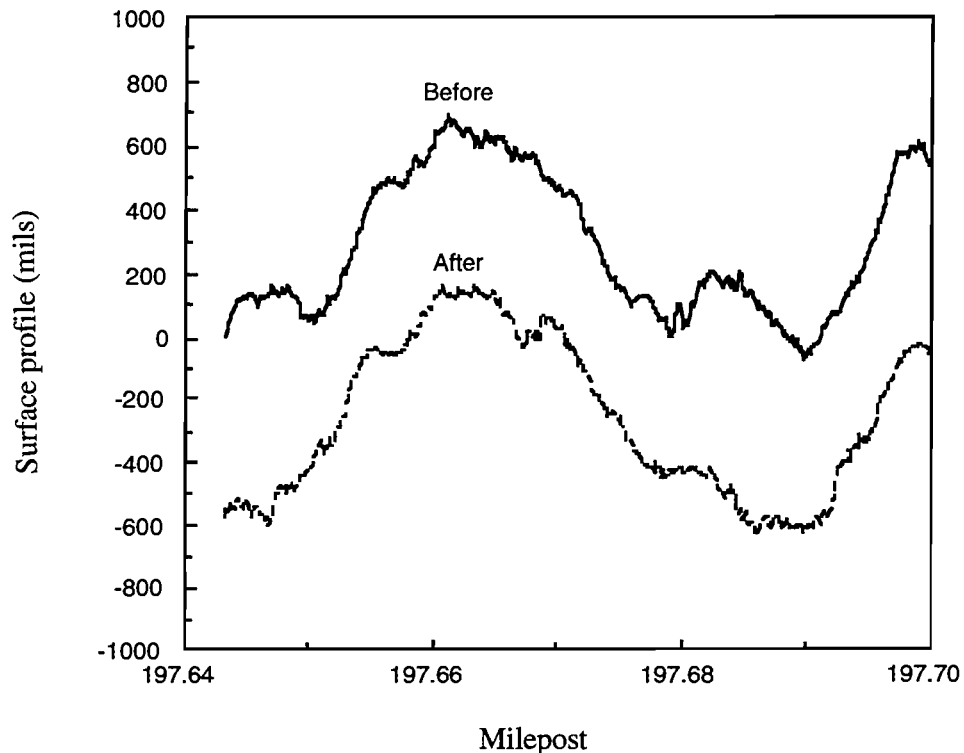


Figure 3.3. Alignment of old and new profile wave forms (1 mil=0.025 mm)

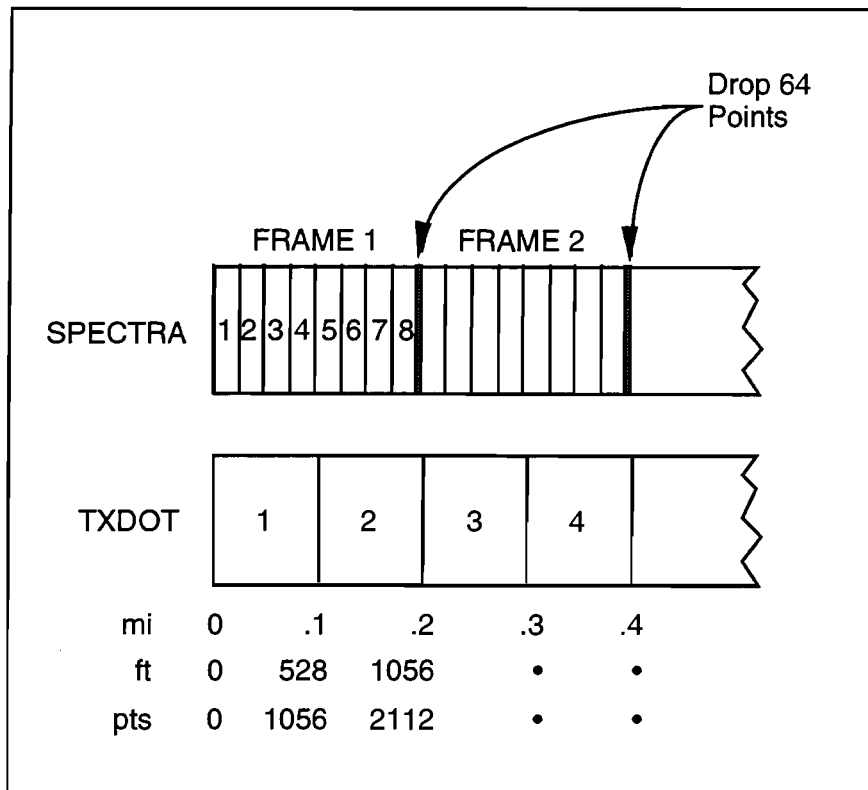


Figure 3.4. Framing scheme for comparing TxDOT and spectra sections

As illustrated in the figure, spectral analysis was performed for eight sequential 39-m (128-foot) pavement sections. Then the results were averaged to provide an overall power distribution for the entire 0.32-km (0.2-mile) frame. SI and IRI values for each 0.32-km (0.2-mile) frame were calculated by taking the mean of the 0.16 km (0.1 mile) numbers provided by TxDOT. Because there was no sufficiently small exact integral multiple of 39 m (128 feet) and 161 m (528 feet), this scheme required dropping 64 points (9.75 m/32 feet) from each frame, using a scheme similar to video “drop-frame synchronization.” Since only 64 points out of 2112 were dropped (3 percent), the analysis process did not affect the accuracy to any great extent.

3.3 RESULTS

Table 3.1 shows the results of the analysis for the first 5 frames (in 0.32 km/0.2 mile increments for a total of 1.6 km/1.0 mile) in detail and the overall results for the entire paving project. The spectral densities reported are given as amplitude in thousandths of an inch for frequency components of 39 m (128 feet), 19.5 m (64 feet), 9.7 m (32 feet), 4.87 m (16 feet), 2.4 m (8 feet), 1.2 m (4 feet), 0.6 m (2 feet), and 0.30 m (1 foot). An increase in amplitude at the lower wavelengths implies rougher pavement. By examining the table, we can observe not only the overall roughness reduction resulting from an overlay (in terms of SI and IRI), but also the roughness reduction at each individual wavelength.

Table 3.1. Roughness measures for milled section before and after overlay

Milepost	Ovly	SI	IRI	Spectral Density for Each Wavelength* (1000 mils ²)							
				128*	64	32	16	08	04	02	01
197.7 to	before	4.51	1.05	528	145	8.08	1.16	.446	.160	.067	.025
197.5	after	4.7	.92	472	122	8.72	1.10	.266	.078	.028	.021
197.5 to	before	4.18	1.31	544	138	8.65	3.30	.298	.047	.053	.008
197.3	after	4.86	.83	479	145	9.66	1.48	.698	.097	.034	.017
197.3 to	before	3.94	1.29	245	47.4	25.1	2.63	.516	.185	.035	.019
197.1	after	4.92	.83	272	49.3	6.76	.956	.421	.07	.014	.029
197.1 to	before	4.39	.96	114	24.7	8.12	2.76	.318	.089	.045	.006
196.9	after	4.38	1.19	114	13.4	4.67	.787	.199	.078	.02	.088
196.9 to	before	4.4	1.08	993	185	22.2	4.42	.653	.141	.082	.026
196.7	after	4.82	.87	1113	120	24.4	4.24	1.46	.374	.086	.028
Entire	before	3.97	1.25	426	102	14.1	2.77	.621	.182	.07	.034
Project	after	4.72	.93	417	62	7.82	1.73	.521	.12	.036	.021

*Wavelength in feet (1 foot =.3048 m)

The results of the analysis show that the roughness scores over the entire project length were improved from an already smooth 3.97 SI to an almost perfect 4.72 SI (1.25 to 0.93 IRI improvement). In the more detailed spectral analysis, some roughness improvement was observed at every wavelength from 39 m (128 feet) to 0.3048 m (1 foot), with the maximum improvement of about 51 percent in the 0.6096-m (2-foot) component.

Figure 3.5 shows the power spectrum distribution of the pavement profile before and after the new overlay. This is just a more detailed, graphic presentation of the information displayed in the last two rows of Table 3.1.

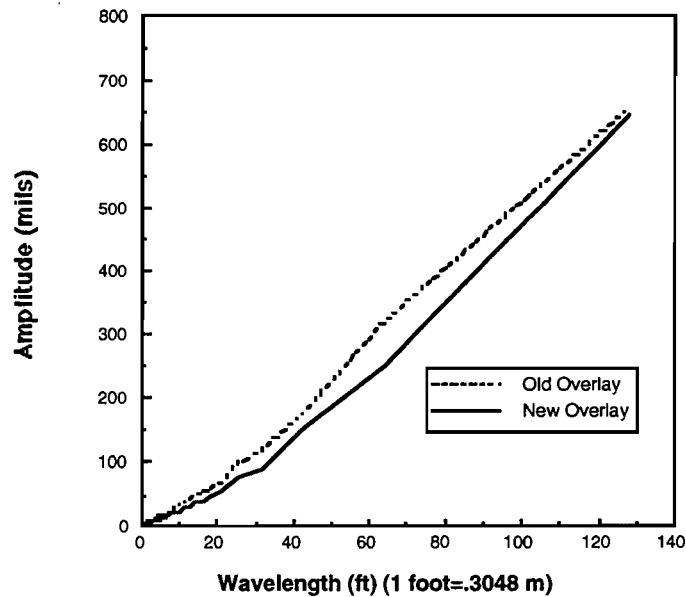


Figure 3.5. Roughness before and after new overlay for project by wavelength (1 mil=0.025 mm)

We can also view the profile measurement results as an absolute reduction in roughness value at each component wavelength. Figure 3.5 shows that the maximum absolute difference occurs at around 18.3 m (60 feet), dropping off in each direction as the component comes to represent such irreducible or unmeasurable quantities as terrain (in the long wavelengths) or microtexture (in the short wavelengths). Figure 3.6 presents the roughness reduction as a percentage for the wavelength. Thus, from this perspective the maximum improvement occurs in the shorter wavelengths. This is to be expected, since surface deterioration, differential rutting, shoving, etc., of the existing surface would occur at short wavelengths.

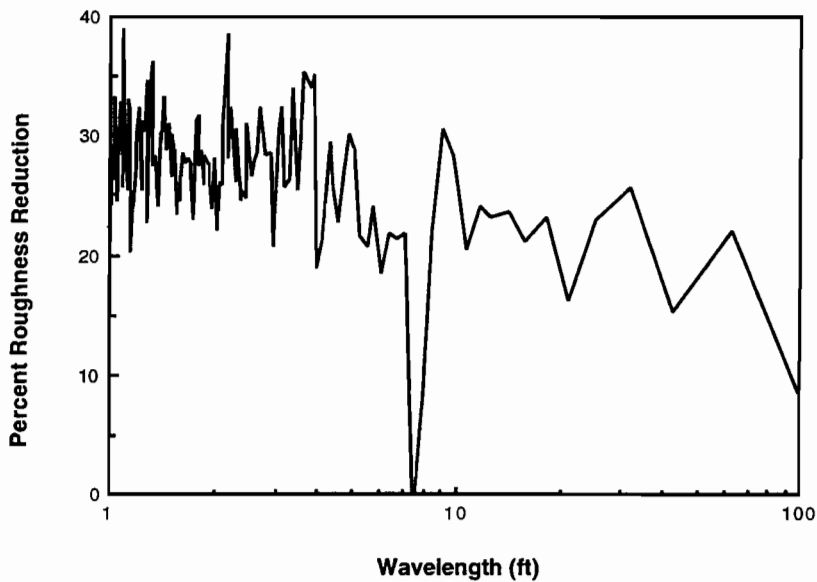


Figure 3.6. Roughness reduction for entire project by wavelength (1 foot=0.3048 m)

Finally, Figure 3.7 shows that, although roughness reduction in every wavelength was observed for the overall study section, that is not necessarily the case for individual analysis frames (0.39.01-m/128-feet analysis sections).

3.4 DISCUSSION OF RESULTS

The existing overlay on the test section was 7 years old and heavily patched, which accounts for the high amplitude in the 0.6096-m (2-foot) wavelength range. Nevertheless, it provided an excellent riding surface in terms of roughness ($SI = 3.97$) up until the day it was replaced.

It was shown in Chapter 2 that the old overlay substantially reduced the number of punchouts that would have been expected if the 21-year-old CRCP pavement had not been overlaid. Using a failure criteria of 6.2 failures/km (10 failures/mile), it can be estimated that the

original CRCP pavement would have reached failure at an age of 15 years, just one year after the initial overlay was placed. Since the section roughness was still low, it can be assumed that the decision to rehabilitate was based on failures rather than ride quality. Looked at from a perspective of ride quality, the overlay was not needed at this time; however, since the section was nearing failure, the addition of the 5.08 cm (2-inch) overlay essentially provided an additional 6 years of life with no deterioration for the existing pavement. The placement of the second overlay added additional ride quality (SI = 4.72) and will presumably extend the pavement life.

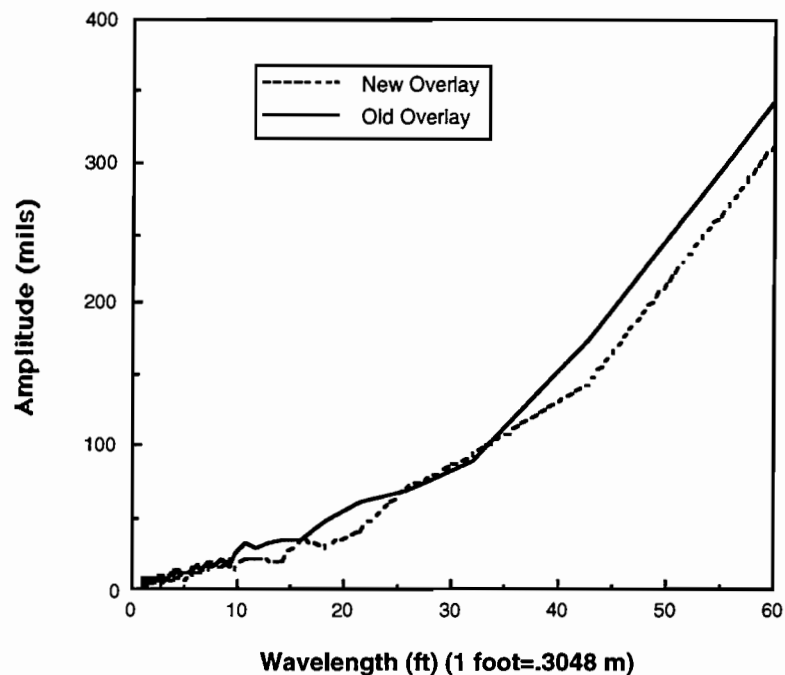


Figure 3.7. Roughness before and after overlay for analysis Frame 1 (1 mil=0.025 mm)

One last note: We mentioned that this section has a swelling clay subgrade. It is possible that roughness introduced by the clay interacted with dynamic loading to cause the rapid deterioration observed in this pavement. By adding the overlay and smoothing the pavement, these dynamic loadings should be eliminated.

3.5 CONCLUSIONS AND RECOMMENDATIONS

The preceding analysis shows the benefit of overlays in terms of roughness reduction. Although the initial state of the test pavement (old overlay over PCC) was still relatively smooth (SI = 3.97), the new overlay reduced the roughness even further to an almost perfect SI of 4.72. Most likely, the decision to rehabilitate this section was based on a condition indicator other than roughness (e.g., visual condition rating).

Using spectral analysis, we could see at exactly which component wavelengths additional smoothness was attained. It is unfortunate that profile data could not be obtained from the milled

section prior to overlay, since it would then have been possible to determine how much of the roughness was due to the underlying PCC layer. It is even more unfortunate that accurate data for overlay thickness has not been forthcoming, since it now seems possible to use the spectral analysis results to develop a model estimating the roughness reduction at each component wavelength as a function of overlay thickness. Such a model could assist pavement designers in specifying overlay thickness.

CHAPTER 4. DEFLECTION ANALYSIS

4.1 DATA MEASUREMENTS

Deflection measurements on IH-30 from Milepoint 188 to Milepoint 198 in the eastbound and westbound lanes near New Boston were performed using the Falling Weight Deflectometer (FWD). The FWD measurement locations were marked every 0.16 km (0.1 mile) with paint on the shoulder of the road in both directions over the entire 16 km (10 miles).

As discussed in previous chapters, the existing ACP overlay was milled off and a portion was recycled and mixed with the new hot mix asphalt pavement overlay. There were some scheduling constraints for the milling process, and the milling machine did not mill more than 3.2 km (2 miles) ahead of the paving machine. Since FWD readings on both the overlaid and non-overlaid sections were requested, it was necessary to get readings between the brooms that swept off excess debris from the milling process and the “tack coat” truck, and to get another set of readings before the old overlay was removed.

In the eastbound direction, a full-lane milling machine was used. Because the machine moved rapidly, it was not possible to get all of the required FWD readings. Obtaining FWD readings was more difficult in the westbound lane, since it was milled half the width of a lane at a time.

The FWD geophone sensors, set to CTR’s specifications, followed the layout depicted in Figure 4.1. Each of the three basic set-ups used for the readings is illustrated in Figure 4.2.

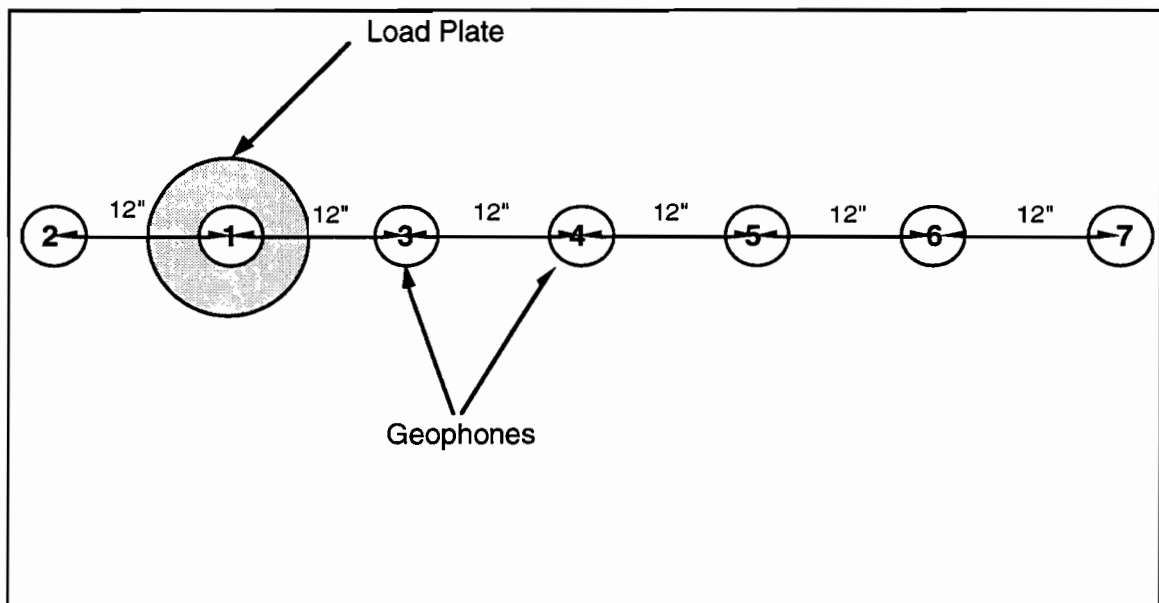


Figure 4.1. FWD 7 geophone configuration (1 inch=2.54 cm)

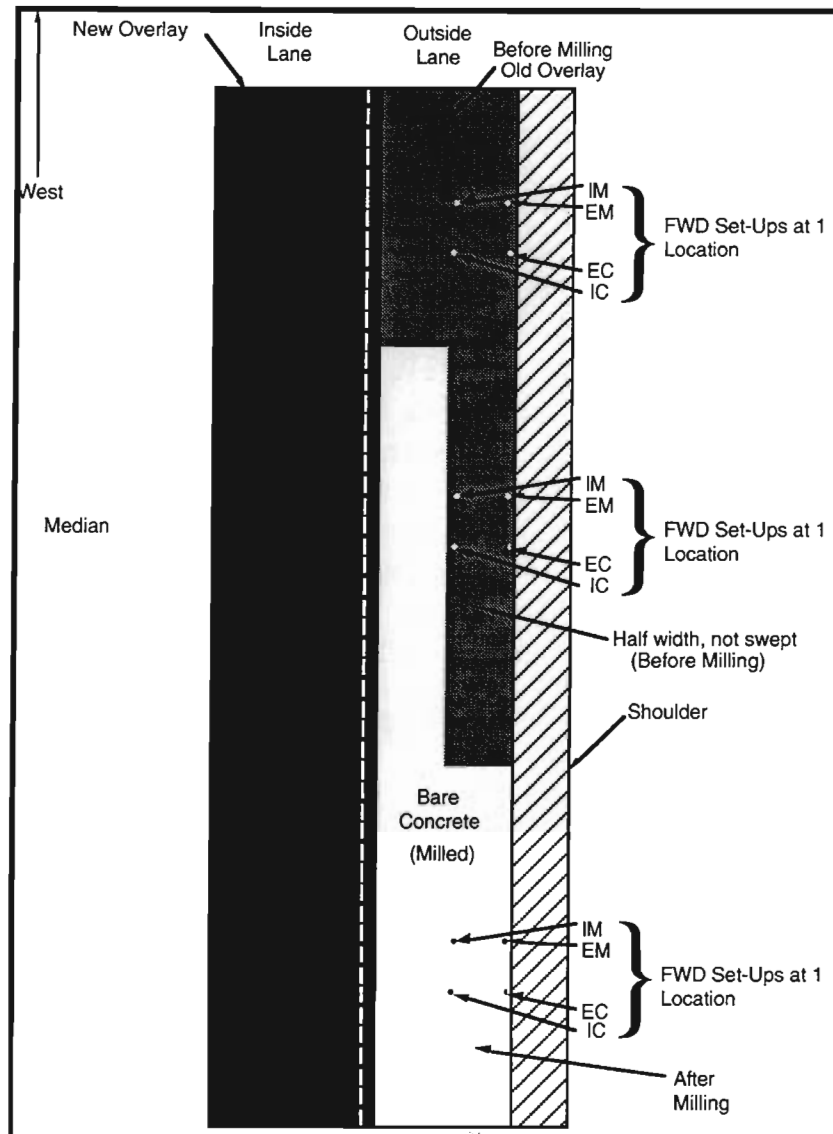


Figure 4.2. Basic FWD set-ups for various stages of before-and-after milling of ACP overlay

After the new overlay was placed, deflections were measured every one-tenth of a mile (.16 km) in both the eastbound and westbound directions before the lanes were open to traffic. The measurements after-overlay proceeded smoothly, since, unlike in the previous set of measurements, there was no interference from the milling process.

The deflections were measured four times at each station; EC (Edge Crack), EM (Edge Mid-span), IC (Interior Crack), and IM (Interior Mid-span) (see Fig. 4.2). While the first drop was at 2,722 kg (6,000 lb), the subsequent drops were at 4,025 kg (9,000 lb), 5,443 kg (12,000 lb), and 6,804 kg (15,000 lb). The three deflection results (before overlay, after milling, and after overlay) are discussed below.

4.2 DELINEATION OF HOMOGENEOUS SECTIONS

The delineation process consists of the determination of unit homogeneous sections based on the FWD deflections measured on the pavement structure. This was accomplished using two methods: one based on engineering judgment, and the other based on the cumulative difference method as recommended by the AASHTO Pavement Design Guide (Ref 2). In the AASHTO process, delineation based on two positions were compared — the edge midspan and the interior midspan conditions. Edge and interior crack conditions were excluded because (1) cracks usually appear irregularly in the pavement, and (2) cracked conditions are not suitable for back-calculation purposes.

The engineering judgment method uses the plots summarizing the deflections and mileposts. There is common agreement in the FWD-related literature that the first FWD sensor represents the material properties directly under the load, while the difference between sensor one and seven readings represents the surface layer properties. Based on this rationale, two kinds of charts were drawn. The first set of charts shows the measurement of four sensors along the stations. The second set of charts shows the differences between sensors one and seven. Based on these charts, section delineation was performed using engineering judgment. A statistical t-test is usually used to obtain the difference of mean values in neighboring sections. An example of these type of plots is presented in Figure 4.3. In this chart, “w1” represents the first sensor reading and “w3” represents sensor three, and so on. The data shown represent the interior midspan deflection data for the westbound lanes. Appendix B contains the complete set of charts.

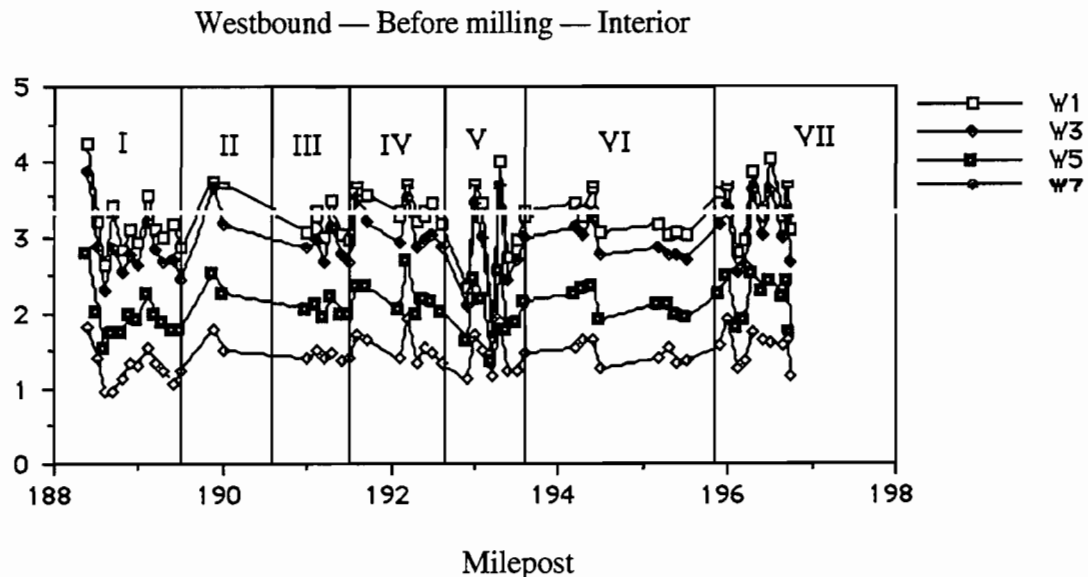


Figure 4.3. Example of chart used in the engineering judgment method on the interior midspan data for the westbound lanes before milling

The cumulative difference method, described in the AASHTO Guide, is a simple way of delineating project sections. First, the z-value is calculated and plotted along the station; next, the boundary for each section is determined based on the point of changing slope of the curve, as shown in Figure 4.4. (These data are the same as those used in Figure 4.3, i.e., interior midspan for westbound lanes.) Similar to the engineering judgment approach, z-value versus milepost chart gives a similar pattern for sensors one or seven.

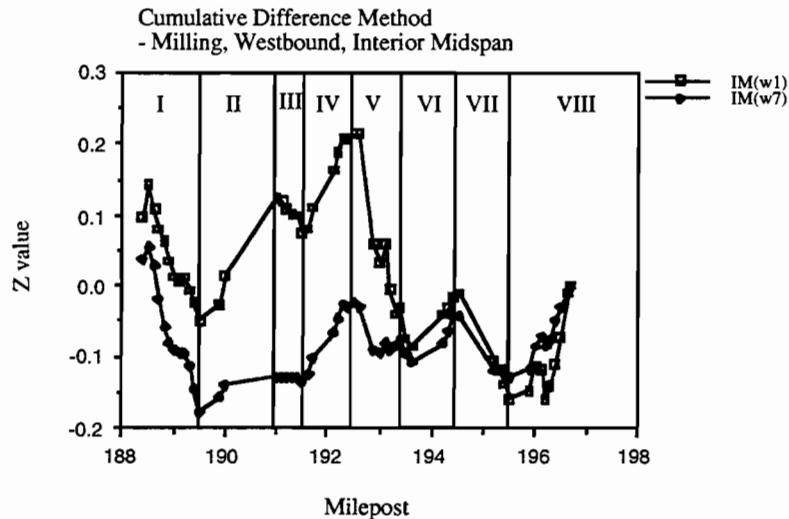


Figure 4.4. Example of chart used for the cumulative difference method on the interior midspan data for westbound lanes

The results of the delineation process using “before-overlay data” are shown in Tables 4.1 and 4.2. Both delineation methods give almost the same results. Little difference is observed between interior and edge condition for the engineering judgment method. The cumulative difference method gives almost identical results for the east or west section. This means delineation done by deflections can generate stable results no matter which delineation process is chosen.

Table 4.1. Delineation results for the two methods (before overlay — eastbound)

i) Engineering Judgment Method								
Interior	I	II	III	IV				
	- 192.1	- 192.8	-194.4	End				
Edge	I	II	III	IV	V	VI		
	- 191.6	- 192.4	-192.8	- 195.8	- 196.3	- End		
ii) Cumulative Difference Method								
Interior	I	II	III	IV				
	- 192.1	- 195.8	-196.2	End				
Edge	I	II	III	IV				
	- 192.4	-195.8	- 196.3	- End				

Table 4.2. Delineation results for the two methods (before overlay — westbound)

i) Engineering Judgment Method

	I	II	III	IV	V	VI	VII	
Interior	- 189.6	- 190.7	-191.6	- 192.6	- 193.5	- 195.0	End	
	I	II	III	IV	V	VI	VII	VIII
Edge	- 188.5	- 189.6	-190.7	- 192.4	- 193.8	- 194.7	- 195.6	- End

ii) Cumulative Difference Method

	I	II	III	IV	V	VI	VII	VIII
Interior	- 189.7	- 190.7	- 191.6	- 192.5	- 193.4	- 195.0	- 195.5	- End
	I	II	III	IV	V			
Edge	- 189.7	- 192.5	- 193.4	- 195.0	- 195.5			

The same analytical procedures were applied for the after-milling conditions. The deflection data obtained after milling were used to make a delineation, with the results compared with the before-milling results. This required special care, insofar as the data collected along the eastbound direction for the after-milling condition could have been disturbed by the milling operations (as discussed in a previous paragraph). Like those for the before-milling condition, the results for the after-milling condition between interior and edge were slightly different, as shown in Table 4.3. An explanation for these results might be the change in the pavement structural system caused by the milling of the old ACP overlay. The existing overlay had been placed to correct undulations in CRCP caused by swelling clay actions. Thus, the ACP overlay will vary in thickness along the roadway to minimize the long wave roughness, i.e., level up. This variation in thickness will have some effect on the load-deflection relationship along the pavement. In addition, after milling, only the rigid layer exists, causing the test results to present different deflection results between the edge and interior section.

Table 4.3. Delineation results from engineering judgment method (after milling — eastbound)

i) Engineering Judgment Method

	I	II	III	IV	V			
Interior	- 192.1	- 192.7	-193.8	- 194.8	- End			
	I	II	III	IV	V			
Edge	- 192.2	- 192.8	-193.3	- 195.8	- End			

ii) Cumulative Difference Method

	I	II	III	IV	V			
Interior	- 192.1	- 192.8	- 194.7	- 195.8	- End			
	I	II	III	IV	V			
Edge	- 192.1	- 192.8	- 194.1	- 195.8	- End			

Table 4.4. Delineation results from two methods (after milling — westbound)

i) Engineering Judgment Method

	I	II	III	IV	V	VI		
Interior	- 189.6	- 191.5	- 192.5	- 193.5	- 195.5	- End		
	I	II	III	IV	V	VI	VII	
Edge	-189.6	- 192.0	- 192.8	- 193.6	- 194.3	- 196.1	- End	

ii) Cumulative Difference Method

	I	II	III	IV	V	VI	VII	VIII
Interior	- 189.7	- 191.1	- 191.5	- 192.7	- 193.5	- 194.5	- 196.3	- End
	I	II	III	IV	V	VI		
Edge	-189.7	- 191.1	- 192.0	- 192.7	- 194.3	- End		

In order to determine the overlay effect, the following criteria were selected:

- 1) Combine before-overlay and after-milling results whenever possible.
- 2) Use after-milling condition if the combination is not possible.
- 3) Use interior midspan conditions for which back-calculations are possible.
- 4) Include, whenever possible, at least five deflection readings in each unit section.

Tables 4.5 and 4.6, based on the section delineation and the criteria established, summarize results for the eastbound and westbound directions, respectively.

Table 4.5. Delineation of test section – Eastbound

(1 mi. = 1.61 km)

Section	I	II	III	IV
From- To	Start-192.1	- 192.8	- 194.7	- End
Distance	4.1	0.7	1.9	3.3

Table 4.6. Delineation of test section – Westbound

Section	I	II	III	IV	V	
From- To	Start-189.7	-190.7	- 191.5	- 192.6	- 193.5	- End
Distance	1.7	1.0	0.8	0.9	0.9	4.5

In summary, the delineation results for the before- and after-milling conditions show a similar pattern, while the Engineering Judgment Method and Cumulative Difference Method

give almost the same results. However, the results from the interior and edge conditions are somehow different.

4.3 LOAD TRANSFER

The discussion of load transfer relative to this study first covers the technique for the FWD measurements. The concepts used for estimating load transfer are covered in the next section, followed by the specific results.

4.3.1 FWD Measurements

As discussed previously, deflections were measured at four positions in order to compare load transfer across cracks. For the before-overlay condition, the test section consisted of 5-cm (2-inch) ACP overlay over an 8-cm (3-inch) CRCP. Four readings were taken depending on the existing crack in the ACP surface, as shown in Figure 4.4.

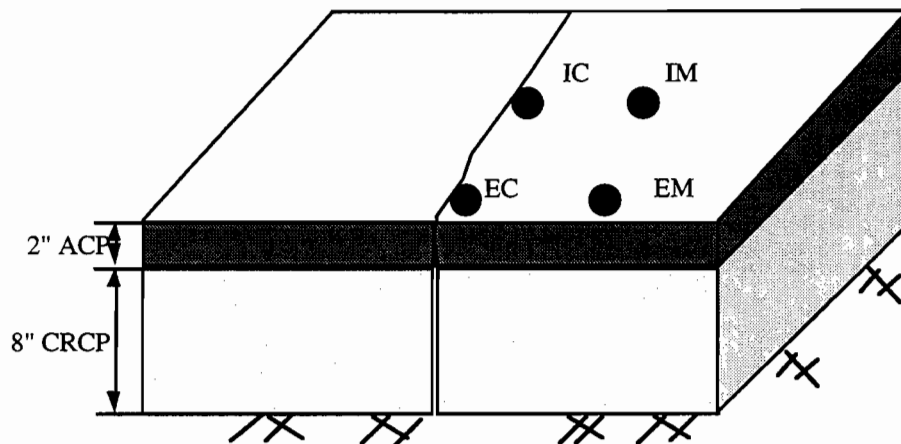


Figure 4.4. Configuration of deflection measurements for the before-overlay on existing condition (1 inch=2.54 cm)

After milling, deflections on the CRCP were taken at four points, as shown in Figure 4.5.

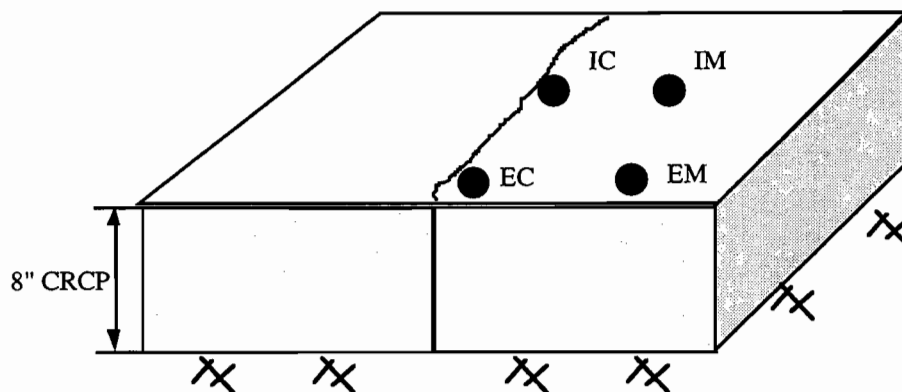


Figure 4.5. Configuration of deflection measurements (after milling) (1 inch=2.54 cm)

4.3.2 Load Transfer at Transverse Cracks in the Composite Pavement

Load transfer at cracks in the composite pavement (asphalt overlay on CRCP) is defined as the ability of the pavement structure to transfer loads across transverse cracks from one side of the crack to the other. The loss of load transfer in CRCP is known to be one of the main causes of punch-outs. In the case of the composite pavement, it is also important to verify the load transfer characteristics at the reflected cracks, since this is one of the main distresses observed in asphalt-overlaid PCC pavements. Consequently, load transfer evaluations provide valuable information about future performance of the composite pavement section.

It has been recognized in the literature that cracking can also be caused by either vertical differential deflection induced by the traffic loads, or horizontal movement resulting from temperature loading (Ref 3). An analysis of the load transfer testing results on the composite pavement may explain why cracking occurred.

The load transfer across joints in JRCP or CRCP has been researched by many investigators. For example, Chao Wei (Ref 4) investigated three procedures for evaluating the load transfer, looking in particular at one method called the Teller procedure. Teller and his colleague evaluated load transfer across a joint using a deflection ratio, as shown in Figure 4.6 (Ref 5). In this approach, if load transfer efficiency (LTE) is zero, then no load is being transferred from the load slab to the adjacent unloaded slab. Likewise, perfect load transfer is considered if the procedure calculates a value of 100 percent for the LTE. This result also means that there is no differential displacement across the crack or joint.

$$LTE = \frac{2 W_u}{W_u + W_l}$$

where :

- LTE = load transfer efficiency (percentage),
- W_u = deflection on an unloaded slab, and
- W_l = deflection on an adjacent loaded slab.

An alternative procedure was suggested by Ricci (Ref 6). Because deflection was measured by a downstream loading arrangement, as shown in Figure 4.7, load transfer efficiency for downstream loading could be calculated as follows:

$$LTE_d = \frac{W_2}{W_3} \times 100$$

where:

- LTed = Load transfer efficiency for downstream loading,
- w_2 = deflection measurement at sensor 2, and
- w_3 = deflection measurement at sensor 3.

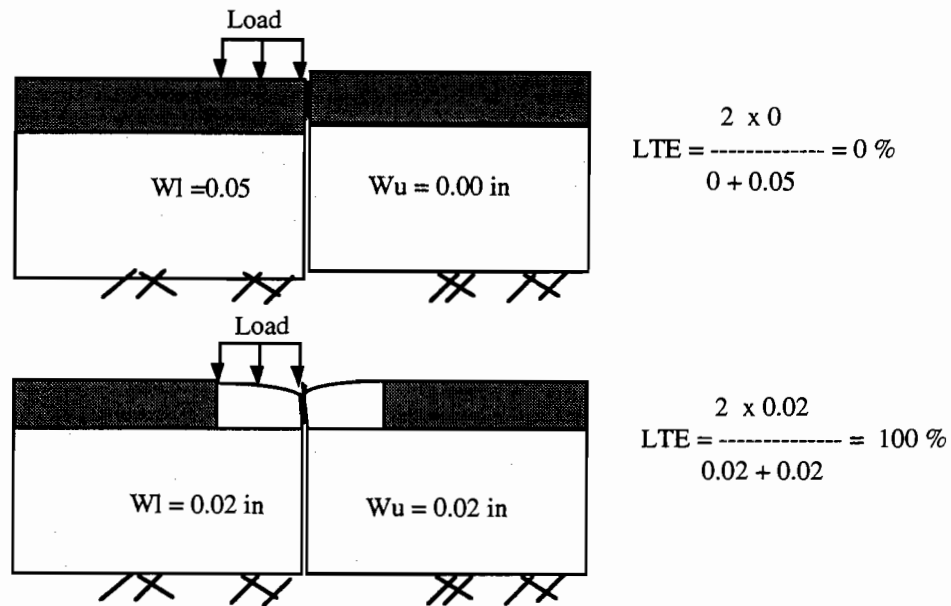


Figure 4.6. Illustration of Teller procedure for assessment of load transfer (1 inch=2.54 cm)

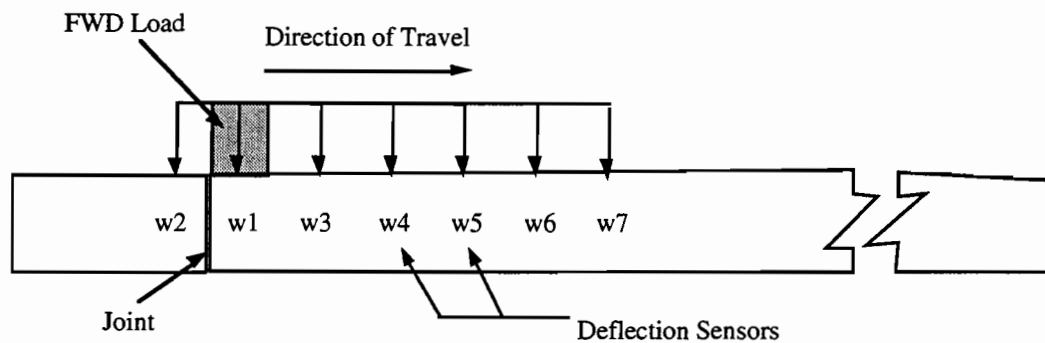


Figure 4.7. FWD deflection sensor locations — Downstream position

4.3.3 Load Transfer Results

Load transfer efficiency using the Ricci or Teller method does not show any significant differences, as may be observed in Tables 4.8 and 4.9. All the previously defined units sections after milling showed over 99 percent of load efficiency. No difference on load transfer was observed at cracks between interior and edge loading positions. This shows that load transfer for the CRCP has been well-preserved by the first overlay. Without the protection of the overlay, the load transfer may have possibly decreased, thus causing such distresses as punch-outs to develop. For the old overlay, which already showed significant reflection cracking, a slightly

higher value of load transfer efficiency was observed, as compared with the after-milling readings. This most likely means that there is zero or little vertical differential movements under traffic loadings. This also shows that the overlay improves the LTE slightly. Assuming a service life for the old asphalt overlay of around 7 years, load transfer for the composite pavement at crack does not seem to have decreased at all.

Table 4.8. Load transfer efficiency – Westbound – Interior crack condition (4,082 kg/9,000 lb)

Unit Section	Before Overlay		After Milling	
	Ricci	Teller	Ricci	Teller
1	101	100	101	100
2	100	100	103	101
3	101	101	100	100
4	100	100	100	100
5	100	100	102	101
6	101	101	101	100

Table 4.9. Load transfer efficiency – Westbound – Edge crack condition (4,082 kg/9,000 lb)

Unit Section	Before Overlay		After Milling	
	Ricci	Teller	Ricci	Teller
1	102	101	101	101
2	101	101	100	100
3	101	100	99	99
4	100	100	100	99
5	101	100	100	100
6	100	100	100	100

Different drop heights may give dissimilar results for the LTE calculations. To study drop-height effects on LTE measurements, we analyzed the westbound testing results. Only interior crack conditions were considered in this study because the previous paragraphs showed that no significant effects exist, owing to the point where deflection is measured. The results observed are similar to the ones reported before. LTE before overlay or after milling also gives over 99 percent for drop loads of 2,722 kg (6,000 lb) to 6,804 kg (15,000 lb), as may be observed in Tables 4.10 to 4.12.

Table 4.10. Westbound – Interior crack condition (2,722 kg/6,000 lb)

Unit Section	Before Overlay		After Milling	
	Ricci	Teller	Ricci	Teller
1	100	101	100	100
2	99	100	103	101
3	101	100	99	100
4	102	101	100	100
5	100	100	102	101
6	101	101	102	101

Table 4.11. Westbound – Interior crack condition (5,443 kg/12,000 lb)

Unit Section	Before Overlay		After Milling	
	Ricci	Teller	Ricci	Teller
1	101	100	101	100
2	99	100	102	101
3	101	101	100	100
4	100	100	100	100
5	100	100	101	100
6	101	100	101	101

Table 4.12. Westbound – Interior crack condition (6,804 kg/15,000 lb)

Unit Section	Before Overlay		After Milling	
	Ricci	Teller	Ricci	Teller
1	101	100	101	100
2	99	99	103	101
3	102	101	101	100
4	100	101	100	100
5	101	100	102	101
6	101	101	101	100

To illustrate the findings discussed above, we compared deflections of sensor two and three for the after-milling case. Sensor two measured deflections after the crack behind load, while seven gives the results without crack. Figures 4.8 and 4.9, which combine all data for drops of 2,722 kg (6,000 lb) to 6,804 kg (15,000 lb) for the eastbound and westbound roadways, respectively, show that the interior crack has almost perfect load transfer up to 6,804 kg (15,000 lb) used in this study. The before-milling condition for the old overlay also gives similar results.

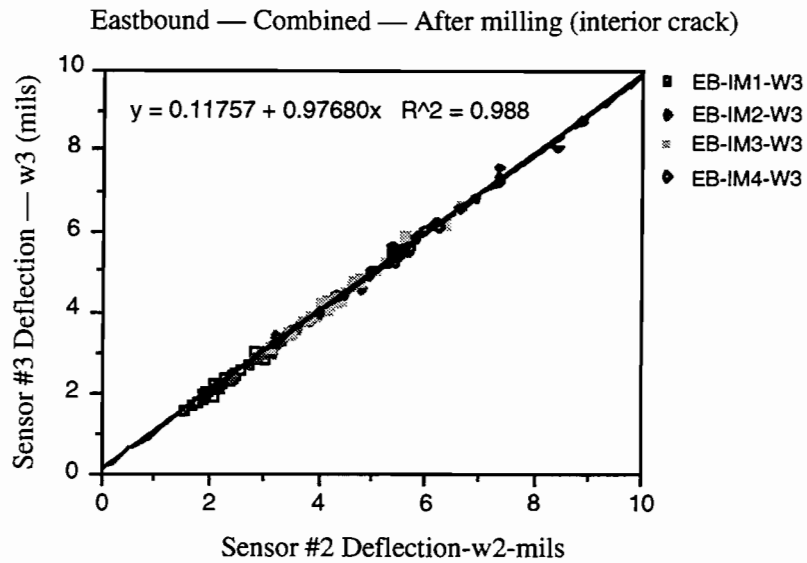


Figure 4.8. Comparison of Sensor 2 and 3 deflection in eastbound roadway for all load drops (6, 9, 12, and 15 kip loads) (1 mil = 0.025 mm)

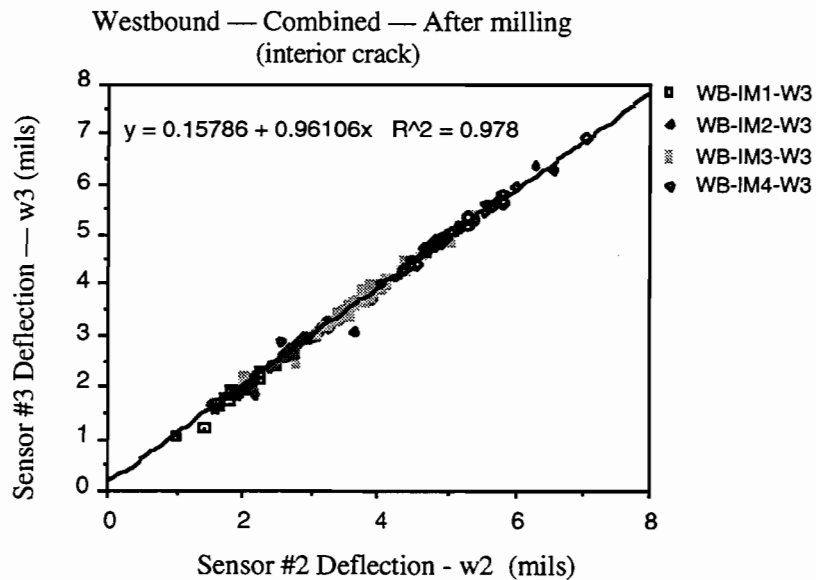


Figure 4.9. Comparison of Sensor 2 and 3 deflection in westbound roadway for all load drops (6, 9, 12, and 15 kip loads) (1 mil = 0.025 mm)

In summary, load transfer was maintained as a result of the ACP overlay, and does not depend on the position or impact loading. In the composite pavement, load transfer efficiency has been maintained during the service life, and the main reason for reflection cracking may not be related to the vertical movement of the slabs across cracks.

4.4 EVALUATION OF OVERLAYS

This section investigates the overlay's structural contribution, since deflections were taken on the surfaces of the initial overlay and the second overlay and also on the milled surface of the CRCP. The information also provided an excellent opportunity for evaluating the change in structural contribution of an aged overlay and a relatively new overlay. Thus, in the following sections, a comparison of the deflections for the old and new overlay will be made; this will be followed by an evaluation of the structural contribution of the overlay in reducing the total pavement structure deflection.

4.4.1 Comparison of Old and New ACP Overlays

Since approximately the same asphalt concrete pavement thicknesses were used, i.e., 5 cm (2 inches), and since the riding quality measurements in Chapter 3 demonstrate approximately the same long wavelength-amplitude relationship exists for the two overlays, it is reasonable to assume that the thicknesses for the overlays are approximately equal at various locations along the pavement. As part of the study, the deflections were taken at the edge and interior for both the cracks and midspan conditions in the eastbound and westbound roadways. Appendix C contains a graph for each of these combinations. In addition, separate graphs are provided for the deflections at Sensors 1 and 7, for a total of 16 plots. The deflection of Sensor 1 was selected because it is primarily an indicator of the pavement structure, and Sensor 7 was selected because it tends to reflect changes in the subgrade. A study of these graphs indicate that they could be combined for a given roadway in a similar manner for the load transfer study in the previous section.

A study of the various charts indicates that the deflections for the two overlay conditions are approximately equal, though there is a scattering of points; accordingly, the deflections for Sensor 1 and Sensor 7 were combined on the same graph, as shown in Figures 4.10 and 4.11, which are for the eastbound and westbound roadways, respectively. An overall look at the data shows a fairly equal distribution around the 45° line, with the slope of the regression lines approaching unity. Thus the impact of the overlays is approximately equal, as would be expected, since the thicknesses are expected to be the same. Although asphalt generally becomes stiffer with age (at the time the measurements were taken, the old overlay was 7 years old and the new overlay was less than 30 days old), it may be concluded that the increased asphalt concrete stiffness has minimal effect of the total pavement deflection.

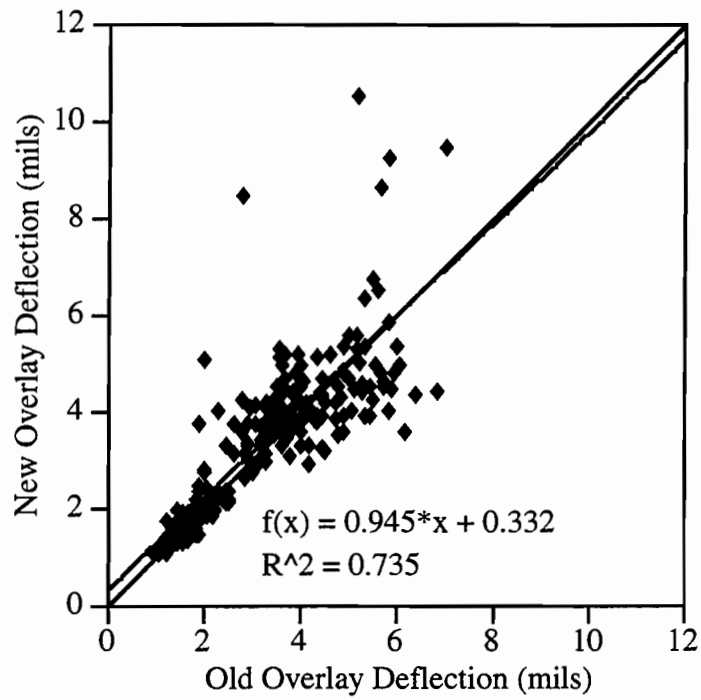


Figure 4.10. Comparison of deflections, old and new overlays (eastbound) (1 mil = 0.025 mm)

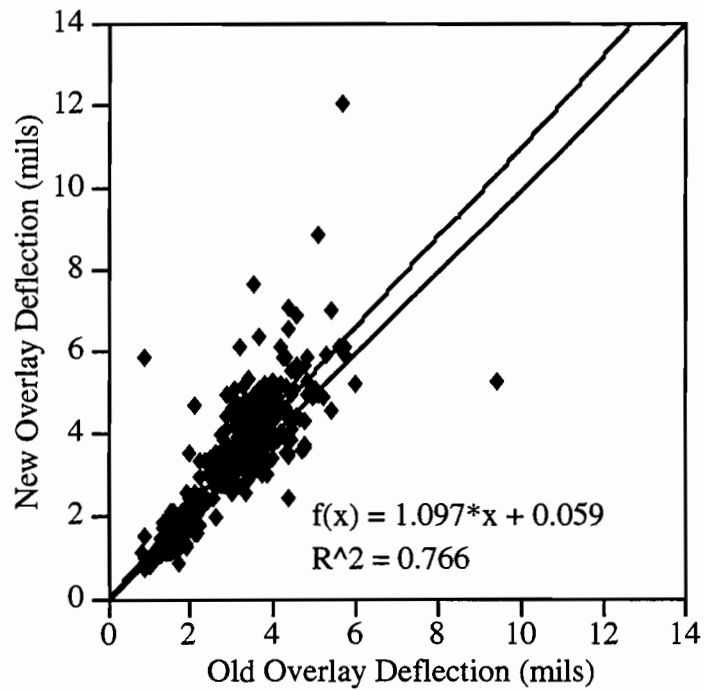


Figure 4.11. Comparison of deflections, old and new overlays (westbound) (1 mil = 0.025 mm)

4.4.2 Overlay Structural Contribution

The previous section established that the deflections for the old and new overlays are approximately equal, and thus both were making approximately equal structural contributions. Therefore, the next logical step is to use the “after” milling condition for establishing the net structural value of the overlay. Figures 4.12 and 4.13 show the net deflection reduction of the pavement structure as a result of the overlay placed in the eastbound and westbound roadways, respectively. The vertical axis presents the deflection on top of the asphalt overlay, whereas the horizontal axis presents the deflection on the milled surface. A 45° line of equality is shown on the plot to provide a net structural evaluation. The regression line and the slope indicate that the net effect of the overlay is actually an increase in deflection of 11 to 15 percent, which reflects the softer asphalt.

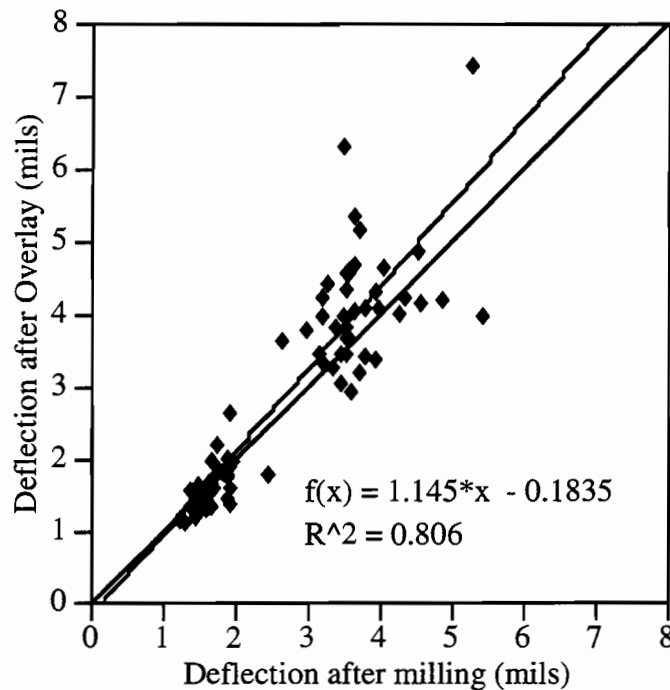


Figure 4.12. Comparison of deflections, new overlays vs. milled (eastbound) (1 mil = 0.025 mm)

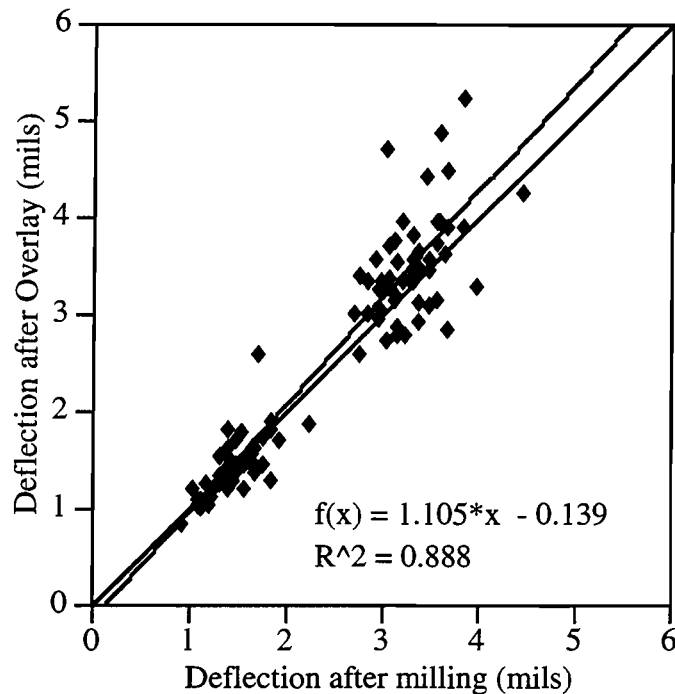


Figure 4.13. Comparison of deflections, new overlays vs. milled (westbound) (1 mil = 0.025 mm)

4.4.3 Summary

Considering both approaches comparing the deflections of the new and old overlay and the net effect of the structural overlay, it appears that the thin asphalt overlay does not contribute significantly to the structural performance of the pavement. Hence, the significant reduction in failures that was experienced after the application of the initial overlay indicates that it was not due to a reduction of the normal load stresses, but rather to the impact load stresses developed by the roughness resulting from swelling clays. Thus, in essence, the initial condition as intended when developed in the original CRCP design was restored (i.e., the number of load repetitions).

4.5 BACK-CALCULATION PROCEDURES

This section briefly reviews back-calculating procedures for estimating layer modulus values (see Appendix B for a more detailed review). The MODULUS program is used to estimate and review the layer properties along the roadway.

4.5.1 Back-Calculation Programs

Back-calculation is a method for estimating the elastic modulus values of existing layers using pavement deflections measured by various devices. Three steps are involved in this process: (1) measuring deflection, (2) performing back-calculation, and (3) verifying the results with core testing results. There are a number of methodologies for back-calculating the properties, as discussed in Appendix D. The overall conclusions from Appendix D are (1) that

all the methods have limitations relative to composite pavements, and (2) that new methodologies are required for composite pavement. As discussed below, we selected the MODULUS program for the analysis of the data.

4.5.2 Results of Deflection Analysis

MODULUS was selected to calculate layer modulus for the section under study. Figures 4.14 to 4.16 show the variation of modulus values for the eastbound roadway. E1 (PCC modulus) back-calculated from the deflections is approximately equal to the modulus of PCC constructed with SRG aggregate in the lab. These data show that the first overlay maintained in general the integrity of the underlying PCC pavement structure.

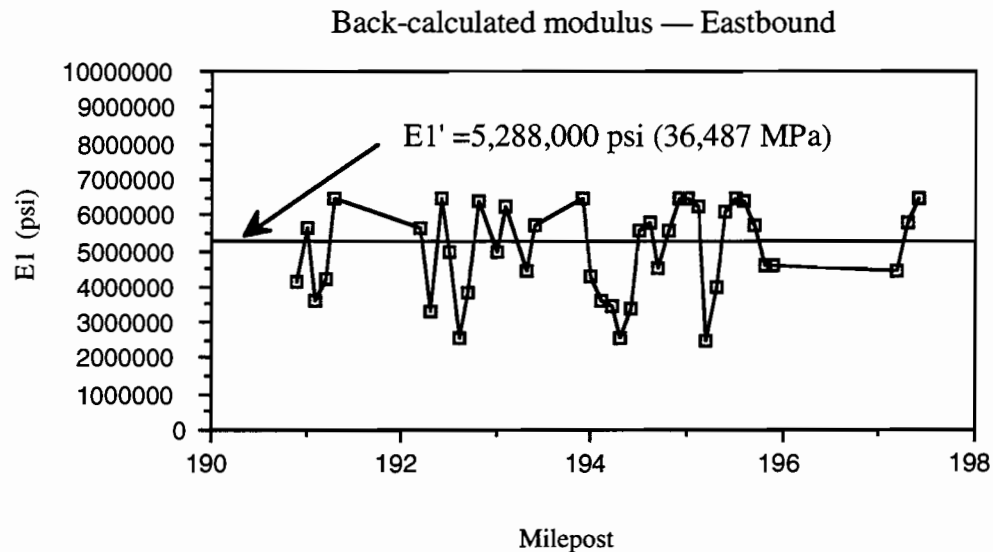


Figure 4.14. Back-calculated modulus ($E1$) variation along the eastbound roadway

The lower values of $E1$ at various locations — that is, less than 20,700 MPa (3,000,000 psi) — may indicate either inherent errors in the back-calculated method or the pending fatigue failure of the concrete. In general, when a material experiences fatigue failure, the stiffness decreases rapidly. Since there are no values above the E value for SRG concrete, then the latter possibility must be given serious consideration. If 27,600 to 31,100 MPa (4.0 to 4.5 million psi) is considered the lower limit of PCC with SRG coarse aggregates, then of the 40 measurements in Figure 4.14, 6 are below 4×10^6 (15 percent) and 11 are below 4.5×10^6 (28 percent). The same observations are also applicable to the cement stabilized layer ($E2$). The variation in the clay stiffness ($E3$) appears as a normal variation.

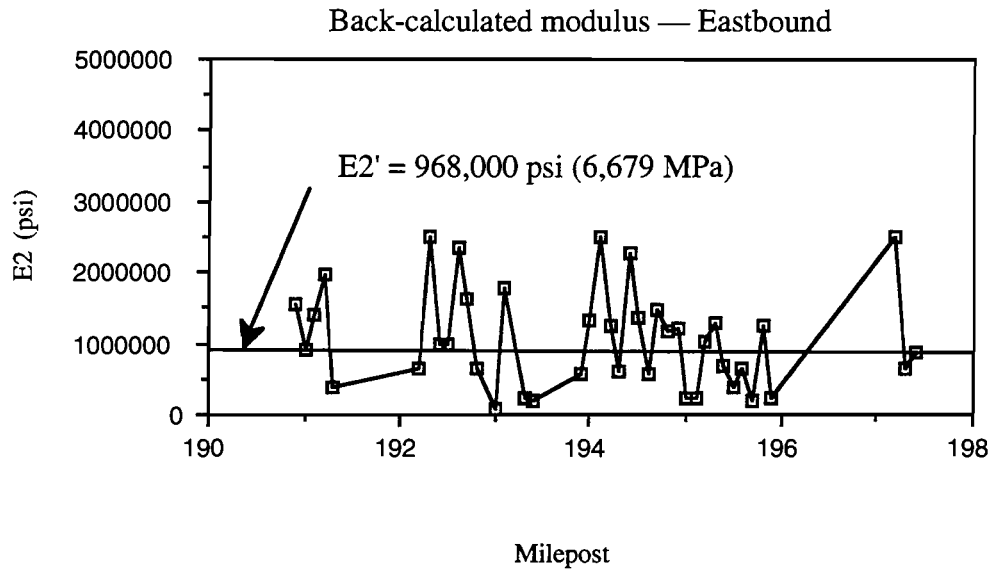


Figure 4.15. Back-calculated modulus ($E2$) variation along the eastbound roadway

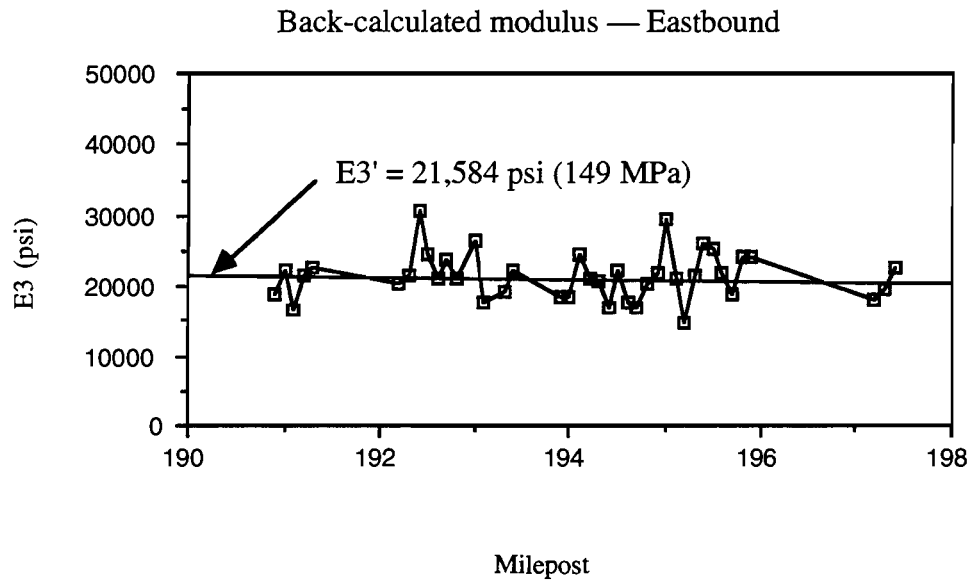


Figure 4.16. Back-calculated modulus ($E3$) variation along the eastbound roadway

CHAPTER 5. DISCUSSION OF RESULTS

In the previous chapters, we reported the behavior and performance of CRC pavements on IH-30 (Bowie County) over the entire history of the pavement (two complete performance periods and the start of a third). This chapter compares the various CTR prediction models developed for TxDOT — models useful not only in predicting behavior and performance, but also in comparing predicted performance with actual performance. Thus, in the following sections, pavement structure behavior is examined in terms of actual and measured deflection, and in terms of material properties.

Next, the pavement structural performance is examined, along with the actual short-term benefit of the overlay, the reasons for its placement, and the long-range performance. The last section then discusses the implications of the observed results on long-term planning, as well as the specific considerations that should be taken into account in the planning and design of CRC pavements.

5.1 PAVEMENT STRUCTURE BEHAVIOR

In Chapter 4, the pavement behavior characteristics were reported in terms of deflection and back-calculated material properties. Thus, this section first compares predicted deflections with the actual deflection measurements, and then discusses the implications of the properties' variability. All predicted deflections and stresses were made using the ELSYM5 program.

5.1.1 Deflection Behavior

Figures 4.22 and 4.23 demonstrate that the deflection measurements on top of the old and new overlays were, for all practical purposes, equal, even though there was a 7-year difference in ages of the ACP overlays. In both cases, a 5-cm (2-inch) overlay was used to eliminate the roughness caused by swelling clay. Thus, the question is: Can this be simulated with predicted values?

This issue is addressed in Figure 5.1, which shows plots of the surface deflection on top of the overlay as a function of the predicted deflection on top of the CRCP for several conditions of surface modulus of elasticity and overlay pavement thicknesses. Figure 5.1a shows the range in deflection as recorded by sensor W1 of the FWD, which is closest to the applied load, and thus more sensitive to stiffness in the surface layer. The slight increase in deflection for the after-overlay condition reflects the addition of the softer asphalt layer. Figure 5.1b shows almost no change in deflection as recorded by sensor W7, which is farthest from the applied load and a better indicator of the deeper structural stiffness of the pavement, subbase, and subgrade. Taken together, these predicted values show very little change in deflection owing to the 5.08-cm (2-inch) overlay; this is comparable to Figures 4.24 and 4.25 that reveal the addition of the asphalt concrete overlay had only a minor influence on the surface deflection — that is, the net effect of the ACP overlay on deflection is very small.

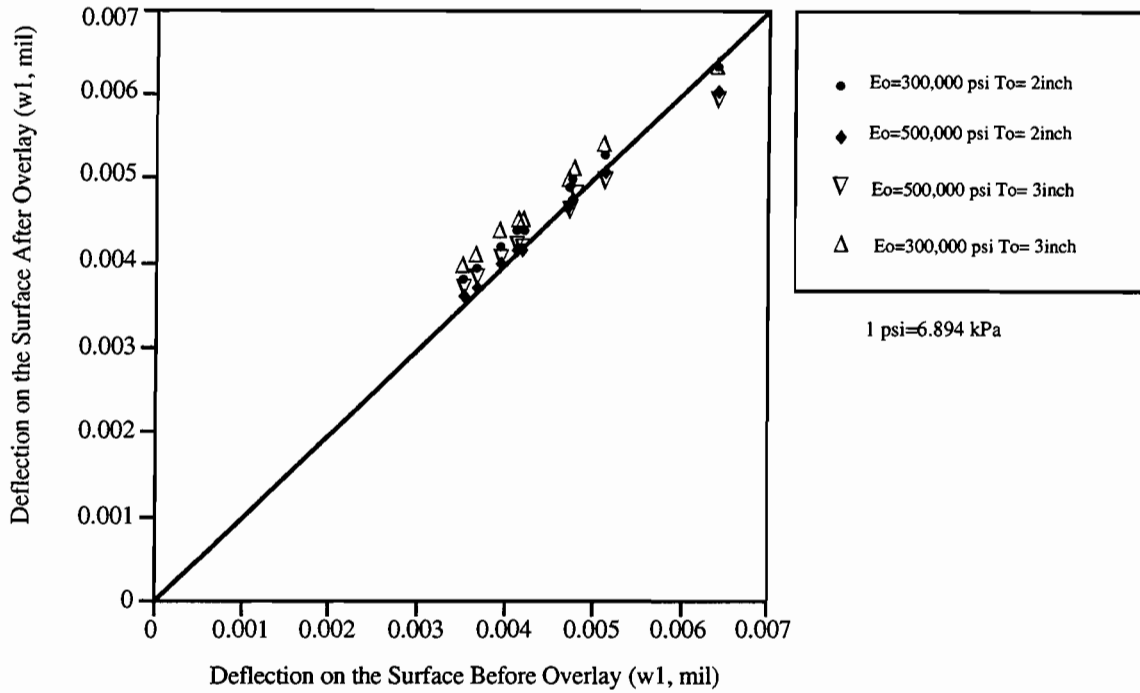


Figure 5.1a. Predicted deflection before and after overlay for several combinations of overlay thickness and modulus as measured directly under the load (1 inch=2.54 cm; 1 mil=0.025 mm)

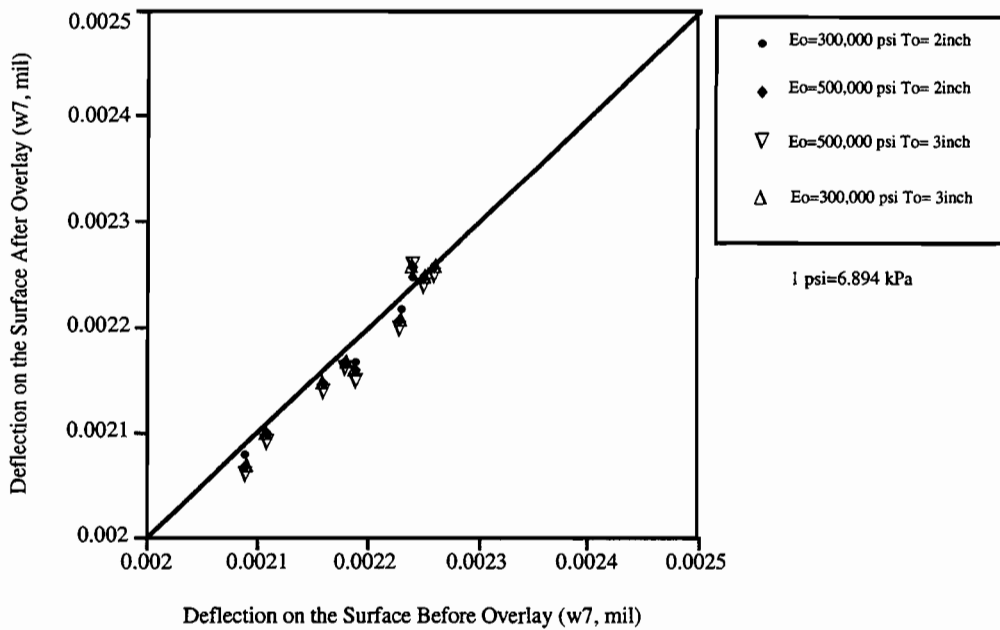


Figure 5.1b. Predicted deflection before and after overlay for combinations of overlay thickness and modulus as measured 5 ft. (1.5 m) from the applied load (1 inch=2.54 cm; 1 mil=0.025 mm)

Figure 5.2 shows a plot similar to that in Figure 5.1, only in this case the tensile stress at the bottom of the PCC is plotted (rather than a deflection). As was the case previously, the effect of the ACP overlay on stress is only minimal.

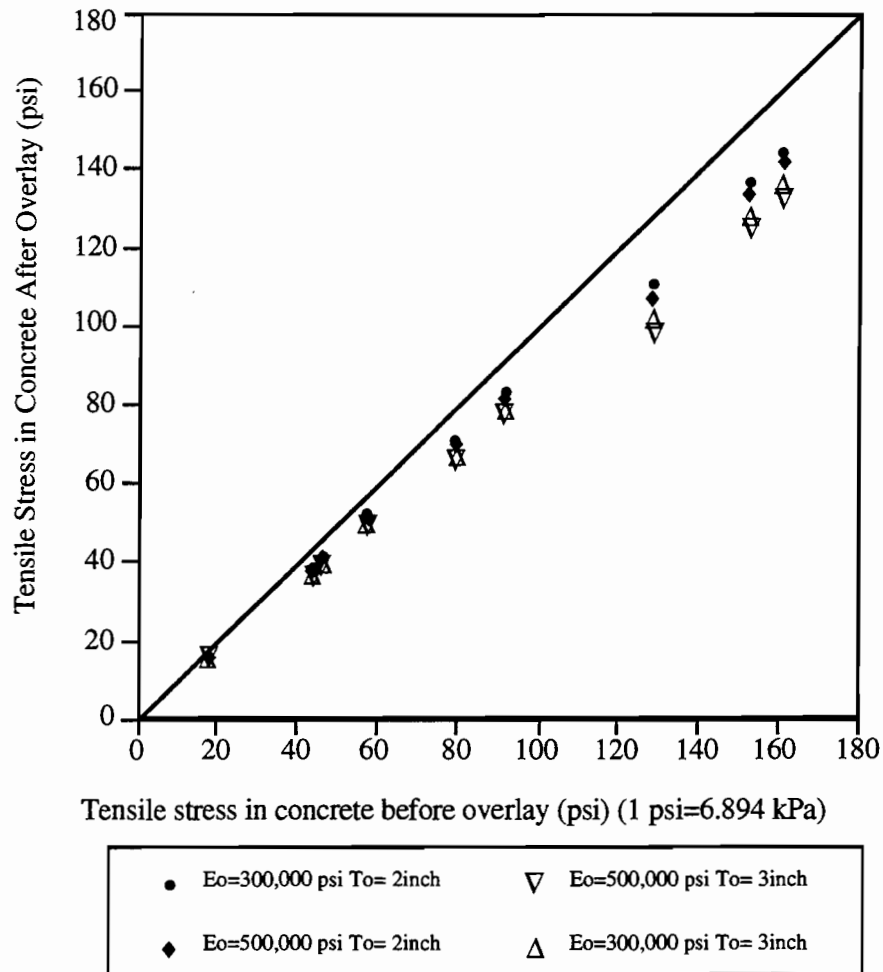


Figure 5.2. Predicted tensile stress at bottom of PCC layer (1 inch=2.54 cm; 1 mil=0.025 mm)

In summary, both the actual and predicted data demonstrate that the asphalt concrete overlay has only a minimal effect on the deflection. Hence, the predicted equations are a good representation of what occurs in the field. Furthermore, the predicted stresses show only a minimal effect in terms of overlay thickness and do not account for the significant change in performance noted in Chapter 2 with the addition of the overlay.

5.1.2 Material Properties

The preceding section showed that, while the 5.08-cm (2-inch) overlay has a significant impact on the pavement performance in terms of punchout failures, it has very little impact on

reducing the deflection or stress. The next major question is the implication of this finding on the slab PCC fatigue life, since the stiffness of a material experiencing fatigue damage will generally decrease, especially as it nears the wearout phase.

Figure 5.3 is a cumulative percentage distribution of the subgrade stiffness for both the Modulus and the RPEDD programs. The values for the RPEDD program are lower than those for the Modulus program, but for both programs the distribution is fairly uniform. This represents one point in time; the overall distribution may shift to a minor extent as the subgrade moisture conditions change, but the distribution will probably remain very similar. There is some indication that these values are probably stable for the subgrades, since the psi value on top of the original ACP overlay had an excellent riding quality after 7 years ($\psi = 3.7$). If there had been moisture changes, the ψ would probably have continued to decrease over time with the swelling clay action.

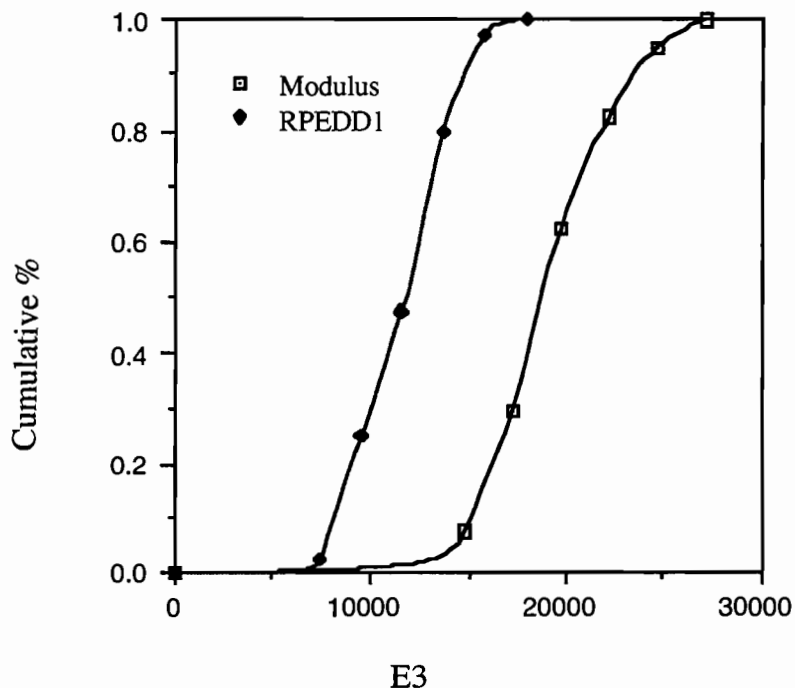


Figure 5.3. Cumulative distribution of subgrade stiffness as estimated by MODULUS and RPEDD programs

Figure 5.4 is a plot similar to the previous one, except that it represents the Cement Stabilized Subbase (CTB). Although the initial modulus values for the CTB were not available, it appears that some of the values may be on the low side. The coefficient variations for these layers are 61 percent and 31 percent for the Modulus and RPEDD1 programs, respectively. For a controlled layer, where quality control was applied, these values appear to be extremely large,

especially in terms of the smaller values for the subbase. This could imply either poor quality control during construction, or the possibility of wearout. It is very doubtful that the quality control permitted the excessive variation shown; thus, we must conclude that some wearout is occurring. One can observe that 40 percent and 8 percent of the observations are below the $2.76 \text{ E}+09 \text{ Pa}$ ($400,000 \text{ psi}$) value for the cement-stabilized subbase for use in the Modulus and RPEDD1 programs, respectively. Thus, we should be concerned about a fatigued deterioration of the cement-stabilized layer.

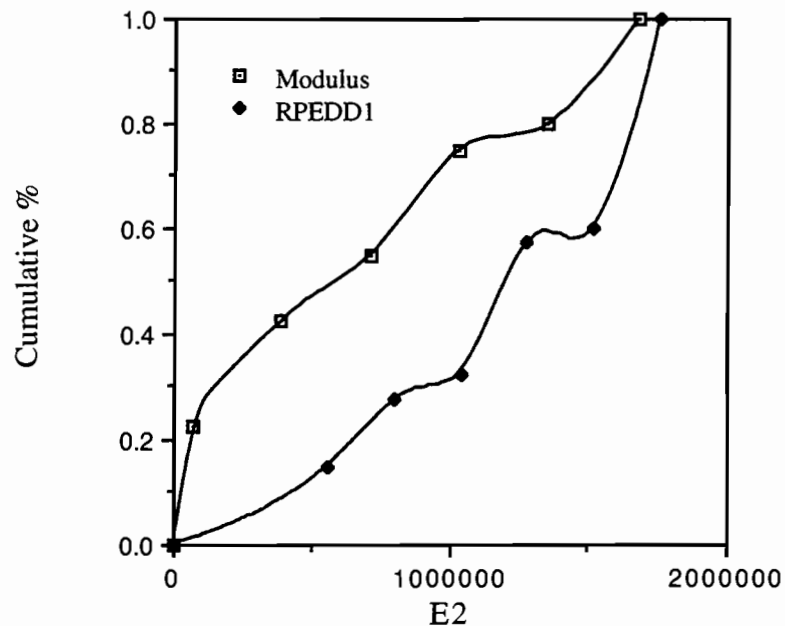


Figure 5.4. Cumulative frequency distribution of subbase stiffness as predicted by MODULUS and RPEDD1 programs

Figure 5.5, also similar to previous figures, shows the plots for the PCC pavement. Although the coefficient of variation of 23 percent and 13 percent for the Modulus and RPEDD distributions, respectively, are substantially smaller than those for the cement-stabilized layer, they are nonetheless still considered large. In fact, the distribution for the MODULUS program back-calculation is well beyond the normal variation of PCC pavements experienced in the field. Previous studies in Texas have shown these percentages to be in the range of 8 to 14 percent (Refs 13, 14). Thus, again, we must conclude that the PCC pavement is experiencing stiffness loss as a result of fatigue consumption. Although it is not as rapid as that for the cement-stabilized subbase, the net result is an ongoing fatigue consumption.

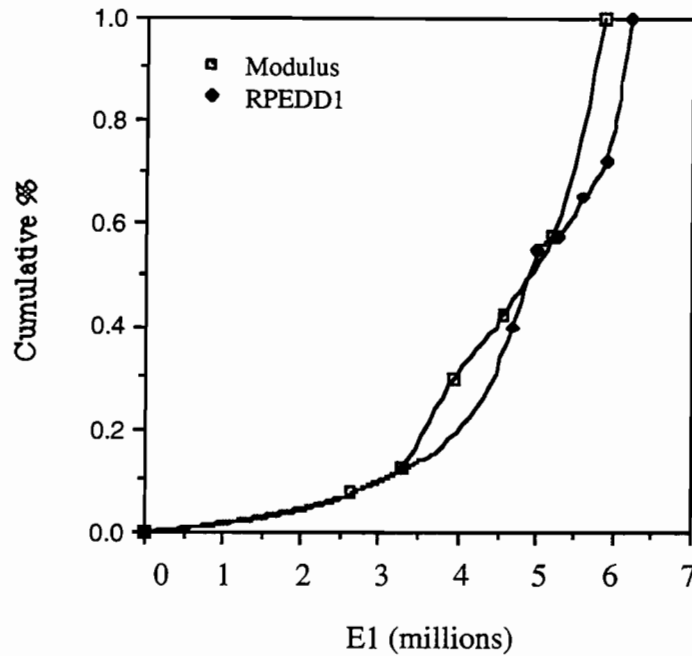


Figure 5.5. Cumulative frequency distribution of PCC stiffness as estimated by the MODULUS and RPEDD1 programs

This fatigue consumption may be illustrated by taking the actual E1 distribution from RPEDD in Figure 5.5 and overlaying on it a normal distribution, as shown in Figure 5.6. For the predicted normal distribution, a typical mean value for the aggregate type was used along with a 10 percent coefficient of variance. The actual field distribution appears to have shifted to the left as expected. Furthermore, the larger E1 values have experienced a much greater shift with the upper part of the curve approaching a vertical line. This may be attributed to the higher stress level associated with the higher E1 values; thus, they will experience fatigue failure first. As further confirmation, note that the predicted normal distribution of E1 has a pattern very similar to that of the E3 distribution in Figure 5.3, where no wearout has occurred.

Thus, in terms of material properties, the pavement may be approaching some degree of wearout, even though this is not reflected in terms of failures. This is to be expected, since the stress levels were not significantly influenced by the addition of the 5-cm (2-inch) asphalt concrete overlay.

5.2 PAVEMENT STRUCTURE PERFORMANCE

In Chapters 2 and 3, the actual pavement structure performance was reported in terms of the history of punchouts and failures and, in Chapter 3, in terms of the serviceability. Thus, the CRCP program and the AASHTO program may be used to prepare the predicted and the actual performance.

5.2.1 CRCP-5 Predicted Performance

Since the previous section demonstrated that the asphalt concrete overlay did not significantly affect the stresses in the PCC pavement, the CRCP program may be used to analyze the before-and-after performance conditions. Since the overlay was placed to reduce the roughness caused by swelling clays, the program may be run using the swelling clay performance curve for siliceous aggregates. The improved riding quality resulting from the asphalt overlay, in essence, indicates that the dynamic impact loading has been removed from the pavement. Thus, an analysis with the non-swelling clay performance curve for siliceous river gravel aggregates may be used to demonstrate that portion of the curve.

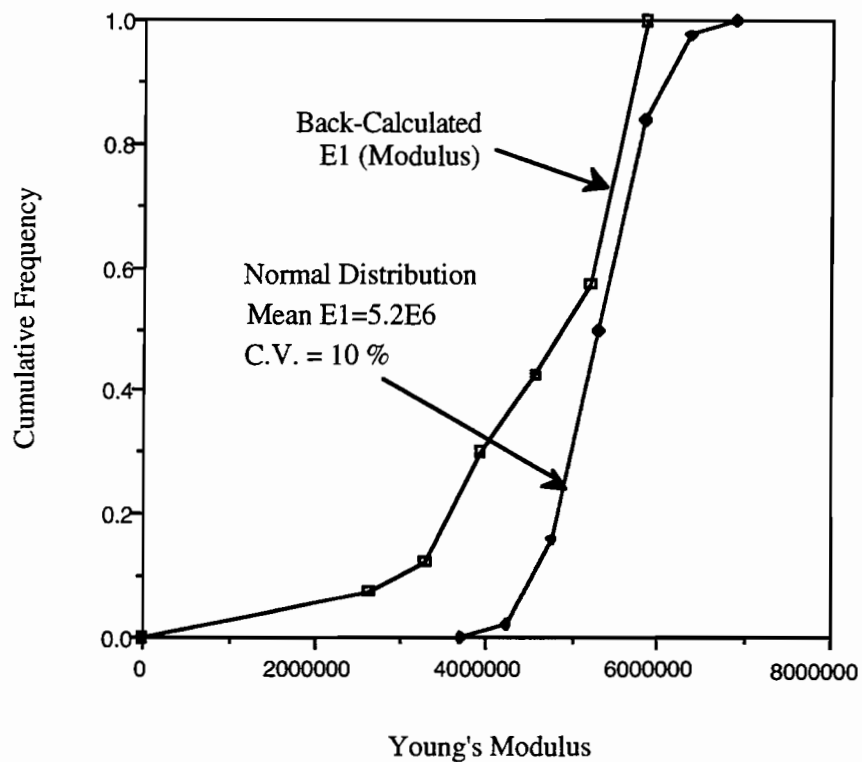


Figure 5.6. *E1 distribution (Modulus) vs. normal distribution*

Accordingly, the CRCP5 analysis program was run using the best available data simulating the project in terms of design, environment, coarse aggregate effect, soil type, and other factors. Figure 5.7 shows a remarkable similarity in the crack spacing distribution predicted by the program and the actual crack spacings as measured by a survey team in 1978. Figure 5.8 shows the same result in terms of the cumulative distribution. For example, the figure shows that for both the predicted and observed distribution, approximately 50 percent of the crack spacings were closer than 0.6858 m (2 1/4 feet) in 1978, just 6 years after construction.

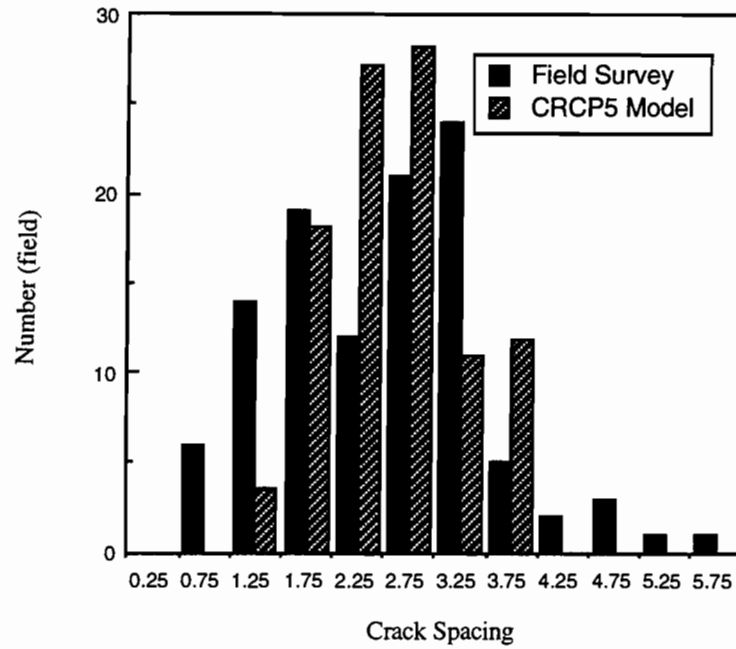


Figure 5.7. Comparison of predicted crack spacing distribution (CRCP5 program) with actual field data (1978 survey)

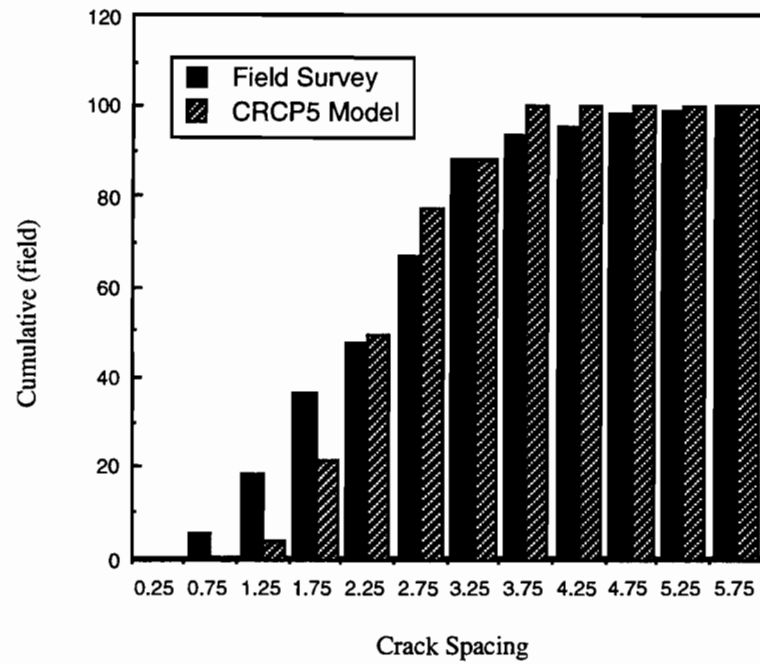


Figure 5.8. Comparison of cumulative crack spacing as predicted by CRCP5 program vs. 1978 field survey

In order for the CRCP5 program to estimate rate of failures from the crack spacing distribution, several inputs are needed. These include coarse aggregate type (siliceous river gravel), soil swelling, reliability level (set at 50 percent to indicate average values), and cumulative traffic exposure. Unfortunately, no detailed ESAL data are available for this pavement section. However, using the average annual daily traffic (AADT) data collected by TxDOT, together with a traffic model developed under TxDOT research project 472 (Ref 1), we can estimate ESALs with a reasonable degree of accuracy. Figure 5.9 shows that, based on this model, the section has experienced a cumulative traffic exposure of approximately 10,000,000 ESALs from construction in April 1972 to the date of first overlay in the spring of 1986.

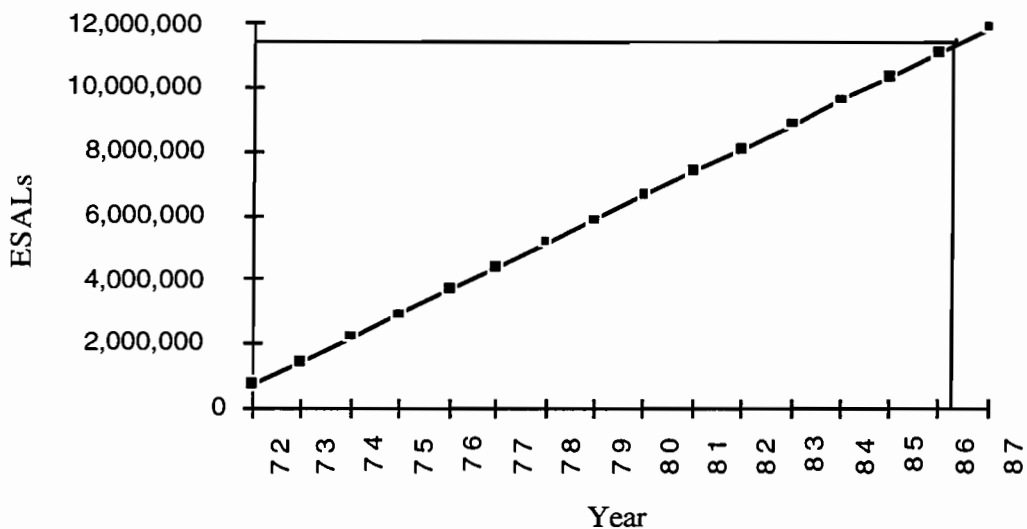


Figure 5.9. Estimated cumulative traffic exposure (ESALs) from construction to overlay

Figure 5.10 presents the predicted failures (in terms of time) for the swelling clay and non-swelling clay relationships. The examination of these curves shows a significant difference between the performance of the pavement, as reflected in Figures 2.2 through 2.6 in Chapter 2.

Thus in Figure 5.11, a simulated predicted performance curve is obtained by overlaying the swelling and non-swelling clay portions of the curve to simulate the time of the overlay on the original CRCP. These data are then compared with the actual performance curve from Chapter 2.

5.2.2 AASHTO Performance

The AASHTO Rigid Pavement Equation was used to estimate the total number of ESALs for various levels of terminal serviceability pavement using an initial value of 4.7. A J-factor of 2.7 was used in this analysis for the CRCP, with Figure 5.12 showing the result. If we use the total equivalencies estimated to this point (11 million ESALs), then the pavement's total ESALs to a terminal level of 17.2 kPa (2.5 psi) may be estimated, assuming the overlay had not been placed

and the swelling clay action had not occurred. The total equivalencies expected during the design life for the facility (using a terminal serviceability of 2.5) is 14 million ESALs. Thus, by ratioing these two values, we can estimate that 79 percent of the total life has been consumed, or that the pavement has a 21 percent remaining life for 95 percent reliability.

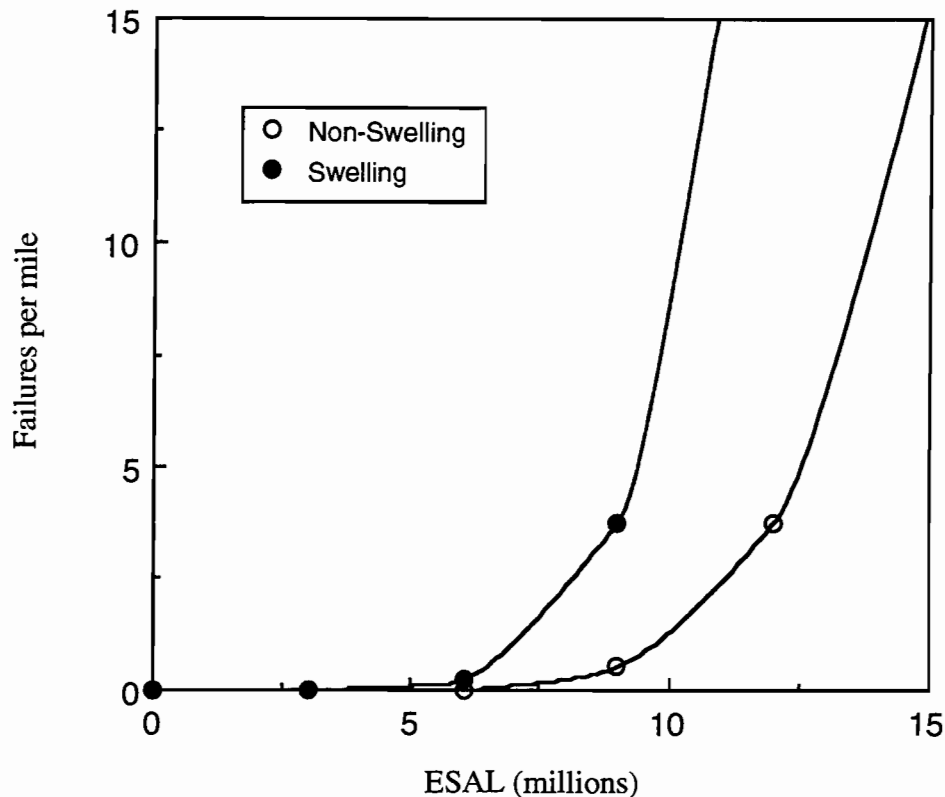


Figure 5.10. CRCP5 predicted failures for swelling and non-swelling conditions

5.3 PLANNING AND DESIGN IMPLICATIONS

Both the observed and simulated performance of CRCP demonstrates that the use of a thin overlay can significantly reduce the rate of failures on a CRCP in areas where swelling clays are found. This type of rehabilitation is recommended in areas where swelling clays increase roughness (reduce psi) and cause dynamic impact of loadings on the pavement that may be observed by excessive oscillations of the truck springs as a truck travels down a pavement. A thin overlay eliminates the roughness, thereby returning truck operations to a normal type of pavement loading. If the dynamic impact loading is not eliminated, a rapid increase in failures will be experienced.

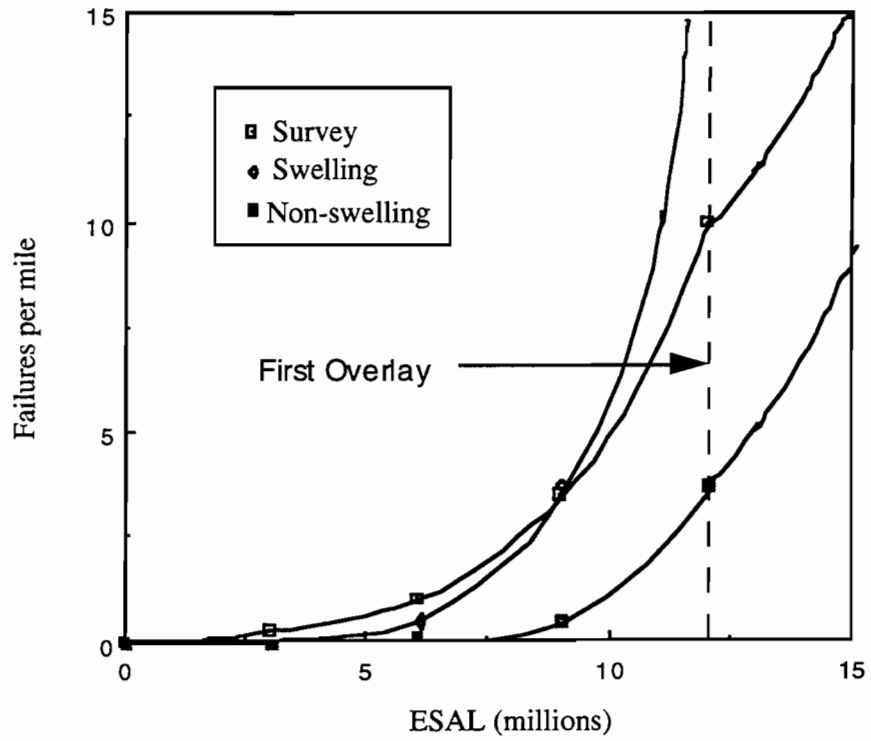


Figure 5.11. Comparison of predicted and actual performance curve (1 mile=1.61 m)

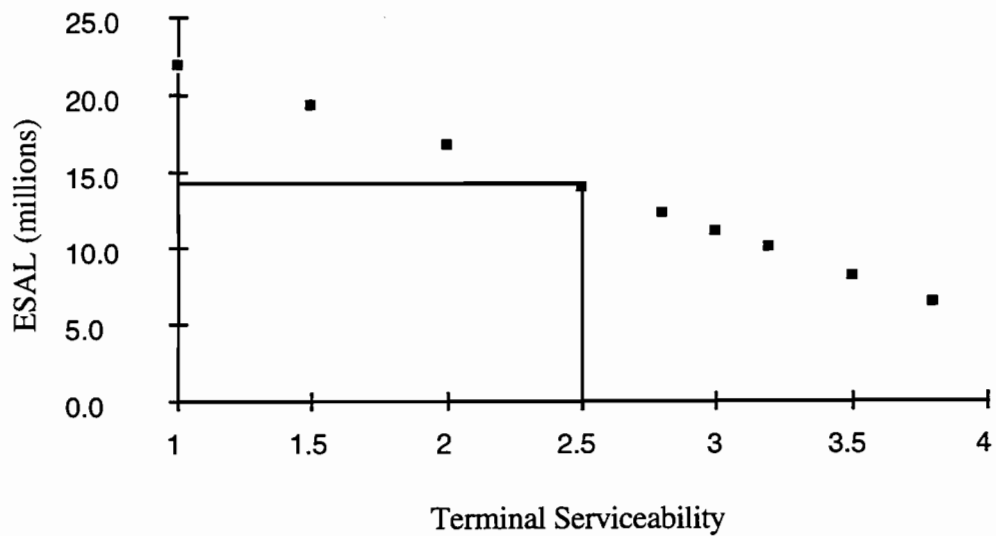


Figure 5.12. AASHTO pavement life prediction for the special study section

Another implication of this work is that the CRCP program may be used in a cost-benefit study to establish the value of using thin overlays to increase the life of a CRCP. Techniques, such as those in Figure 5.7, may be used to simulate the performance curves and to perform economic analyses.

The next implication is that an excessive life extension must not be assigned through the use of a thin ACP overlay. Basically, this procedure rehabilitates the pavement's condition to that of the original performance curve, as intended. The pavement on IH-30 indicates that wearout is being experienced, as shown in Figures 5.4 and 5.5. Thus, at some point a rapid increase in punchouts will be observed, as pavement fatigue failure starts to occur. This concept is illustrated by Figure 5.13, which demonstrates the stages of CRCP service life as a function of the average crack spacing or segment length. There are three stages: the early, rapid change period; a very stable period; and, finally, the fatigue failure period. Our survey indicates that the IH-30 pavement is at the boundary of the Phase 2 and Phase 3 stages of crack development. The shorter crack spacings in Phase 3 will result in a rapid increase in punchouts. Thus, from a planning standpoint, the pavement should be observed closely; in addition, deflections should be taken on a more permanent structural rehabilitation of the pavement, i.e., an unbonded CRCP overlay. There is still some possibility of using a bonded CRCP overlay (i.e., removing the asphalt overlay), but such usage is considered a gray area.

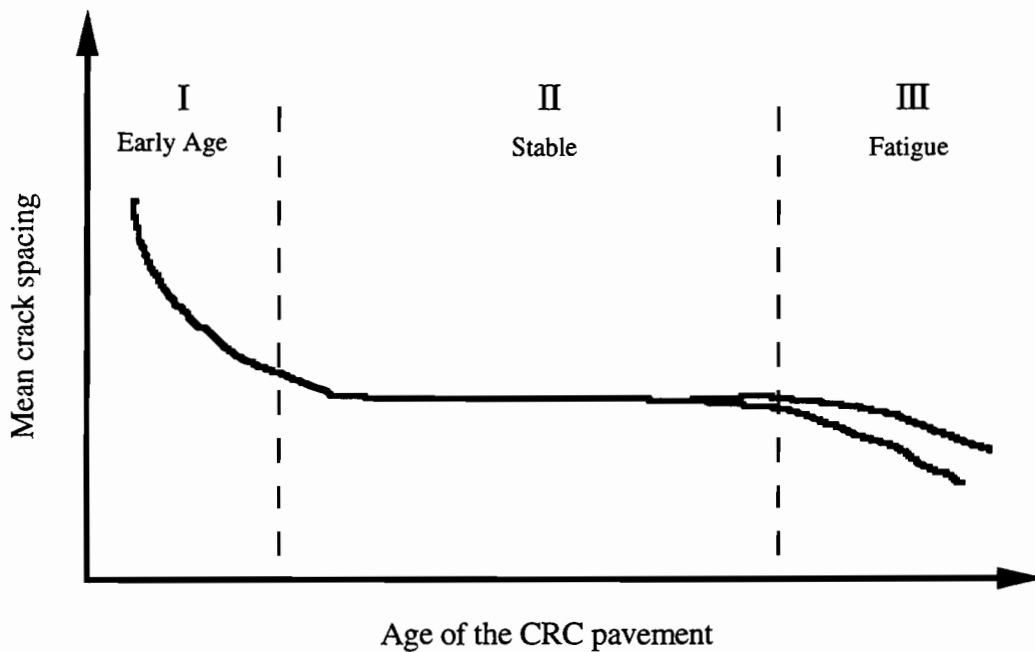


Figure 5.13. Stages in the life of a CRC pavement

Finally, the implication of this study is that a well-developed pavement database can be instrumental not only in explaining existing pavement performance, but also in designing new pavements.

CHAPTER 6. CONCLUSIONS AND RECOMMENDATIONS

While the conclusions and recommendations presented here are based on the single diagnostic case study undertaken in Bowie County, the study section itself — a typical 20.32-cm (8-inch) CRC pavement — is representative of the type of pavement most commonly placed across the state during the Interstate Highway construction program (late 1950s to the late 1970s). Having only a 20-year design life, many of these 20- to 30-year-old pavements are now overlaid, typically with an ACP overlay of the type studied here. The effectiveness of the rehabilitation methods used for the study section is therefore of great interest to planners in terms of what may be done with the rest of the state's aging CRCP inventory. An ACP overlay, if effective, is certainly a low-cost alternative to total reconstruction. But, as some may wonder, is it only a temporary solution?

6.1 CONCLUSIONS

This study strongly indicated that thin ACP overlays are an effective rehabilitation strategy for pavements whose conditions are similar to those studied in this project. In this case, the CRCP — constructed on active clay and experiencing an increasing rate of punchouts and failures — was treated with a thin layer of ACP. The following are the general conclusions of this study:

- The thin overlay significantly reduced the failures occurring as a result of (1) the dynamic impact loadings developed by high-speed heavy trucks, and (2) the surface roughness caused by swelling clay action. The fact that the protective layer (ACP) also reduces environmental PCC deterioration is a secondary benefit.
- As for the long-term effect on normal fatigue, the thin overlay does not significantly increase the structural capacity or reduce the stress caused by normal loading (i.e., eliminate the dynamic impact stresses). The significant or marginal loss of stiffness on the PCC layer for approximately 15 percent and 28 percent of the observations may warrant some concern. The fact that the project is two years beyond the design life and probably way beyond the ESAL's predicted life brings the overall problem somewhat into focus.
- The benefits of a pavement data base are self-evident, since this study would not be possible without access to the 20-plus years of data.

From the visual condition survey (Chapter 2):

- The first ACP overlay reduced the visual distress from an average of about 10 failures/mile to zero failures/mile. At the time this overlay was removed, 6 years later, only minimal additional failures/mile had developed. It can be extrapolated from the pre-overlay failure rate that the PCC pavement would have developed between 15 and 20 failures/mile (or possibly more) had it not been overlaid (Figure 2.2). Thus, the overlay afforded 5 to 6 additional years of pavement surface at a relatively low cost.

- Although it was difficult to count failures in the exposed PCC surface after milling, it is clear that the rate of failure development in the underlying PCC was greatly slowed by the addition of the overlay.

From the roughness study (Chapter 3):

- The decision to replace the ACP overlay in 1993 was not based on roughness, but rather on surface deterioration, since the old overlay was still maintaining a relatively smooth 3.97 SI (1.25 IRI) surface after 6 years of service (though there was short wavelength roughness).
- The new, 1993 overlay further reduced the overall roughness of the section and increased riding quality to a 4.72 SI (0.93 IRI).
- The new, 1993 overlay reduced roughness at all significant wavelengths, from less than 0.3048 m (1 foot) to about 36.576 m (120 feet). Wavelengths shorter than 0.3048 m (1 foot) were considered microtexture, while wavelengths longer than 30.48 m (100 feet) were considered “built into the road” as hills, dips, etc.
- The short wavelength roughness reduction, i.e., 0.3048 m (1 foot) to 36.576 m (120 feet), probably reflects the elimination of the deteriorated ACP.

From the deflection analysis (Chapter 4):

- The old overlay preserved the integrity of the underlying PCC pavement structure. This is evident from the fact that the majority of the E_1 (PCC modulus) back-calculated from the deflections is approximately equal to the modulus of concrete constructed with SRG aggregate in the lab.
- Load transfer in the PCC pavement was maintained.

6.2 RECOMMENDATIONS

- Placing a thin ACP overlay, i.e., average 5.08-cm (2-inch) thickness, can extend the life of a PCC pavement experiencing dynamic impact loading as a result of swelling clay.
- The ACP overlay should be placed immediately on PCC pavements where swelling clay roughness has increased the failure rate.
- This specific project should be scheduled for a major structural overlay in the near future, in order to reduce the rate of fatigue consumption.
- The merits of continuing the pavement data base have been demonstrated by this project.

REFERENCES

1. Dossey, T., and A. Weissmann, "A Continuously Reinforced Concrete Pavement Database," Research Report 472-6, Center for Transportation Research, The University of Texas at Austin, November 1989.
2. "AASHTO Guide for Design of Pavement Structure 1986," AASHTO, 1986.
3. Treybig, Harvey J., B. Frank McCullough, Phil Smith, and Harold von Quintus, "Overlay Design and Reflection Cracking Analysis for Rigid Pavement," Vol. 1, Development of New Design Criteria, Austin Research Engineers, Austin, Texas, 1978.
4. Wei, Chao, B. Frank McCullough, W. Ronald Hudson, and Kenneth Hankins, "Development of Load Transfer Coefficient for Use with the AASHTO Guide for Design of Rigid Pavement Based on Field Measurements," Research Report 1169-3, Center for Transportation Research, The University of Texas at Austin, February 1992.
5. Teller, L. W., and E. C. Sutherland, "The Structural Design of Concrete Pavement: Part 4 — The Study of the Structural Action of Several Types of Transverse and Longitudinal Joint Design," *Public Roads*, Vol. 17, September 1936.
6. Ricci, E., A. H. Meyer, W. Ronald Hudson, and K. H. Stokes, "The Falling Weight Deflectometer for Nondestructive Evaluation of Rigid Pavement," Research Report 387-3F, Center for Transportation Research, The University of Texas at Austin, November 1985.
7. Hall, Kathleen T., and Alaeddin Mohseni, "Back-Calculation of Asphalt Concrete-Overlaid Portland Cement Concrete Pavement Layer Moduli," Transportation Research Board No. 1293, Transportation Research Board, Washington, D.C., January 1991.
8. Anderson, M., "A Data Base Method for Back Calculation of Composite Pavement Layer Moduli," *Nondestructive Testing of Pavements and Back-calculation of Moduli*, ASTM STP 1026, Philadelphia, PA, 1989.
9. Uzan, Jacob, T. Scullion, C. H. Michalak, M. Paredes, and R. L. Lytton, "A Microcomputer-Based Procedure for Back-Calculation Layer Moduli from FWD Data," Research Report 1123-1, Texas Transportation Institute, Texas A&M University, College Station, Texas, July 1988.
10. Teller, L. W., and E. C. Sutherland, "The Structural Design of Concrete Pavements: Part 4 — The Study of the Structural Action of Several Types of Transverse and Longitudinal Joint Designs," *Public Roads*, Vol 17, Nos. 7 and 8, September and October 1936.
11. Uddin, Waheed, A. H. Meyer, W. Ronald Hudson, and K. H. Stokoe II, "A Structural Evaluation Methodology for Pavements Based on Dynamic Deflections," Research Report 387-1, Center for Transportation Research, The University of Texas at Austin, August 1985.

12. Scullion, Tom, and Chester Michalak, "Modulus 4.0 User's Manual," Research Report 1123-4, Texas Transportation Institute, Texas A&M University, College Station, January 1991.

APPENDIX A:
SAS Spectral Analysis Program


```

/*****
/*
/* SPECTRA PROC / T. DOSSEY 11/3/93
/*
/* THIS PROGRAM RUNS A SPECTRAL ANALYSIS OF ROAD PROFILE.
/*
/*
/*****

GOPTIONS DEVICE=TEK4105 GPROTOCOL=GSAS7171;
CMS FI OUT DISK DOWN1 DATA A;
CMS FI OUT2 DISK DOWN2 DATA A;
CMS FI IN DISK BEFORE I30 A;

/***** READ THE SURFACE PROFILE *****/
DATA TEST; POINTS=256;INFILE IN;

/**** SKIP DOWN TO START ****/
/*DO I=1 TO 3168;INPUT; END; */
    DO FRAME=1 TO 119;

/**** READ NEXT 256 FOR ANALYSIS *****/
    DO I=1 TO POINTS;
        INPUT RWP LWP; AMP=RWP;
        OUTPUT;
    END; END; STOP;

/***** Create Plot of INPUT DATA *****/
SYMBOL1 C=RED V=NONE I=JOIN;
SYMBOL2 C=BLUE V=NONE I=JOIN;
OPTIONS OBS=MAX; /*
PROC GPLOT; PLOT AMP*I=1; RUN; */
DATA _NULL_; SET TEST; FILE OUT; PUT FRAME I AMP;
PROC SPECTRA P S COEF CENTER OUT=B ADJMEAN WHITETEST; BY FRAME;
VAR AMP;RUN;
DATA TEST2; SET B; HZ=FREQ/3.14159; WL=1/HZ;

/***** PRINT & PLOT RESULTS. SPECTRA PRODUCES NO PRINTOUT. **/
/* PROC PRINT;
AXIS1 COLOR=GREEN LOGBASE=10 LOGSTYLE=EXPAND;
PROC GPLOT; PLOT S_01*WL=1 P_01*WL=2 /OVERLAY HAXIS=AXIS1;
PROC GPLOT;PLOT SIN_01*WL=1 COS_01*WL=2 /OVERLAY HAXIS=AXIS1;

/**** OUTPUT DATA TO FILES FOR DOWNLOADING TO MAC *****/
DATA _NULL_; SET TEST2;FILE OUT2;PUT FRAME WL S_01 SIN_01; */
PROC SORT DATA=TEST2; BY WL; RUN;
PROC MEANS NOPRINT DATA=TEST2; BY WL; VAR S_01 SIN_01;
OUTPUT OUT=X MEAN=MS MSIN; RUN;
DATA _NULL_; SET X; FILE OUT2; PUT WL MS MSIN;

```


Appendix B:

Deflection Plots along Milepost

I. Before Construction (old overlay, do nothing)

Eastbound — 4,082 kg (9,000 lb)

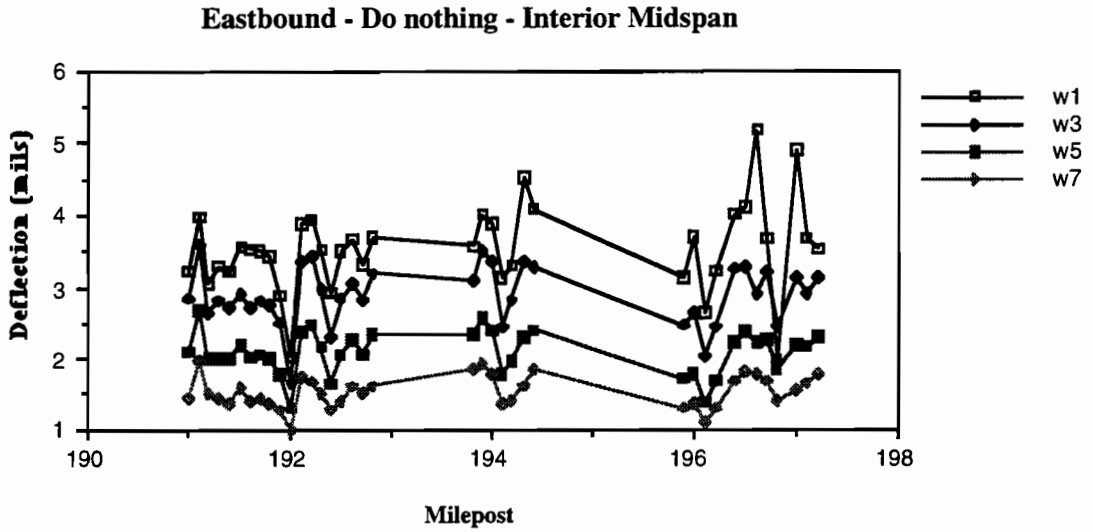


Figure B.1. Eastbound — Interior Midspan (1 mil=0.025 mm)

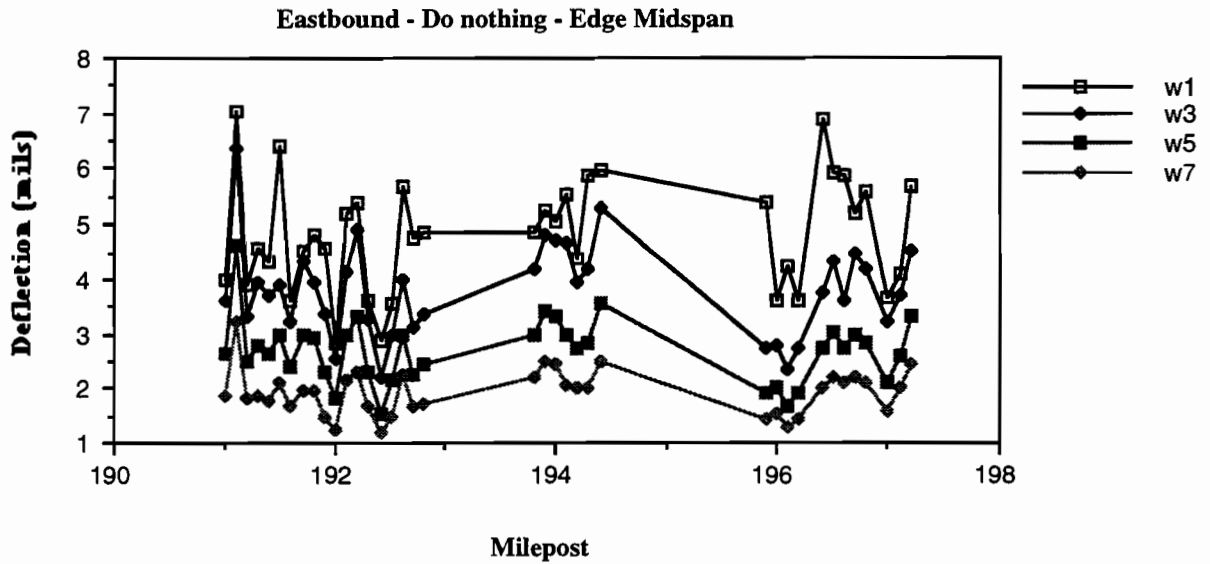


Figure B.2. Eastbound — Edge Midspan (1 mil=0.025 mm)

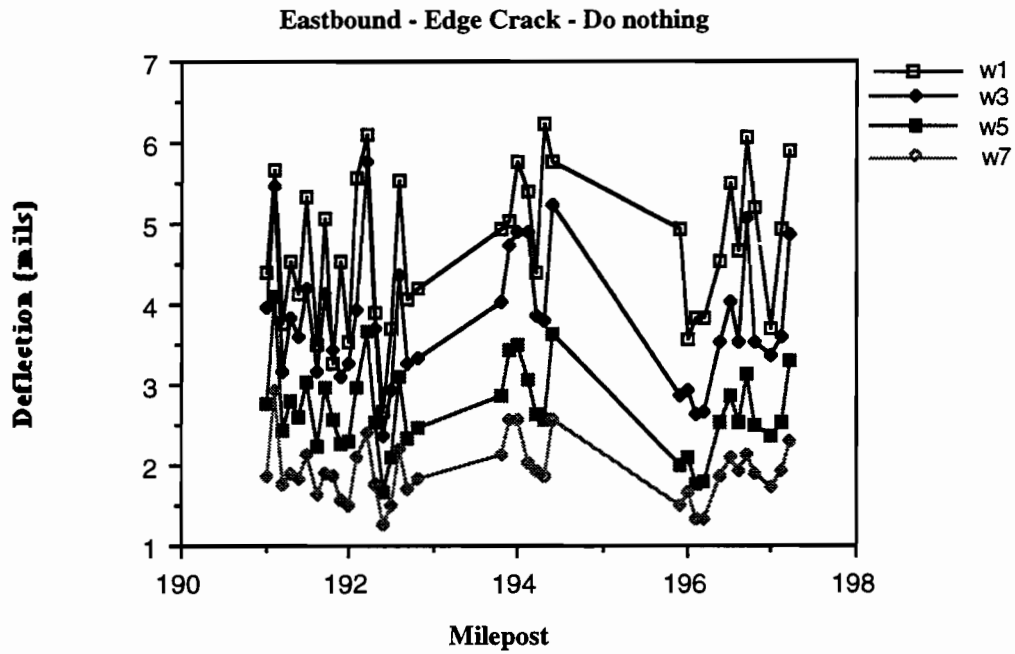


Figure B.3. Eastbound — Edge Crack (1 mil=0.025 mm)

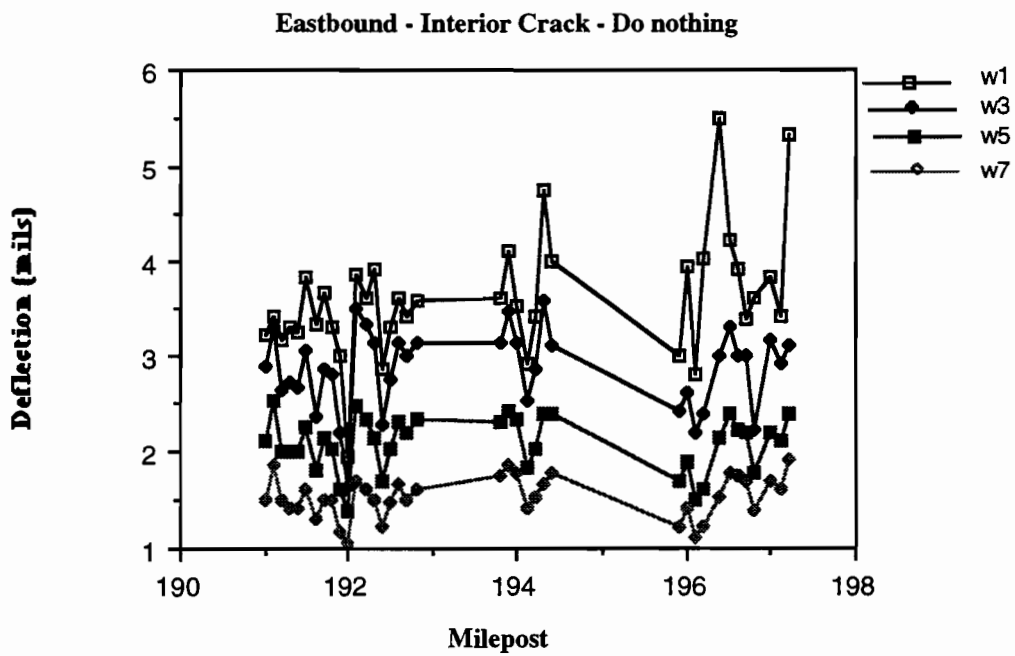


Figure B.4. Interior Crack (1 mil=0.025 mm)

Westbound — 4,082 kg (9,000 lb)

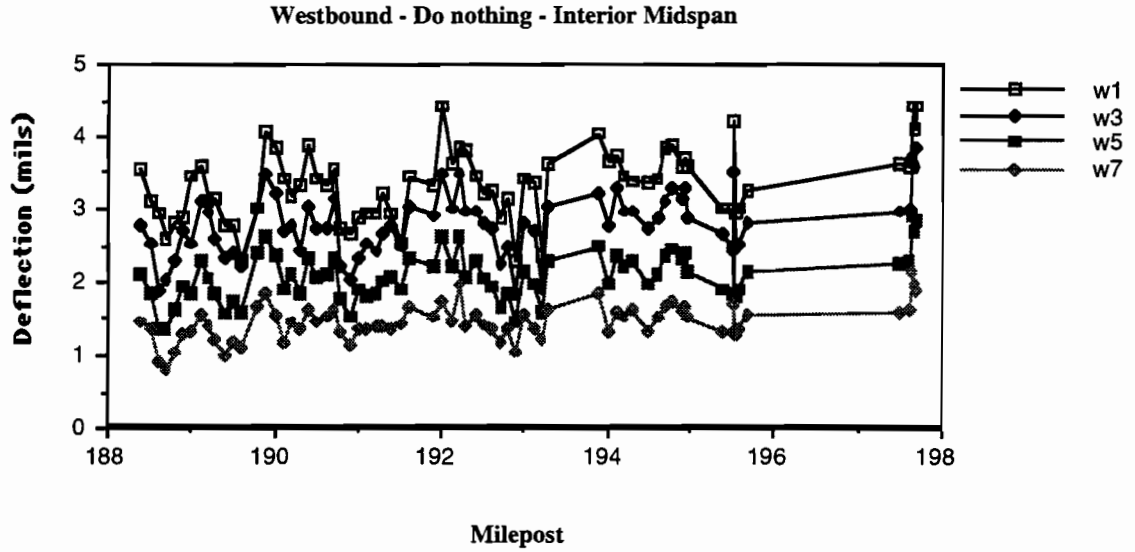


Figure B.5. Westbound — Interior Midspan (1 mil=0.025 mm)

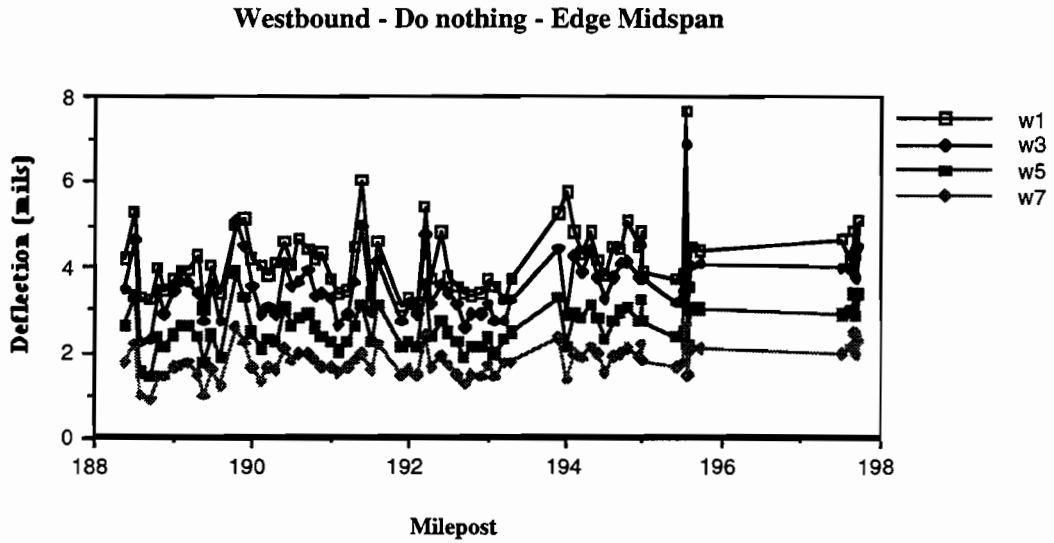


Figure B.6. Westbound — Edge Midspan (1 mil=0.025 mm)

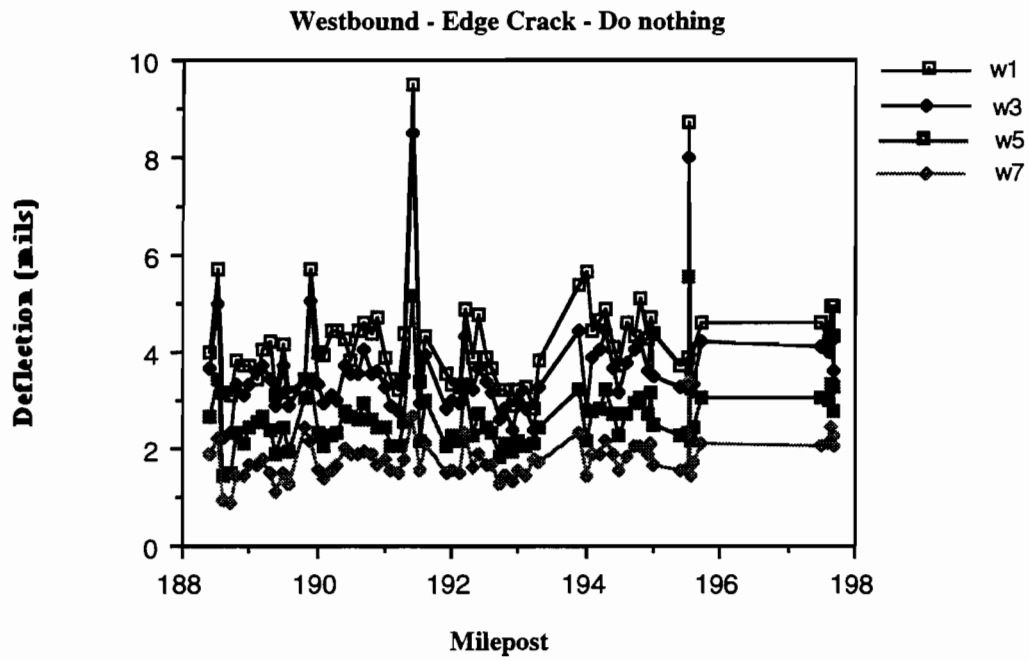


Figure B.7. Edge Crack (1 mil=0.025 mm)

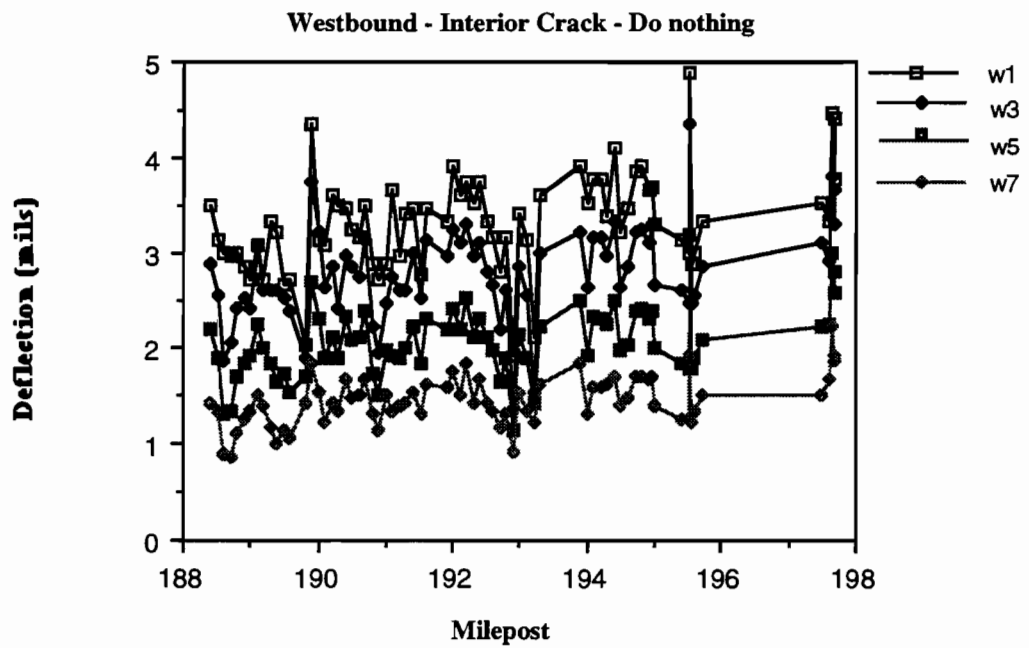


Figure B.8. Interior Crack (1 mil=0.025 mm)

II. After Milling

Eastbound — 4,082 kg (9,000 lb)

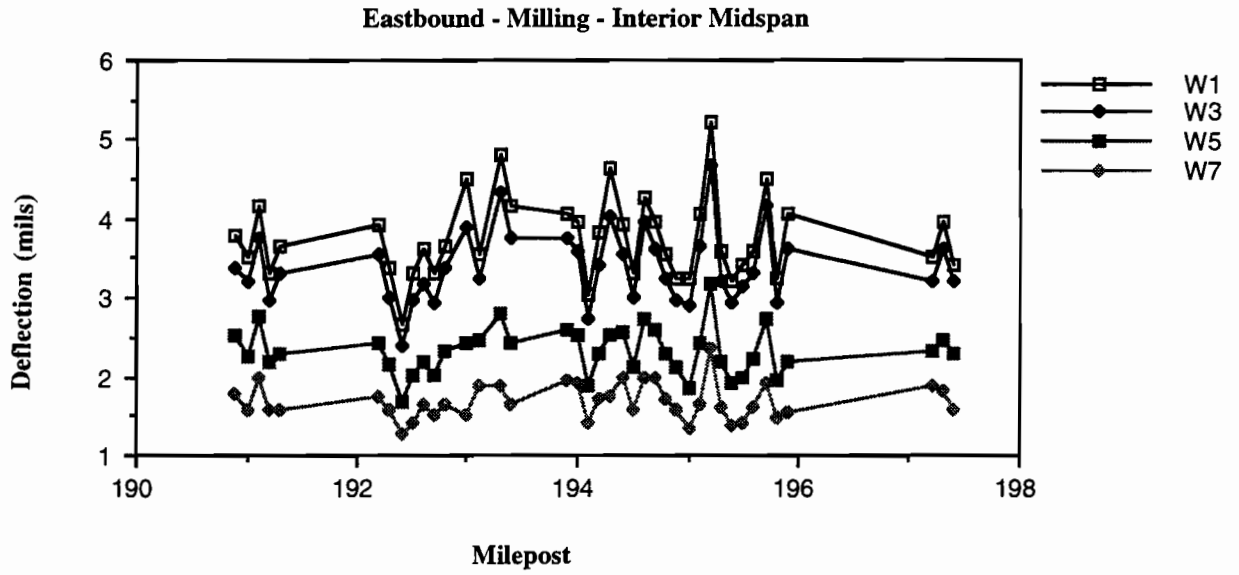


Figure B.9. Eastbound — Interior Midspan (1 mil=0.025 mm)

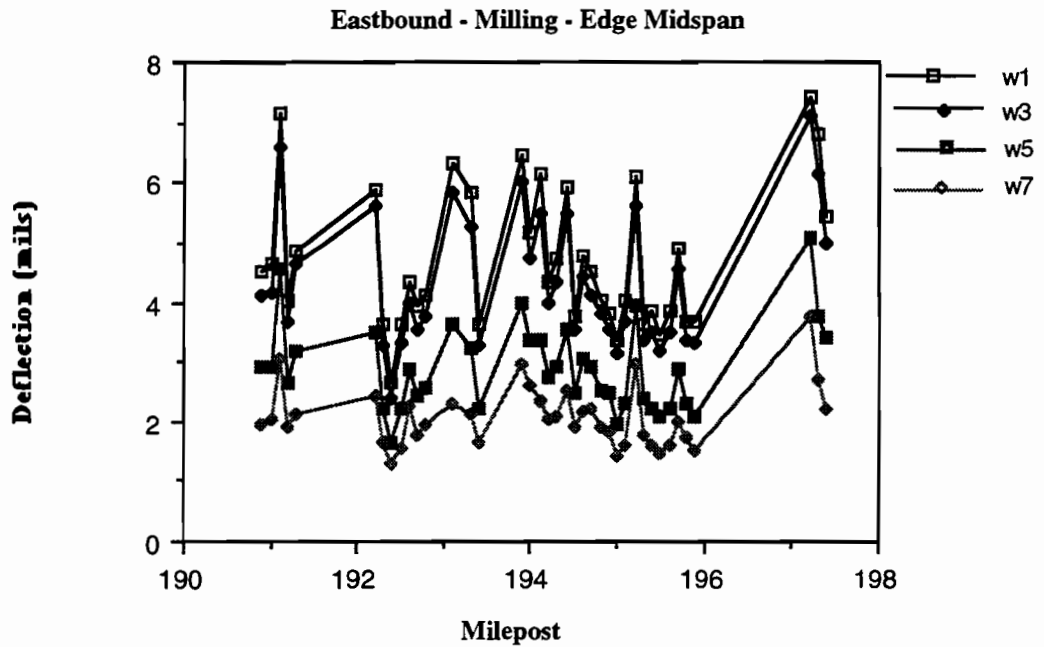


Figure B.10. Eastbound — Edge Midspan (1 mil=0.025 mm)

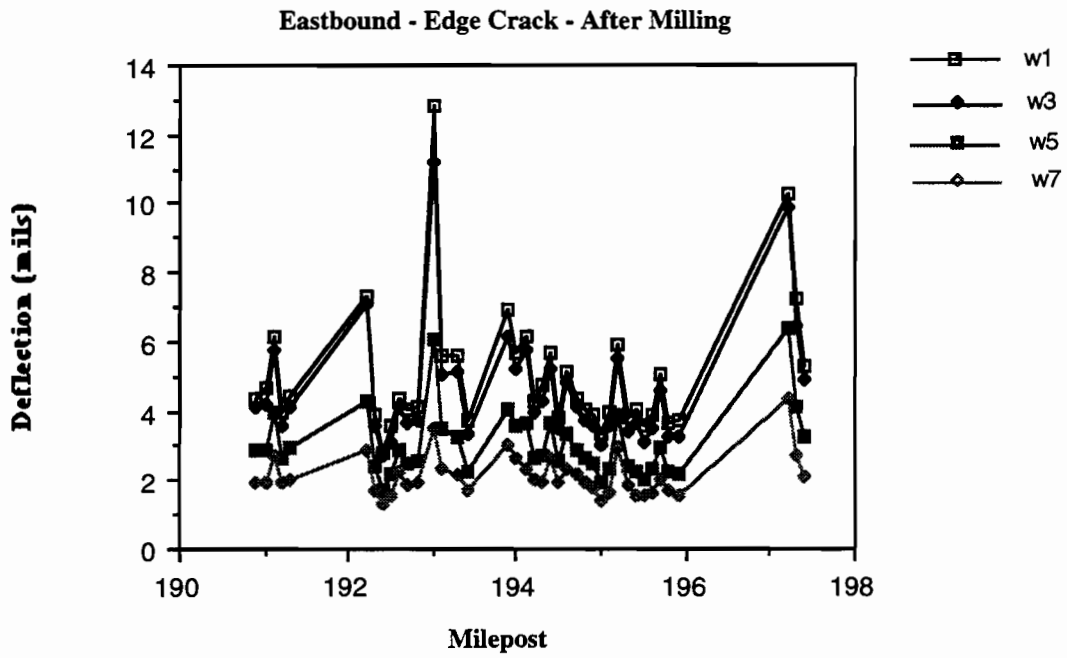


Figure B.11. Edge Crack (1 mil=0.025 mm)

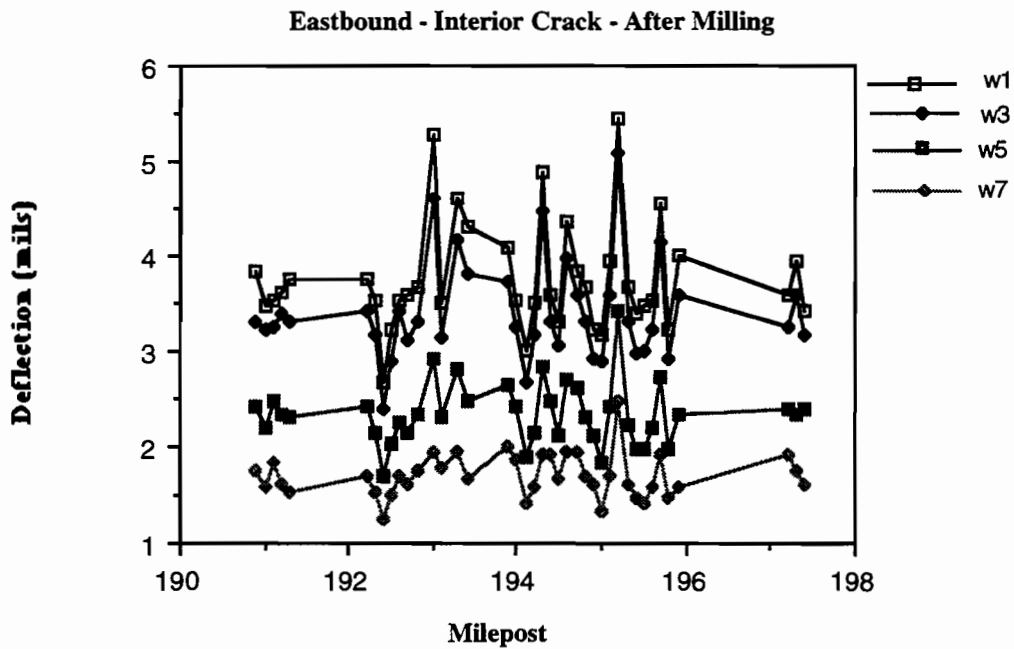


Figure B.12. Interior Crack (1 mil=0.025 mm)

II-2 Westbound — 4,082 kg (9,000 lb)

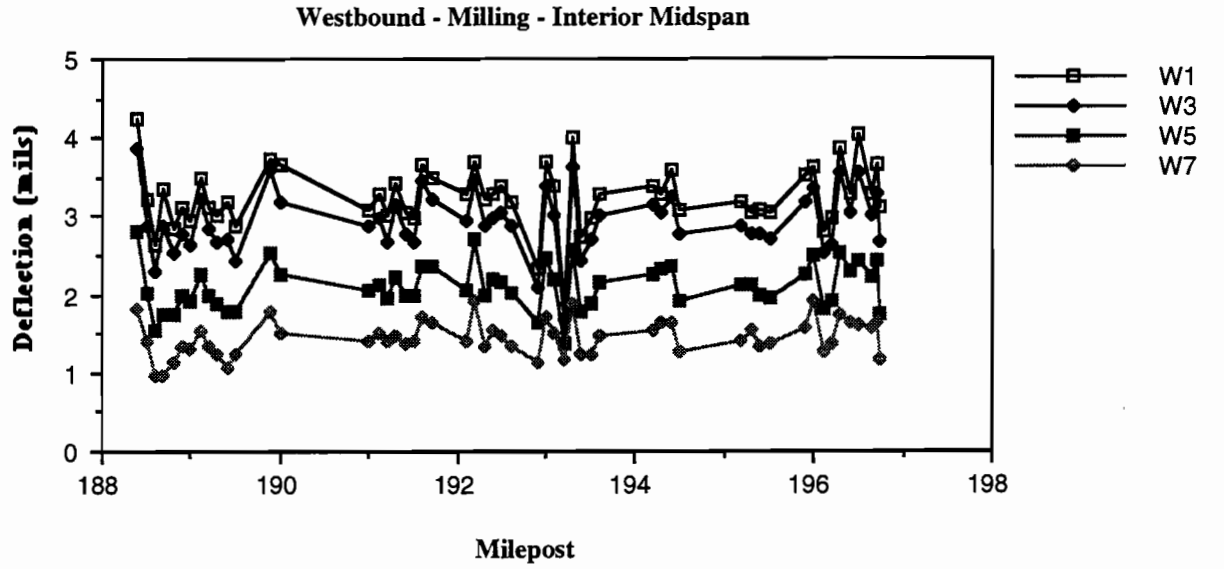


Figure B.13. Interior Midspan (1 mil=0.025 mm)

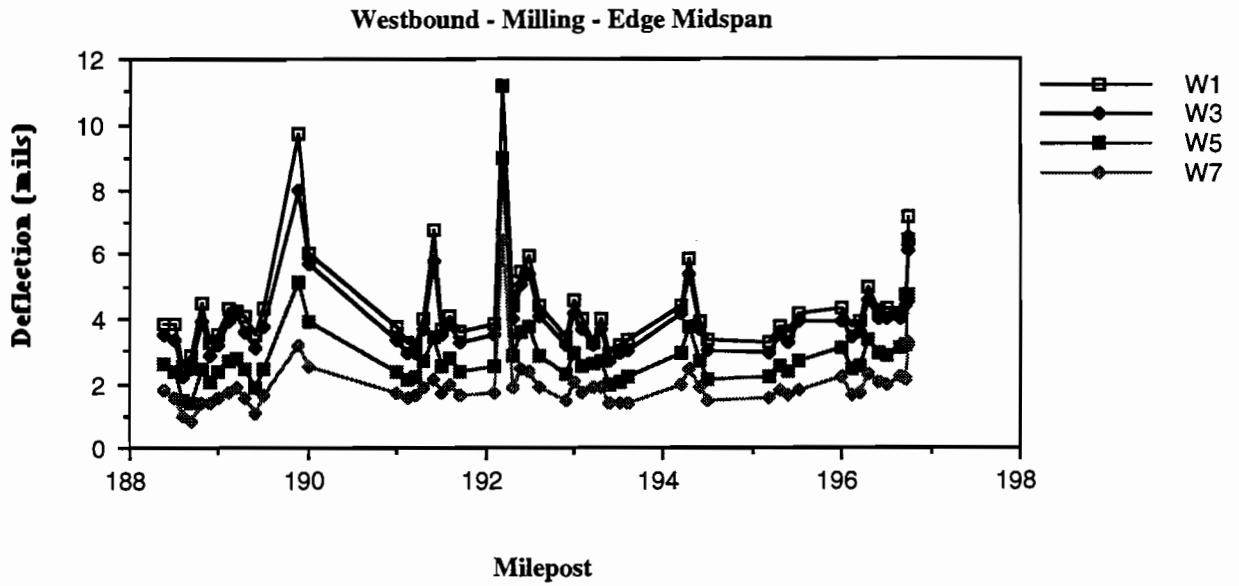


Figure B.14. Edge Midspan (1 mil=0.025 mm)

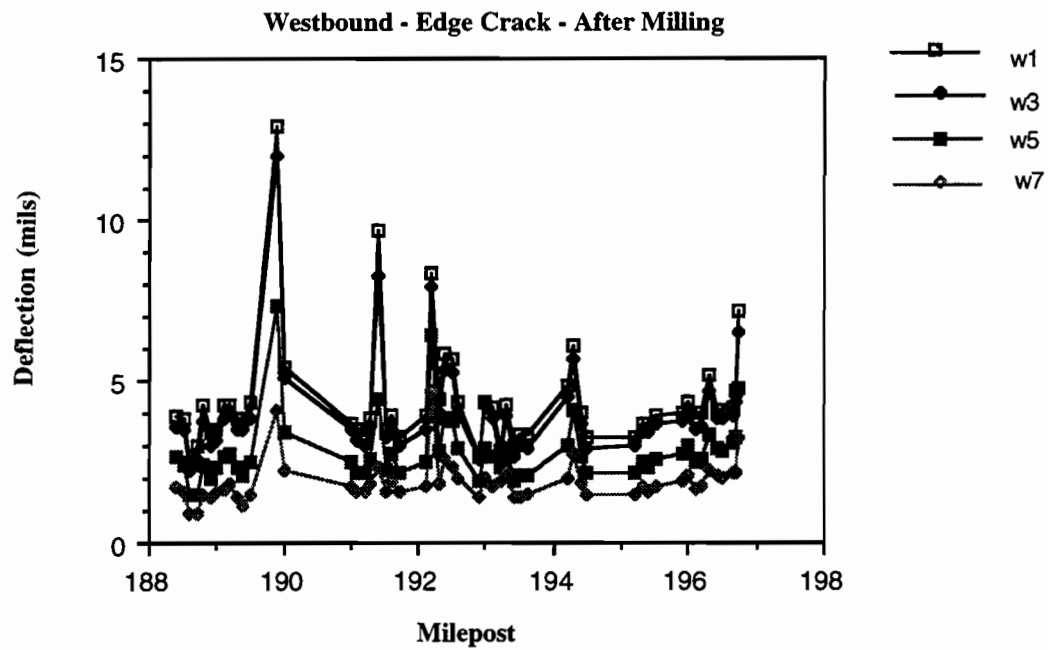


Figure B.15. Edge Crack (1 mil=0.025 mm)

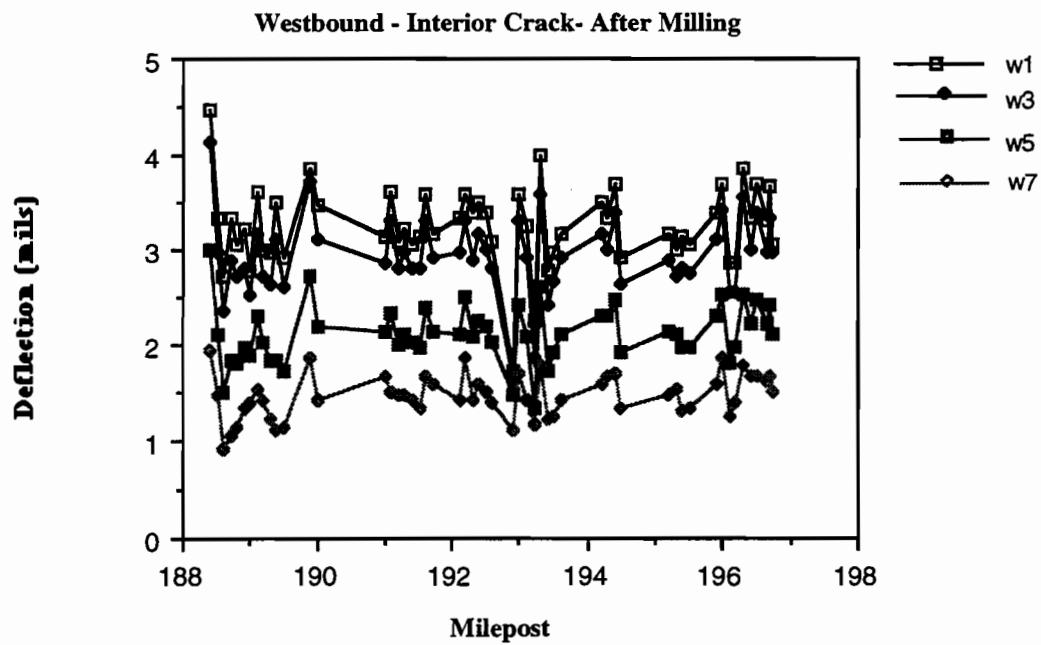


Figure B.16. Interior Crack (1 mil=0.025 mm)

Eastbound — 4,082 kg (9,000 lb)

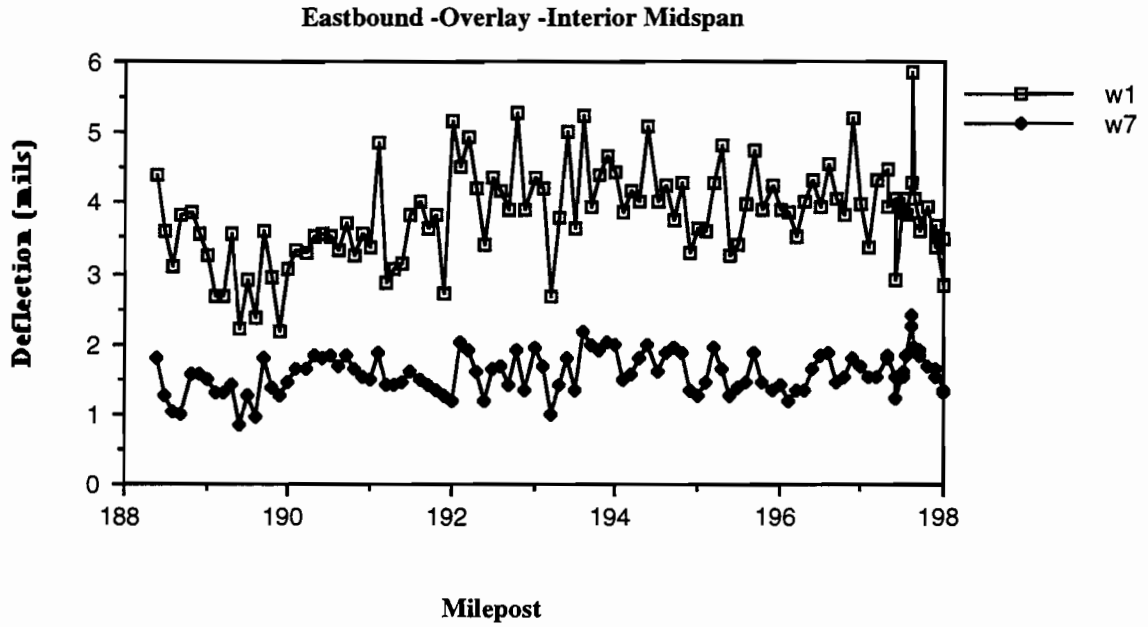


Figure B.17. Interior Crack (1 mil=0.025 mm)

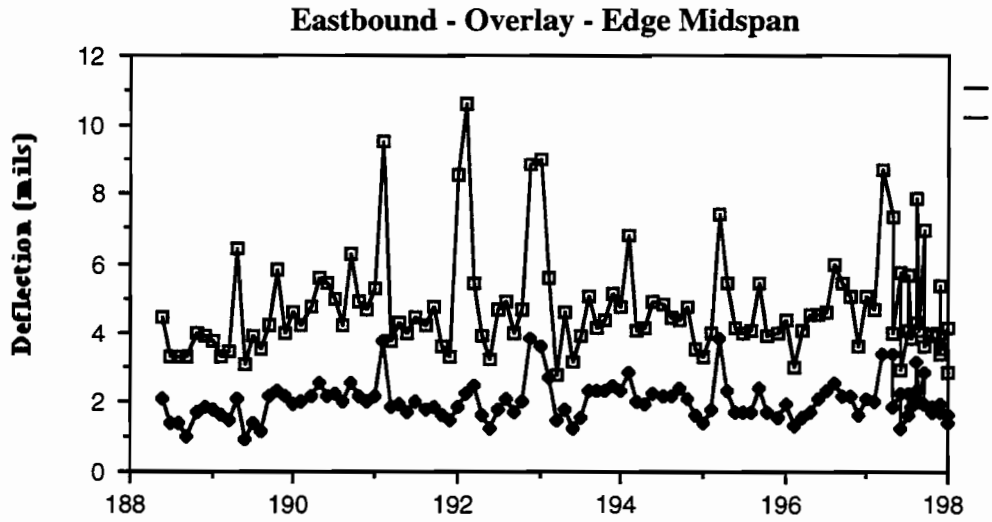


Figure B.18. Edge Crack (1 mil=0.025 mm)

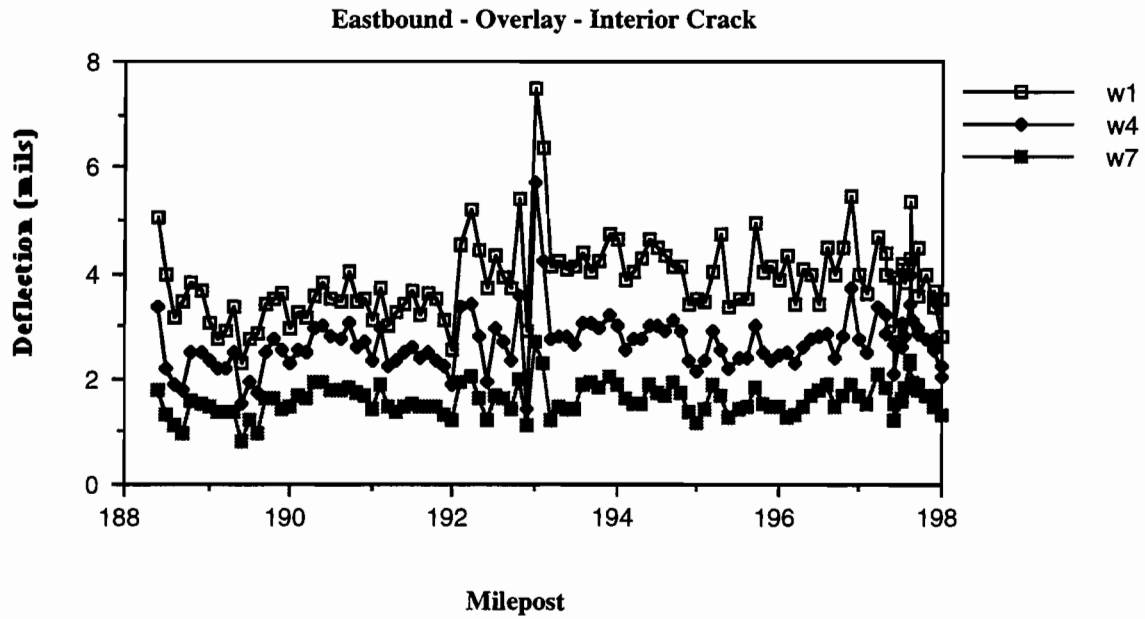


Figure B.19. Interior Crack (1 mil=0.025 mm)

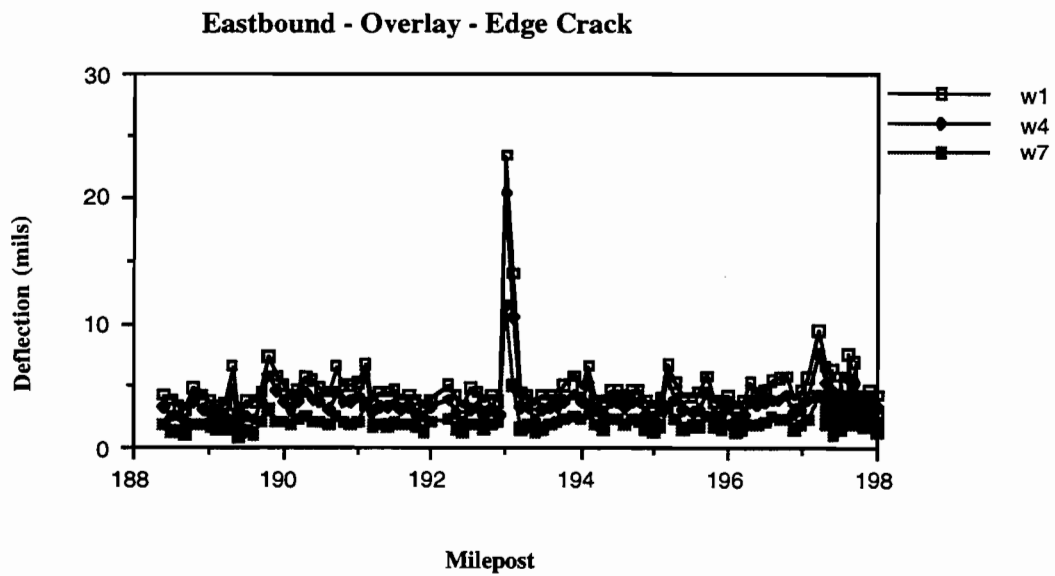


Figure B.20. Edge Crack (1 mil=0.025 mm)

Westbound Direction — 4,082 kg (9,000 lb)

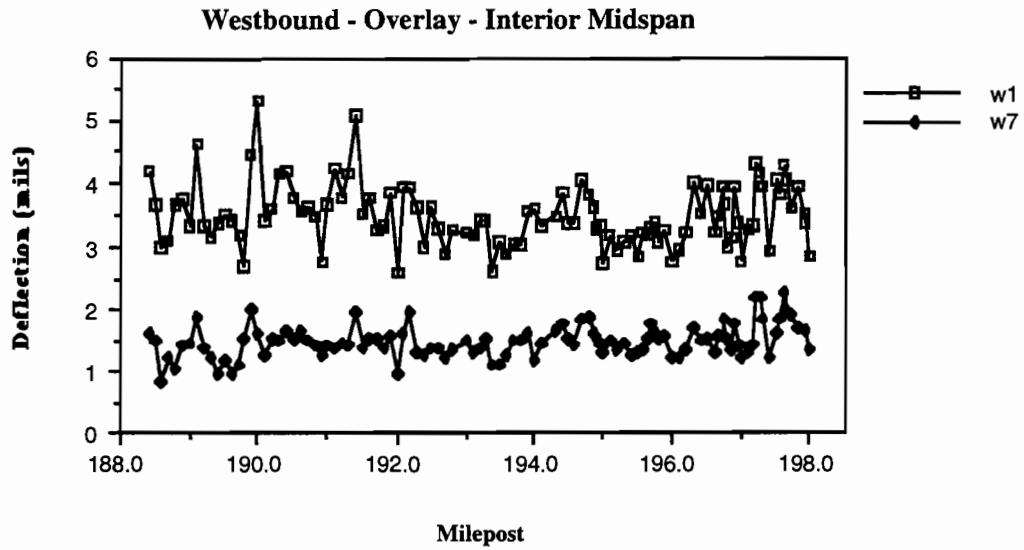


Figure B.21. Interior Crack (1 mil=0.025 mm)

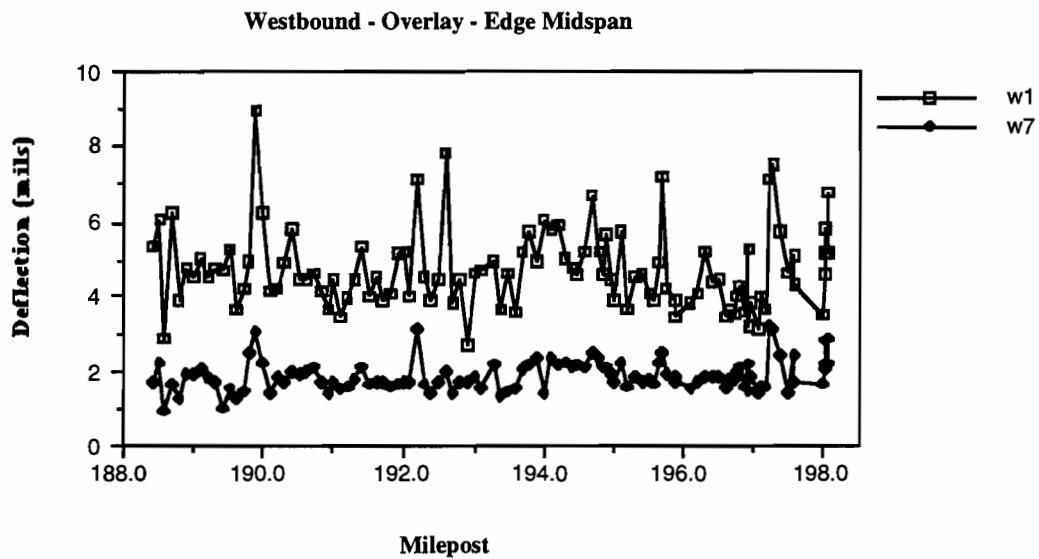


Figure B.22. Edge Crack (1 mil=0.025 mm)

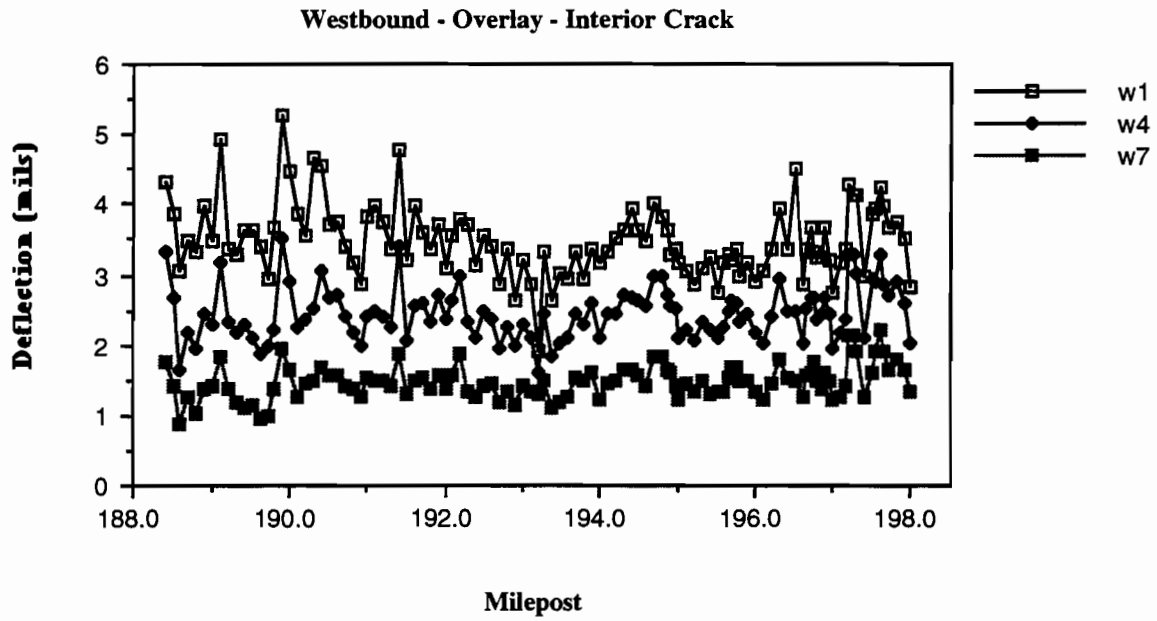


Figure B.23. Interior Crack (1 mil=0.025 mm)

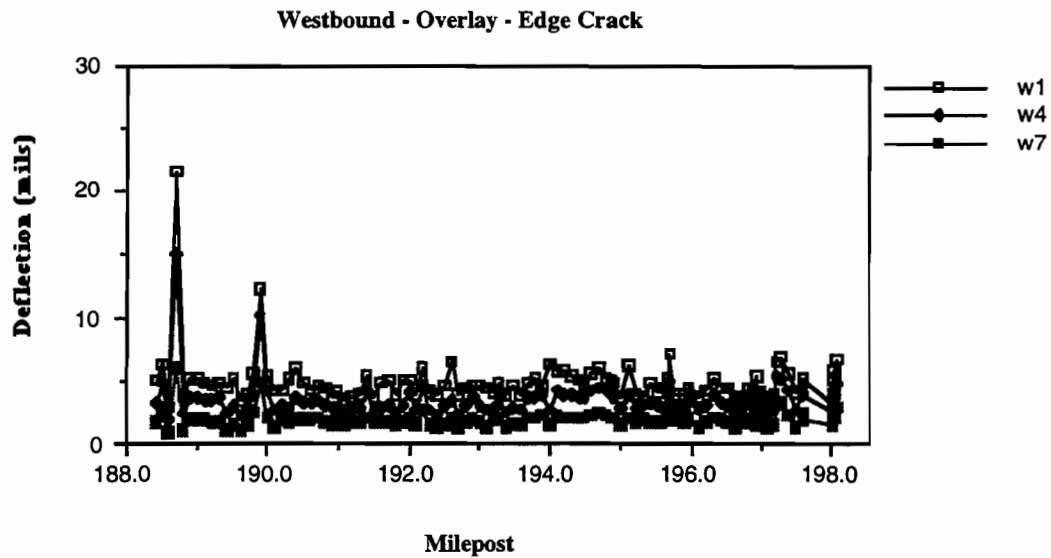


Figure B.24. Edge Crack (1 mil=0.025 mm)

Appendix C:
Comparison of Deflection Between Old and New Overlay
(9,000 lb / 4082 kg Load)

C-1 Edge Crack

C-1-1 Edge Crack — Eastbound

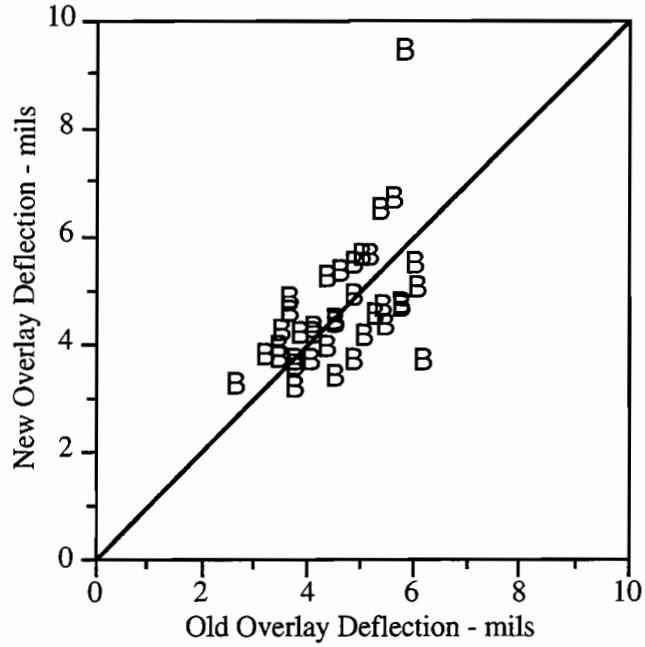


Figure C.1. Comparison of deflection between new and old overlay (w1) for crack of the edge in eastbound roadway (1 mil=.025 mm)

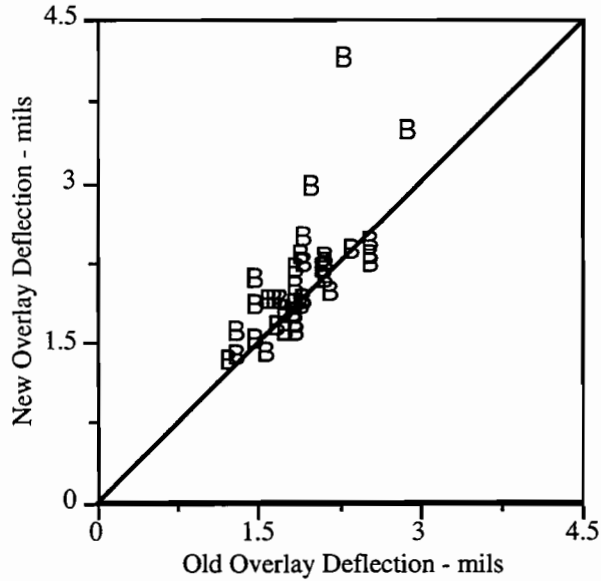


Figure C.2. Comparison of deflection between new and old overlay (w7) (1 mil=.025 mm)

C-1-2 Edge Crack — Westbound

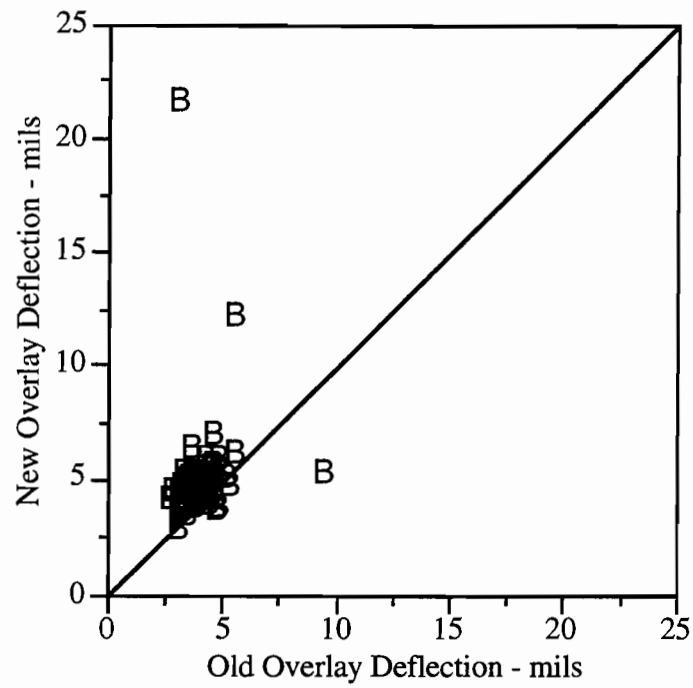


Figure C.3. Comparison of deflection between new and old overlay (w1) (1 mil=.025 mm)

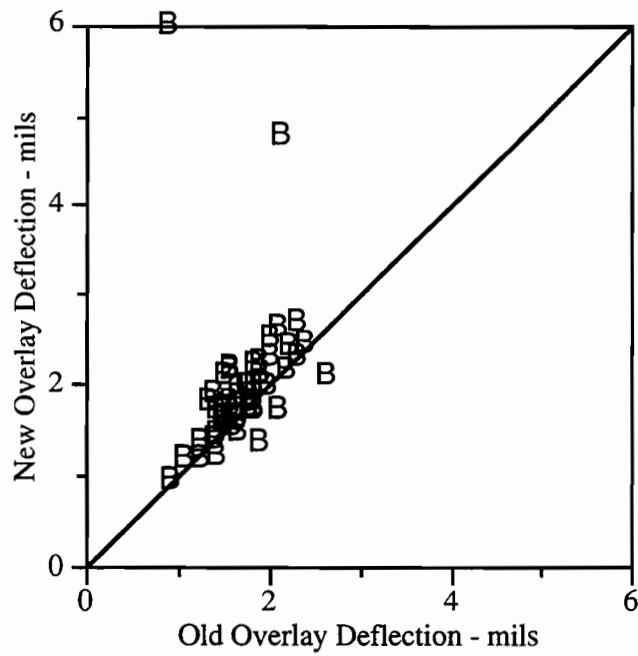


Figure C.4. Comparison of deflection between new and old overlay (w7) (1 mil=.025 mm)

C-2 Edge Midspan

C-2-1 Edge Midspan — Eastbound

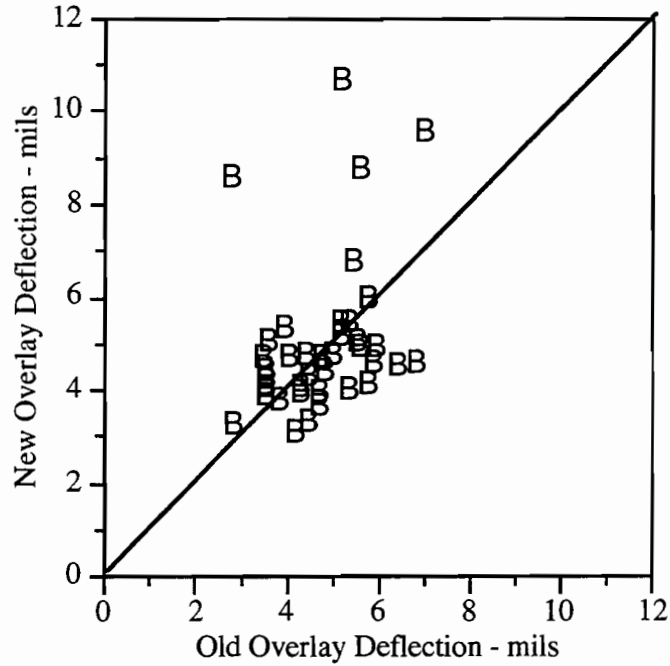


Figure C.5. Comparison of deflection between new and old overlay (w1) (1 mil=.025 mm)

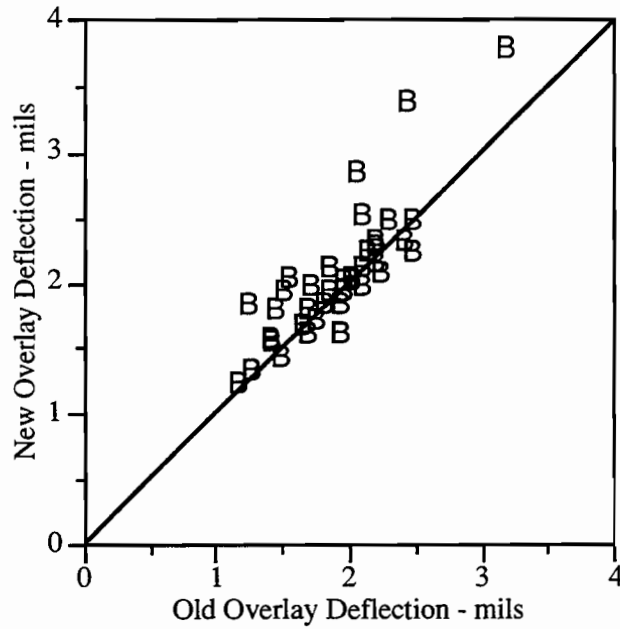


Figure C.6. Comparison of deflection between new and old overlay (w7) (1 mil=.025 mm)

C-2-2 Edge Midspan — Westbound

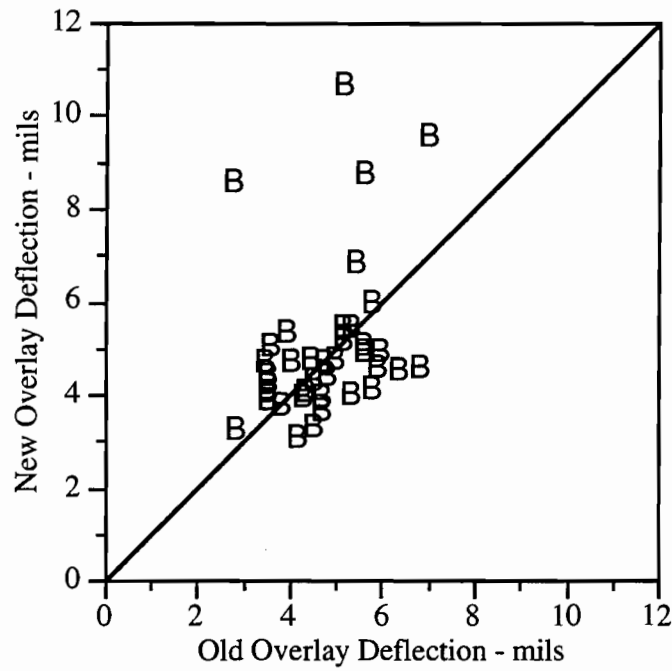


Figure C.7. Comparison of deflection between new and old overlay (w1) (1 mil=.025 mm)

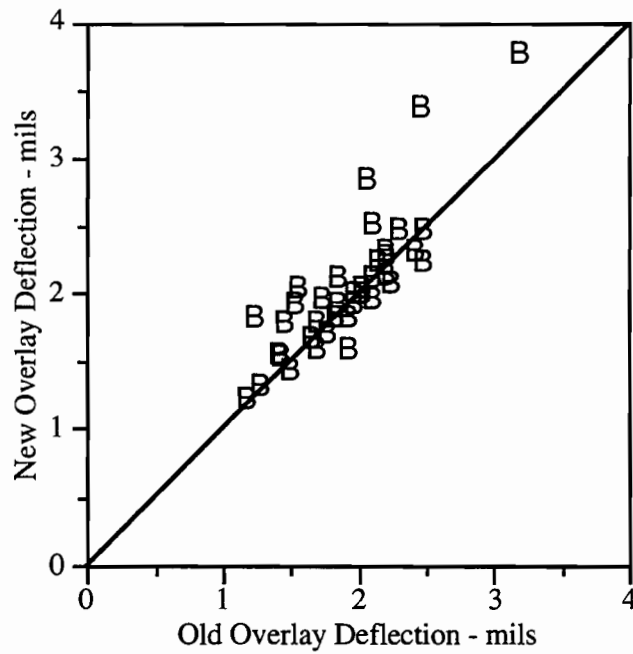


Figure C.8. Comparison of deflection between new and old overlay (w7) (1 mil=.025 mm)

C-3 Interior Crack

C-3-1 Interior Crack — Eastbound

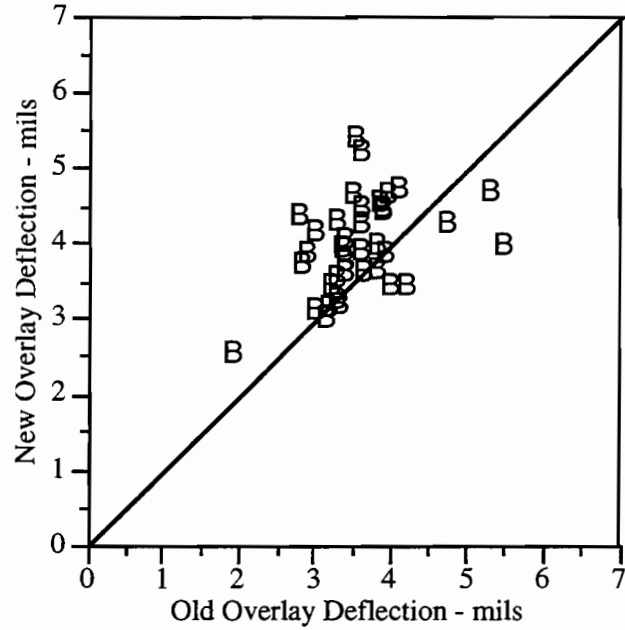


Figure C.9. Comparison of deflection between new and old overlay (w1) (1 mil=.025 mm)

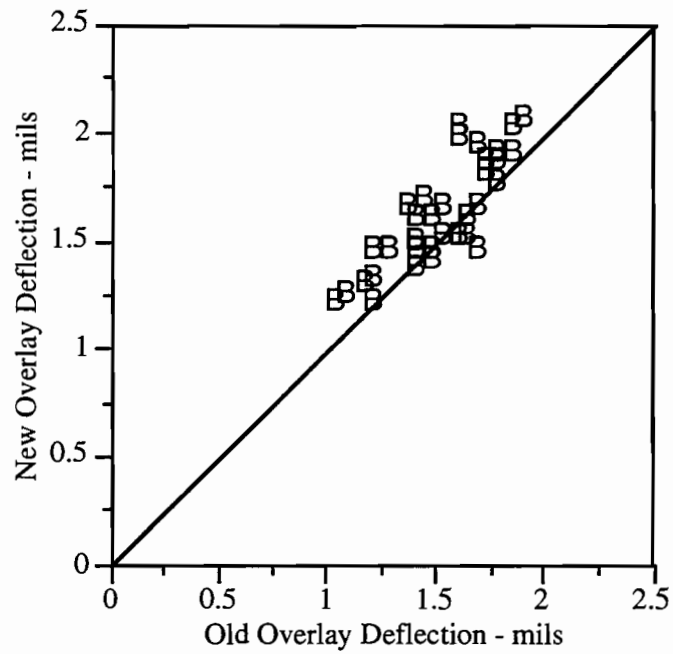


Figure C.10. Comparison of deflection between new and old overlay (w7) (1 mil=.025 mm)

C-3-2 Interior Crack — Westbound

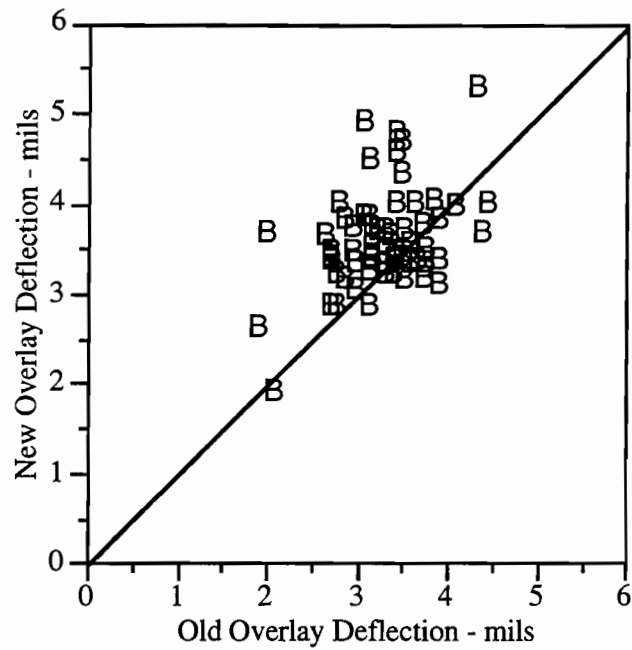


Figure C.11. Comparison of deflection between new and old overlay (w1) (1 mil=.025 mm)

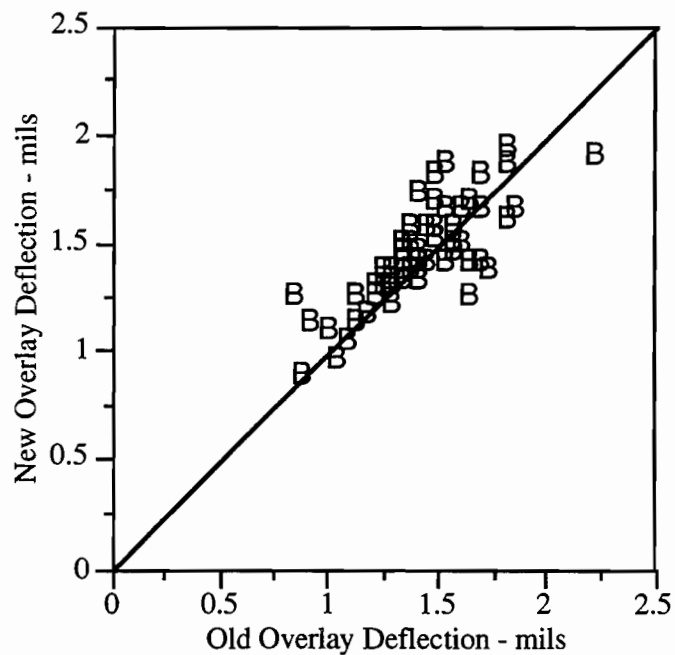


Figure C.12. Comparison of deflection between new and old overlay (w7) (1 mil=.025 mm)

Appendix D:
Analysis of Back-Calculation
Procedures for Composite Pavements

Three available methods were considered in this analysis. The first method, called an *iterative back-calculation process*, makes repeat calls to an elastic layer subroutine in order to match measured deflections to predicted layer moduli. The procedure converges either when the measured and predicted deflections match within a given tolerance level set by the user, or when the maximum number of iterations set by the user is reached. Examples of this method are RPEDD1, BISDEF, CHEVDEF, WESDEF, ELSDEF, and BOUSDEF (Ref 7). A major disadvantage of this methodology is the computational time required, particularly when many layers are involved. Another drawback is that seed values and ranges for the layer moduli — values based on engineering experience — are required. The second family of computerized procedures is based on a data base that stores back-calculation program results for possible deflection basins. While these run considerably faster than iterative programs, they are limited insofar as they can be applied only to situations comparable to those stored in the database. COMDEF is the only program developed specifically for AC/PCC composite pavements (Ref 8). COMDEF needs seven sensors spaced 12 inches (30.48 cm) apart. The fact that it cannot accommodate fewer sensors or other spacing makes it unfit for analysis of the FWD results for our test section.

While MODULUS was developed originally for flexible pavements (Ref 9), Hall and others (Ref 7) have demonstrated that it can be used for composite pavement analysis as well.

The last family of programs available uses a closed-form back-calculation approach. ILLIBACK is possibly the only program that is available presently that used this approach. However, it is designed to model only PCC pavements.

Following the literature review, we selected MODULUS 4.0 and RPEDD1 to perform the back-calculation procedures. Back-calculation programs generally require the following information to describe the pavement system: impact loading and a possible range of moduli. Data required for operating RPEDD1 and performing back-calculations for the test section include the following (Ref 10):

- 1) FWD deflection data
 - State, country, highway, lane
 - Load, (radius = 5.9 in. [14.9 cm], loading = 9000 lb [4,082 kg])
 - Deflection (w1-w7, mils)

- 2) Input parameters needed to perform the analysis
 - Characteristics of the FWD
 - Plate Radius (in.)
 - Sensor position in relation to the plate
 - Weighting factor of sensor (0-1, 0 will delete that sensor)
 - Pavement system and thickness
 - Surface: CRCP (thickness = 8 in. [20.32 cm])
 - Base: Cement stabilized base (thickness = 6 in. [15.24 cm])
 - Subgrade: Soil

Table D.1. Boundary values for moduli and Poisson ratio

Layer	Minimum	Maximum	Poisson Ratio
Surface	2,000,000	6,500,000	0.15
Base	50,000	2,000,000	0.30
Subgrade	5,000	50,000	0.40

MODULUS 4.0 underwent the following enhancements since it was first developed:

- 1) Automatic calculation of a depth to a stiff layer
- 2) Automatic calculation of weighting factors for each sensor
- 3) Detection of non-linearity in subgrade
- 4) The use of the Corps of Engineers' WES5 linear elastic program

Because it was originally developed for designing flexible pavement, the program requires a feasibility study to check the consistency of the results for rigid pavement applications. For this consistency check, three loading conditions were chosen. Subgrade stiffness and base thickness were selected to study the sensitivity of the output. Table D.2 presents results of MODULUS runs. The values in the table represent the average value of stiffness at each station along the eastbound section.

Table D.2. Output of the Modulus program

Base Thickness	Subgrade Modulus*	**	Impact Load								
			9000 lb (4082 kg)			12000 lb (5443 kg)			15000 lb (6804 kg)		
			E1	E2	E3	E1	E2	E3	E1	E2	E3
6 in. (15.2 cm)	5,000	Mean	5002	1021	21.6	4943	961.3	20.8	4860	915	21.3
		STD	1208	615.8	3.5	1187	633.6	3.1	1192	578	3.3
		COV	24	60.3	16	24	65.9	14.8	25	63.2	15.6
	20,000	Mean	5288	968.0	21.6	5103	908	20.9	5008	878.5	21.3
		STD	1192	590.3	3.3	1201	585.5	3.2	1262	544.7	3.3
		COV	23	61	15.1	24	64.4	15.3	25	62.0	15.3
	50,000	Mean	5288	968.0	21.6	5103	908	20.9	5008	878.5	21.3
		STD	1192	590.3	3.3	1201	585.5	3.2	1262	544.7	3.3
		COV	23	61	15.1	24	64.4	15.3	25	62.0	15.3
8 in. (20.3 cm)	5,000	Mean	5217	556.0	21.3	5096	555.1	20.4	4900	549.1	20.8
		STD	1248	390.0	3.2	1241	411.0	3.0	1101	355.5	3.0
		COV	24	70	15	24	74.0	14.6	22	64.7	14.4
	20,000	Mean	5318	544.6	21.3	5092	571.1	20.4	4950	555.8	20.8
		STD	1227	380.3	3.2	1239	428.7	3.0	1113	371.7	3.0
		COV	23	69.8	15	24	75.0	14.5	22	66.9	14.4
	50,000	Mean	5318	544.6	21.3	5092	371.7	20.4	4950	555.8	20.8
		STD	1227	380.3	3.2	1239	428.7	3.0	1113	371.7	3.0
		COV	23	69	15	24	75.0	14.5	22	66.9	14.4

* Subgrade Moduli: psi

**Mean, STD: Ksi

COV: %

Based on the results presented in Table D.2, the following conclusions may be drawn:

- 1) For a given loading increase, back-calculated moduli decrease — though the variation is not critical.
- 2) If stiffness of the subgrade is chosen over 20,000 psi, the subgrade effect may be ignored.
- 3) Base thickness produces higher variability on the calculated stiffness. A thickness of 6 inches (15.2 cm) results in higher base stiffness and lower surface stiffness.
- 4) The program usually gives higher variability in base stiffness. Thus, the user should take care in the selection of base thickness and stiffness ranges.

RPEDD1, developed by CTR, was also evaluated, with its results compared with MODULUS. Table D.3 shows the comparison of the results of MODULUS and RPEDD1 under the same conditions when the base thickness is 6 inches (15.2 cm) and the same possible stiffness ranges are selected for the layers. Unlike MODULUS, RPEDD1 requires seed values that represent the starting points of the iteration. Values of 4,000,000 psi for E1, 1,000,000 psi for E2, and 20,000 psi for E3 were used as seed values. The comparison shows that large differences exist in back-calculated stiffness between the two programs, though the mean values are very similar for the surface layer (PCC). In general, the RPEDD1 program yields higher stiffness values for the upper layer (PCC and CTB), and a lower value for the subgrade.

Based on information presented in Tables D.3 and D.4 and in Figures D.1 to D.3, the following conclusions can be drawn:

1. MODULUS gives higher moduli values than RPEDD1.
2. Large difference exists between two programs for the surface layer.
3. Subgrade modulus shows a linear relationship between the programs.

The overall conclusion is that back-calculations of pavement layer properties of thin asphalt overlay on a rigid section are unreliable at this point. New methodologies and models are needed in this area.

Table D.3. Results of back-calculation programs (eastbound)

Program Station	Modulus			RPEDD1		
	E1	E2	E3	E1	E2	E3
190.9	6499986	683789	20034	4976000	1801800	12070
191.0	5767600	925687	22447	6500000	2000000	13210
191.1	4063440	1273426	16852	5698000	677300	10890
191.2	4391924	1936955	21518	6500000	1903500	14400
191.3	6499986	383791	22906	4879000	1239900	14880
192.2	5229436	720809	20465	6500000	1454700	11490
192.3	3985711	1999995	21669	5256000	2000000	14020
192.4	6499986	1400535	29455	6500000	2000000	20000
192.5	4855004	1070239	24689	4714000	1985900	16210
192.6	2910560	1999995	21303	4985000	1415200	14030
192.7	3704099	1763613	23791	4704000	1945700	16240
192.8	6368687	636868	21282	4940000	1383200	13960
193.0	4936693	68575	26498	4740000	672200	15230
193.1	6333410	1747782	17748	6500000	2000000	11820
193.3	4550567	209999	19320	5999000	616300	10230
193.4	5735771	195957	22388	5211000	1179600	12680
193.9	6499986	557623	18587	4966000	1285800	11350
194.0	6499986	543417	19392	6500000	965800	11880
194.1	4432915	1999995	24863	6491000	2000000	16570
194.2	3502733	1313338	21318	4860000	1307300	13800
194.3	2638543	590833	20991	5016000	660200	11800
194.4	4275892	1699989	16999	6500000	1019800	11170
194.5	6294277	1205197	22480	5892000	2000000	14660
194.6	5858890	563030	17674	5735000	863200	10890
194.7	6010243	1056095	17362	6500000	888800	11370
194.8	5853241	1172985	20644	4961000	1693100	13750
194.9	6499986	1259949	22091	6500000	2000000	14500
195.0	6499986	214790	29492	4801000	1812400	17720
195.1	6217650	211755	21229	5278000	1430600	11460
195.2	2663052	988765	14785	6500000	560300	7460
195.3	4027889	1371872	21732	4871000	1479200	14060
195.4	6125210	688143	26127	5019000	2000000	16940
195.5	6499986	364698	25522	5051000	1421800	16300
195.6	6399487	645262	21915	4923000	1501800	14170
195.7	5704294	190143	19014	4698000	721700	11440
195.8	4754858	1263786	24407	4751000	2000000	16140
195.9	4619562	228415	24055	6062000	852600	13300
197.2	5614976	1824588	18248	6055000	2000000	12060
197.3	5186416	813033	19649	4890000	1309500	12200
197.4	6499986	933359	22424	5395000	2000000	14580
MEAN (psi)	5287823	967977	21584	5520425	1451230	13523
STD (psi)	1191545	590285	3251	712593	502646	2400
COV (psi)	22.53%	60.98%	15.06%	12.91%	34.64%	17.75%

Table D.4. Absolute differences between Modulus and RPEDD1

Station	Absolute Difference * (E1)	Absolute Difference (E2)	Absolute Difference (E3)
190.9	1,523,986	1,118,011	7,964
191.0	732,400	1,074,313	9,237
191.1	1,634,560	596,126	5,962
191.2	2,108,076	33,455	7,118
191.3	1,620,986	856,109	8,026
192.2	127,0564	733,891	8,975
192.3	1,270,289	5	7,649
192.4	14	599,465	9,455
192.5	141,004	915,661	8,479
192.6	2,074,440	584,795	7,273
192.7	999,901	182,087	7,551
192.8	1,428,687	746,332	7,322
193.0	196,693	603,625	11,268
193.1	166,590	252,218	5,928
193.3	1,448,433	406,301	9,090
193.4	524,771	983,643	9,708
193.9	1,533,986	728,177	7,237
194.0	14	422,383	7,512
194.1	2,058,085	5	8,293
194.2	1,357,267	6,038	7,518
194.3	2,377,457	69,367	9,191
194.4	2,224,108	680,189	5,829
194.5	402,277	794,803	7,820
194.6	123,890	300,170	6,784
194.7	489,757	167,295	5,992
194.8	892,241	520,115	6,894
194.9	14	740,051	7,591
195.0	1,698,986	1,597,610	11,772
195.1	939,650	1,218,845	9,769
195.2	3,836,948	428,465	7,325
195.3	843,111	107,328	7,672
195.4	1,106,210	1,311,857	9,187
195.5	1,448,986	1,057,102	9,222
195.6	1,476,487	856,538	7,745
195.7	1,006,294	531,557	7,574
195.8	3,858	736,214	8,267
195.9	1,442,438	624,185	10,755
197.2	440,024	175,412	6,188
197.3	296,416	496,467	7,449
197.4	1,104,986	1,066,641	7,844
Mean	1,106,122	608,071	8,061

*: Absolute Difference (E_i) = | E_i RPEDD1 - E_i Modulus |

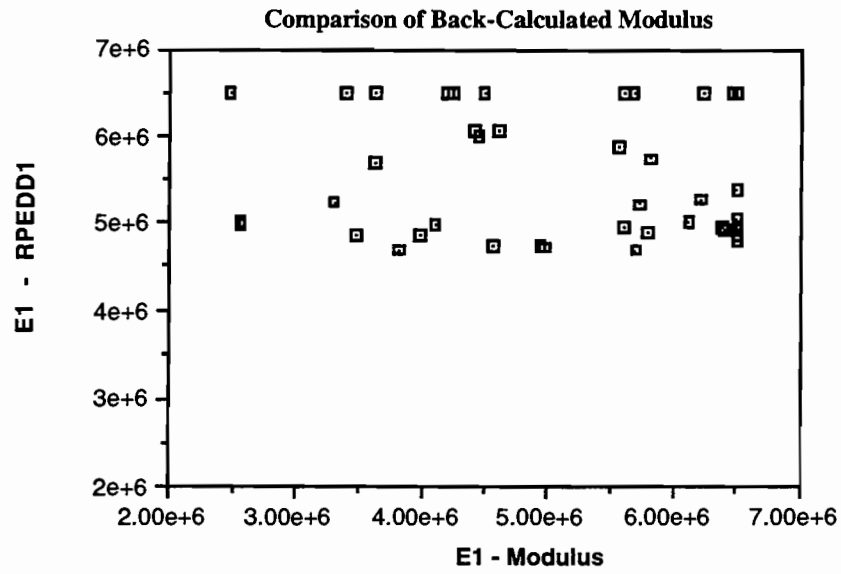


Figure D.1. Comparison of back-calculated Modulus in eastbound — E1

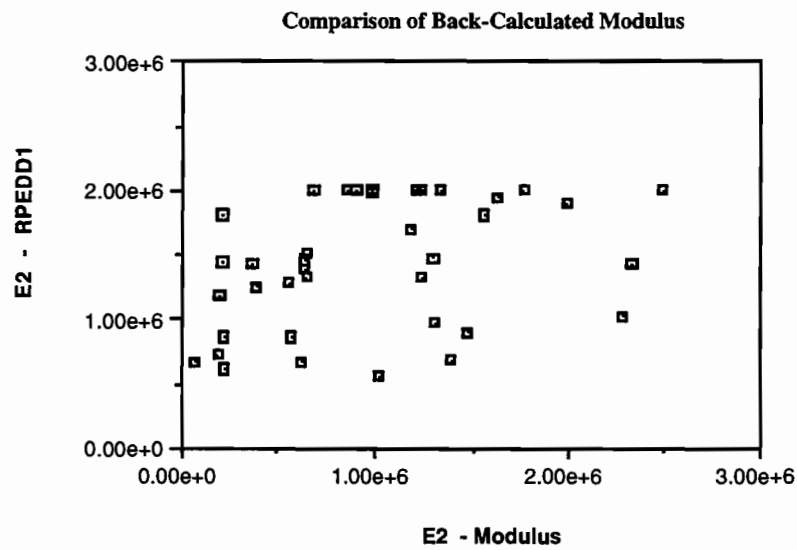


Figure D.2. Comparison of back-calculated Modulus in eastbound — E2

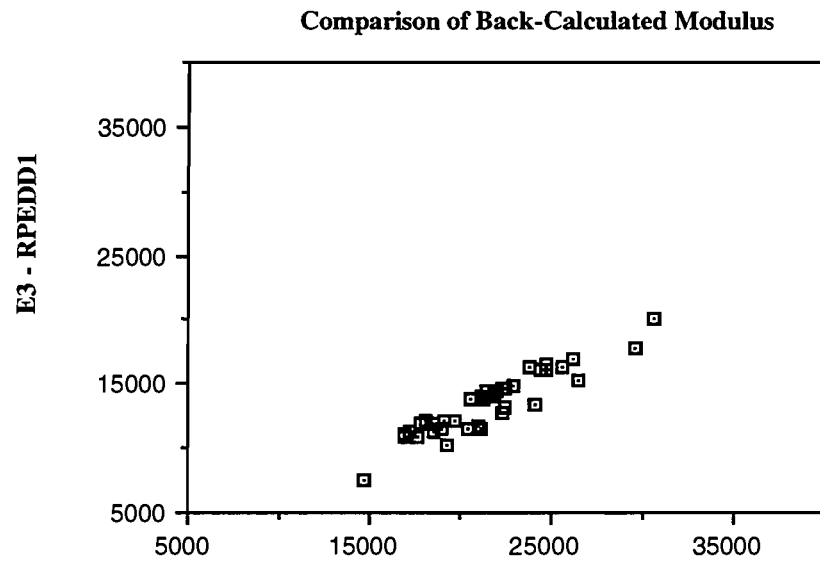


Figure D.3. Comparison of back-calculated Modulus in eastbound — E3

